



मुंबई
**CLIMATE
ACTION PLAN**

**CLIMATE & AIR POLLUTION RISKS
AND VULNERABILITY ASSESSMENT
FOR MUMBAI, INDIA**

Acknowledgments

The climate & air pollution risks and vulnerability assessment was carried out for the Mumbai Climate Action Plan (MCAP). This report is a comprehensive study including a description of methods, data sources and tools used to complete the analysis. A summary of this report is included in the MCAP in the baseline assessment section. This study was conducted by the World Resources India, Ross Centre for Sustainable Cities, in collaboration with the Brihanmumbai Municipal Corporation.

We'd like to sincerely thank the individuals listed below for their support and contributions to this report:

Project Lead

Lubaina Rangwala – Program Head, Urban Development

Authors

Ananya Ramesh – Senior Project Associate, Urban Development

Bhanu Khanna – Senior Program Associate, GeoAnalytics

Bina Shetty – Program Head, GeoAnalytics

Raj Bhagat P – Senior Program Manager, GeoAnalytics

Amrita Chakraborty – Senior Project Associate, Urban Development

Analysts

Janhavi Mane – Program Associate, GeoAnalytics

Aditya Sharma – Program Associate, GeoAnalytics

Linda Regi – Program Associate, GeoAnalytics

Jyoti – Program Associate, GeoAnalytics

Abhimanyu S – Program Associate, GeoAnalytics

Editing, Report Design & Graphic Visualization

Abhinand Gopal – Senior Program Communications Associate, GeoAnalytics

Sonali Chakraborty – Editor, Writer

This report should be referred to as

'Climate & Air Pollution Risks and Vulnerability Assessment, March 2022'

All maps in this report have been prepared by the GeoAnalytics Team at WRI India.

Disclaimer: All maps are for informative purposes only, with representational delimitation of jurisdictional boundaries.

Contact for this report: Lubaina Rangwala at lubaina.rangwala@wri.org

Table of Contents

List of Figures	4
List of Abbreviations	6
List of Tables	7
1. Mumbai's Vulnerability to Climate & Air Pollution Risks	8
1.1 Climate Context	9
1.2 Projected Risks	12
1.3 Climate & Air Pollution Risks and Vulnerability Assessment	13
2. Climate Risk Context	16
Urban Heat Risk	18
Urban Flooding Risk	23
Landslide Risk	26
Coastal Risks	27
Air Pollution Risk	32
3. Demographic Context	40
4. Vulnerability Assessment	44
Socio-economic Aspects	49
Physical Environment Aspects	50
Infrastructure and Service Aspects	52
5. Impact Analysis	60
Impact on Lives	61
Impact on Livelihoods	61
Impact on Services	62
6. Conclusion	66
References	71
Annexure: Figures and Illustrations	74
Endnotes	106

List of Figures

Figure 1A: BMC Ward-wise Population Density	9
Figure 1B: Mumbai's Landscape	10
Figure 2: Framework of Vulnerability Assessment Illustrating the Three Aspects and Respective Parameters	14
Figure 3: Annual Air Temperature Anomalies between 1973 and 2020	19
Figure 4: Inter-annual Air Temperature Trend between 1973 and 2020	19
Figure 5: Statistically Significant Shift in Mean Annual Air Temperature Based on Change-point Analysis between 1973 and 2020	19
Figure 6: Inter-annual Variation in Frequency of Caution and Extreme Caution Events between 1973 & 2020	20
Figure 7: Land Surface Temperature by Land use and Land Cover in Mumbai	21
Figure 8: Ward-wise Distribution of Mean LST in Comparison with Percentage Share of Roofing Material Type	21
Figure 9: Ward-wise Distribution of Mean LST in Comparison with Mean NDVI Share (% Area)	22
Figure 10: Duration of Extreme Rainfall Events	24
Figure 11: Frequency of Extreme Rainfall Events (ERE) between 2011 and 2020	24
Figure 12: Inter-annual Spatial Variation in Frequency of Different Rainfall Events between 2011 and 2020	24
Figure 13: (a) Daytime (b) Nighttime, Average Annual Sea Surface Temperature between 2003 and 2020	28
Figure 14: Annual Sea level Trends from Radar Tide Gauge Sensor between 2011 and 2021	29
Figure 15: Storm Surge associated with Cyclone Tauktae, May 2021	29
Figure 16: Mumbai Mangrove Area Assessment, Year 2008-2010 vs 2018-2021	30
Figure 17: Mumbai Coastline Change, Year 1990 vs 2020	31
Figure 18: Average Annual Concentration of PM10 and PM2.5 from July 2015 to March 2021	33
Figure 19: Annual Average Concentrations of Sulphur Dioxide (SO ₂), Nitrogen Dioxide (NO ₂) and Ammonia (NH ₃) from April 2010 to March 2021 in Mumbai	34
Figure 20: Station-wise Annual Average Concentration of NO ₂ at Fixed Monitoring Stations from April 2010 to March 2021	34
Figure 21: Annual Average Concentrations of Carbon Monoxide (CO) in Mumbai from July 2015 to March 2021	35
Figure 22: 2D Timeseries of Weekly Average Concentrations of PM2.5 for Bandra and Colaba Monitoring Stations from: a) June 2019 to May 2020 and b) June 2020 to May 2021	36
Figure 23: 3D Timeseries of Hourly Average Concentration of PM2.5 for Bandra and Colaba Monitoring Stations, Mumbai, June 2019 to May 2021	37
Figure 24: Total Vertical Column Density of SO ₂ , CO, & NO ₂ – Mean of June 2019 to May 2020	38
Figure 25: Annual Average Concentration of PM2.5 from June 2019 to May 2021	39
Figure 26: Indoor PM2.5 Concentrations by Type of Fuel Use in Mumbai	39
Figure 27: Temporal Analysis showing Change in Serviced Area under Different Traffic Conditions during a Day	58
Figure 28: Population Potentially at Risk due to Floods	63

Figure 29: Impact on Employment Hubs due to Floods	64
Figure 30: Mass Transit Stations with Limited Physical Access during Floods	65
Figure 31: Mumbai's Vulnerability Assessment	70
Figure 32: Mean Land Surface Temperature (October month: 2017-2019)	75
Figure 33: Ward-wise Mean Land Surface Temperature (October month: 2017-2019)	76
Figure 34: Mean Normalised Difference Vegetation Index (2015-2020)	77
Figure 35: Stormwater Drainage Network and Built-up Footprint	78
Figure 36: Landslide Prone Locations and Informal Settlements	79
Figure 37: Flooding Hotspots and Informal Settlements	80
Figure 38: Annual Average Concentration of PM10 and PM2.5 for SAFAR Monitoring Stations from July 2015 to March 2021	81
Figure 39: Station-wise annual average Carbon Monoxide (CO) Levels at Monitoring Stations in Mumbai from July 2015 to March 2021	81
Figure 40: Monthly Variation using Mean Weekday and Weekend Concentrations of PM2.5 ($\mu\text{g}/\text{m}^3$) for June 2019 to May 2020	82
Figure 41: Monthly Variation using Mean Weekday and Weekend Concentrations of PM2.5 ($\mu\text{g}/\text{m}^3$) for June 2020 to May 2021	83
Figure 42: Ward-wise Effective Literacy Rate	85
Figure 43: Ward-wise Effective Female Literacy Rate	86
Figure 44: Access to Educational Institutions	87
Figure 45: Gender Imbalance – Sex Ratio	88
Figure 46: Social Composition – Percentage of SC/ST Population	89
Figure 47: Access to Information based on Asset Ownership - Information Access via Broadcast Media	91
Figure 48: Access to Information based on Asset Ownership - Information Access via Telephone	91
Figure 49: Home Ownership	92
Figure 50: House Condition	93
Figure 51: Access to Daily Urban Recreation Spaces	94
Figure 52: Access to Drinking Water	95
Figure 53: Access to Drinking Water	96
Figure 54: Access to Sanitation	97
Figure 55: Access to Sanitation	98
Figure 56: Access to Sanitation	99
Figure 57: Access to Clean Cooking Fuel	100
Figure 58: Access to Electricity	101
Figure 59: Access to Mass Transit Stations on a Regular Day	102
Figure 60: Access to Healthcare	103
Figure 61: Access to Fire Services	104
Figure 62: Access to Flood Shelters	105

List of Abbreviations

AWS	Automatic Weather Station	PM	Particulate Matter
BMC	Brihanmumbai Municipal Corporation	SAFAR	System of Air Quality and Weather Forecasting and Research
CAAQMS	Continuous Ambient Air Quality Monitoring Stations	SAPCC	State Adaptation Action Plan on Climate Change
CAP	Climate Action Plan	SC	Scheduled Castes
CPCB	Central Pollution Control Board	SEEPZ	Santacruz Electronic Export Processing Zone
CRZ	Coastal Regulation Zone	SRA	Slum Redevelopment Authority
CSMIA	Chhatrapati Shivaji Maharaj International Airport	SST	Sea Surface Temperature
CSMT	Chhatrapati Shivaji Maharaj Terminus	ST	Scheduled Tribes
DP	Development Plan	SWD	Storm Water Drains
ERE	Extreme Rainfall Events	TIRS	Thermal Infrared Sensor
ESA	European Space Agency	TOA	Top of Atmosphere
GDP	Gross Domestic Product	TROPOMI	TROPOspheric Monitoring Instrument
GIS	Geographic Information System	USGS	United States Geological Survey
HH(s)	Household(s)		
IPCC	Intergovernmental Panel on Climate Change		
IMD	Indian Meteorological Department		
INCOIS	Indian National Centre for Ocean Information Services		
JNPT	Jawaharlal Nehru Port Trust		
LPG	Liquified Petroleum Gas		
LST	Land Surface Temperature		
MMR	Mumbai Metropolitan Region		
MPCB	Maharashtra Pollution Control Board		
MSL	Mean Sea Level		
NAAQS	National Ambient Air Quality Standards		
NOAA	National Oceanic and Atmospheric Administration		
NDVI	Normalized Difference Vegetation Index		
NDWI	Normalized Difference Water Index		
NWS	National Weather Station		
OLI	Operational Land Imager		
OSM	OpenStreetMap		

List of Tables

Table 1: Climate Risk Context Indicators _____	16
Table 2: Urban Heat Risk – Assessment Parameters and Attributes _____	18
Table 3: Urban Flooding Risk – Assessment Parameters and Attributes _____	23
Table 4: Landslide Risk – Assessment Parameters and Attributes _____	26
Table 5: Coastal Risks – Assessment Parameters and Attributes _____	27
Table 6: Annual and Daily Permissible Limits for Various Air Pollutants as per the National Ambient Air Quality (NAAQ) Standards, CPCB _____	32
Table 7: Air Pollution Risk – Assessment, Parameters and Attributes _____	32
Table 8: Demographic Context Indicators _____	41
Table 9: Demographic Context – Assessment Parameters and Attributes _____	42
Table 10: Vulnerability Assessment Indicators _____	44
Table 11: Access to Information – Assessment, Parameters and Attributes _____	49
Table 12: Home Ownership – Assessment Parameters and Attributes _____	50
Table 13: House Condition – Assessment Parameters and Attributes _____	51
Table 14: Access to Daily Urban Recreation Spaces - Assessment Parameters and Attributes _____	51
Table 15: Access to Drinking Water – Assessment Parameters and Attributes _____	52
Table 16: Access to Sanitation – Assessment Parameters and Attributes _____	53
Table 17: Access to Clean Cooking Fuel – Assessment Parameters and Attributes _____	54
Table 18: Access to Electricity – Assessment Parameters and Attributes _____	54
Table 19: Access to Mass Transit – Assessment Parameters and Attributes _____	55
Table 20: Access to Healthcare – Assessment Parameters and Attributes _____	56
Table 21: Access to Fire Services – Assessment Parameters and Attributes _____	57
Table 22: Access to Flood Shelters – Assessment Parameters and Attributes _____	58
Table 23: Impact Analysis _____	60
Table 24: Ward-wise Summary – Climate & Air Pollution Risks and Vulnerability Assessment _____	66

Chapter 1:

Mumbai's Vulnerability to Climate & Air Pollution Risks

Introduction

The Climate & Air Pollution Risks and Vulnerability Assessment report analyses risks faced by Mumbai city, using historical climate data. This analysis was used as part of the Mumbai Climate Action Plan's (CAP) baseline assessment studies. The Mumbai CAP is the Brihanmumbai Municipal Corporation (BMC)'s first effort to develop a 30-year roadmap for Mumbai to achieve a 'net zero' target by 2050. WRI India provided technical support for the Mumbai CAP, and as part of this effort, completed the city's first ever spatial vulnerability assessment to identify differential vulnerabilities

based on socio-economic, demographic characteristics that increase risk exposure and sensitivity in poor, underdeveloped neighborhoods. A complex framework of indicators – covering social, physical, and infrastructural aspects – is correlated with spatial and temporal risk analyses and qualitative and quantitative assessments. This composite approach helped develop targeted and effective solutions in the Mumbai CAP. This report is a detailed account of the summary of findings presented in the Mumbai CAP, describing the data sources, analytical methods used, and potential impacts analysed.



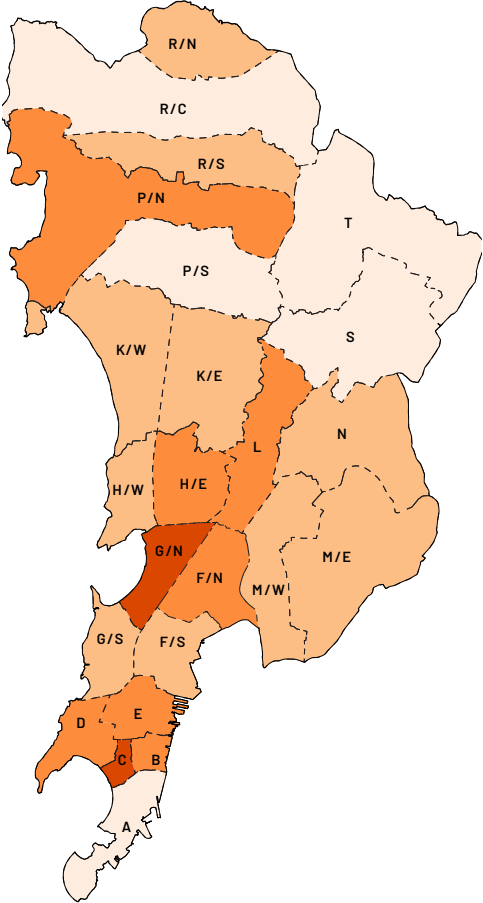
Image Credit: Wikimedia Commons

1.1 Climate Context

Mumbai is the most populous city in India and, globally, the 7th largest in terms of population. Projected to be the 6th largest by 2030 (UNDESA, 2018) it comprises two districts – Mumbai City and Mumbai Suburban. Surrounded by the sea on three sides, Mumbai is separated from the mainland by the Thane Creek and Harbour Bay and divided for administrative purposes into six zones comprising 24 wards. According to the 2011 Census, population density in these two districts exceeds 20,000 persons/km², whereas the national average is 382 persons/km² and the state average is 365 persons/km² (TERI, 2014, p. 40). According to the Slum Rehabilitation Authority (SRA), around 55% of Mumbai’s population lives in slums and about 65% are employed in the informal sector (Bhowmik, 2010). This makes the impact and experience of climate risks highly varied across the city and across different socio-economic groups.

Mumbai faces two major climate challenges – urban flooding and increasing heat. Being a coastal city, Mumbai experiences high levels of humidity and resulting humid heat. Coastal risks due to storm surge, coastal inundation and sea intrusion are also exacerbated during the monsoon months. Demographic diversity impacts sensitivity to climate risks,

Figure 1A | BMC Ward-wise Population Density



Population Density (number of persons/km²):
 □ 0-20k □ 20-40k □ 40-60k □ 60-100k

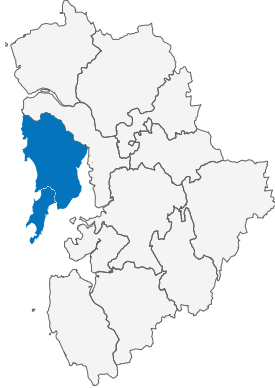
Source: Census 2011



Maharashtra
 Area: 307,713 km²
 Density: 365 persons/km²



Mumbai Metropolitan Region
 Area: 6,328 km²
 Density: 3,700 persons/km²



Brihanmumbai Municipal Corporation (BMC)
 Area: 437.71 km²
 Density: 28,471 persons/km²

Figure 1B | Mumbai's Landscape



- | | | | | | |
|------------|----------|---------------|---------|--------------|----------|
| Water Body | Mangrove | BMC Boundary | Airport | Railway Line | Sea Port |
| Forest | Mudflat | National Park | Station | Highway | |

Source: WRI India; Contains modified Copernicus Sentinel Data(2022)

adding a layer of complexity to understanding differential vulnerabilities and resilience capacities.

According to the Maharashtra State Adaptation Action Plan on Climate Change (SAPCC) 2014 (TERI, 2014), which provides state, regional and city level climate vulnerability context, 40% of Maharashtra's geographic area is drought prone and 7% is flood prone, with deficient rainfall reported once every five years. The state experienced severe and successive droughts in 1970-1974 and 2000-2004. Severe drought conditions occur once every eight to nine years. Mumbai city in particular, due to its geographical condition, is susceptible to heavy rainfall and prone to flooding almost annually. The fact that Mumbai was created by reclaiming land between seven separate islands is one of the primary reasons for its flooding. The Mean Sea Level (MSL) of Mumbai is very close to the Indian MSL at 0.01m. The average high tide level is 2.5m, the annual highest peak tide level being 2.75m. The average low tide level is -2m (i.e., two meters below the MSL). Between 2004 and 2007, Mumbai experienced flooding annually, incurring heavy losses and damages (Kuruppu, Bee, & Schaer, 2018). In July the city witnessed the worst flooding in its history (Gupta, 2007) that claimed over 900 lives and resulted in losses of over INR450 crore (TERI, 2014, p. 42).

The low-lying areas of the island city have a history of flooding five to six times a year, generally for a few hours when high intensity rainfall is coupled with high tides. Areas are just 2.25m to 3m above MSL, which are similar to flood levels in the creeks. In areas such as Saat Rasta, Lower Parel, and Grant Road, the land level is below the high tide level. Large areas along the coast including Juhu Aerodrome and Khar are at 3m, making them vulnerable to submergence. Only low tide phases (about 10 to 12 hours in a day, when water recedes below MSL) provide relief during storm events by draining out accumulated surface water. Anthropogenic activities have not factored in the city's estuary nature, landscape ecology and diverse demography, exacerbating the problem. These activities include unsustainable use of resources, reclamation of low-lying areas, poor condition and capacity of drainage system, development of eco-sensitive zones such

as wetland and mangrove areas leading to a loss of holding ponds and biodiversity, incorrectly designed levels of outfalls, development patterns increasing run-off coefficient, to name a few. This is evident in the fact that while the Mumbai Metropolitan Region (MMR) increased in area from 149km² in 1971 to 1,000km² by 2010 with an expansion in the area under industry from 45km² to 140km², its forest area declined from 1,045km² to 879km² and area under agriculture reduced from 2,098km² to 1,381km² (TERI, 2014).

Another major risk is urban heat. Mumbai experiences high temperatures not only during summer but also in the post monsoon months when humidity levels increase heat stress. Low-income households and informal settlements are at a higher risk (Mehrotra, Bardhan, & Ramamritham, 2018) given the limited access to water and sanitation services and nature of their living environment (metal roofs and tarpaulin roofs exacerbate heat risks). Heat stress also impacts productivity and thereby livelihoods and the economy. According to National Oceanic and Atmospheric Administration (NOAA) projections, 60% of Mumbai's year will comprise high heat days by 2040, where temperatures can exceed 32°C.

Mumbai is vulnerable to climate change induced hazards including sea level rise, heavy rainfall, storm surge and tropical cyclones. It is also susceptible to landslides as a result of heavy rain that causes many fatalities and physical damage every monsoon. By 2030, at the state level, relatively increased rainfall intensity is projected for Northern Maharashtra as compared to baseline rainfall for the other parts of the state. Research Climate Central shows a large part of Mumbai is at risk of being submerged by 2050 (Kulp & Strauss, 2019). With a business-as-usual scenario and no corrective action initiated to address the impending climate risks, Mumbai's total losses for a 100-year return period event is projected to be greater than factor 3 by the 2080s. The contribution of indirect losses to total losses would increase from 14% in the present-day situation to 18% in the 2080s (Hallegatte, et al., 2010, p. 34). Also, by 2080, the likelihood of urban floods such as the July 2005 event is more than double (Ranger, et al., 2010).

1.2 Projected Risks

Climate change is projected to affect populations across the globe with increased water shortages, droughts, heat waves, limited food supply, poorer air quality and increased frequency of extreme events, affecting lives and livelihoods (IPCC, 2014, p. 13). By 2050, global temperatures are expected to increase between 1.5°C and 5°C in many locations (McKinsey Global Institute, 2020) and it is estimated that there will be 25 million to 1 billion climate migrants the world over (Bose, Faleiro, & Singh, 2020). Global statistics on Internally Displaced People (IDP) reveal that new displacements in 2019 stood at 33.4 million, the highest since 2012. Of this, over 70% were due to weather-related disasters. And in South Asia, 38.3% of the total displacements were triggered due to disasters such as monsoons, floods and tropical storms (IDMC, 2020). While everyone will experience these changes in some form or the other, countries with lower per capita GDP are expected to be at greater risk. Poor communities are more vulnerable to climate-related shocks due to lower coping capacities (McKinsey Global Institute, 2020, p. 25) (Hallegatte, et al., 2016) (Eckstein, Künzel, & Schäfer, 2021). Depending on the region, half to two-thirds of Asia's cities with 1 million or more inhabitants are exposed to one or multiple hazards, with floods and cyclones the most important (Hijioka, et al., 2014).

The IPCC Fifth Assessment Report (Hijioka, et al., 2014) analyses climatic drivers and estimates potential future risks for Asia in the near term between 2030 and 2040, and in the long term between 2080 and 2100. According to this assessment, Asia is bound to face medium to very high risk of water shortage in arid areas and a decline in agricultural productivity in the near and long term, impacting food production and security, causing malnutrition. Coastal and marine systems are also projected to be under increasing stress with rising sea levels, increased rates of coastal erosion, degradation of mangroves, salt marshes, saltwater intrusion, high sea surface temperatures. Increased riverine, coastal and urban flooding is projected

with very low to medium risk in the near term and medium to very high risk in the long term, leading to widespread damage to livelihoods, infrastructure and increased flood-related deaths and injuries. Asia is also projected to face more frequent and intense heat waves and intensified heat island effects, resulting in very high risk of heat related mortalities in the long term, especially in vulnerable groups such as outdoor workers and informal settlement residents. Consequently, Asia will witness exacerbated poverty, inequalities and new vulnerabilities with medium to very high risk.

While South Asia¹ is projected to be one of the most vulnerable regions to climate-induced disasters, more than half of all South Asians were affected by one or more climate-related disasters in the last two decades (World Bank, 2021). Primary climate risks in South Asia include flooding, food and water insecurity, and extreme heat due to rising temperatures. Climate-induced yield reduction is projected to be as high as 23% in South Asia by 2080 (Hallegatte, et al., 2010, p. 51). By 2030, the region is projected to incur an annual average economic loss of USD160 billion due to climate change and by 2050 it could see over 40 million climate migrants due to rising sea levels (World Bank, 2013).

The Climate Risk Index 2021 ranked India among the top 10 most-affected countries in 2019 (Eckstein, Künzel, & Schäfer, 2021). Absolute losses incurred by India in 2019 from extreme weather events amounted to nearly USD69 billion (in purchasing power parity), the highest of any country in the world (World Bank, 2021, p. 66). India has a 10% likelihood of experiencing a lethal heat wave in climate exposed regions, leading to reduced productivity due to lost working hours by 2050 (McKinsey Global Institute, 2020, p. 18). And it is likely to witness a 10% loss in GDP per capita by 2100 due to climate change, higher than the global average of about 7% (World Bank, 2021).

1 - South Asia includes eight countries - Afghanistan, Bangladesh, Bhutan, India, Maldives, Nepal, Pakistan, and Sri Lanka

Nearly 60% of India's land area is prone to earthquakes of moderate to very high intensity; 12% of land is prone to floods and river erosion; 5,700km of coastline is prone to cyclones and tsunamis; 68% of the cultivable land is vulnerable to drought; hilly areas are at risk from landslides and avalanches; and 15% of landmass is susceptible to landslides (*World Bank, 2021, p. 66*).

Climate change benefits and addressing Greenhouse Gas (GHG) emissions can be concurrently achieved while pursuing clean air targets. Tangible outcomes such as lower fatalities and improved air quality help strategize targeted interventions at source across multiple stakeholders. This can harness many other allied benefits such as better public health and higher productivity. According to the World Health Organization, 14 of the 20 most polluted cities across the G20 economies are in India and over 50% of cities studied throughout the country have critical levels of PM10 pollution. In

2017, outdoor air pollution caused around 6,70,000 premature deaths in the country, a six-fold increase since 2000 (*World Bank, 2021, p. 68*). Air pollution generated by burning fossil fuels is attributed to 4.5 million premature deaths worldwide every year, over 1 million occurring in South Asia in 2018 (*World Bank, 2021, p. 7*). Among the South Asia Region (SAR) countries, India has the highest share of Global GHG emissions (7.1%) of which 72% is generated by the energy sector (*World Bank, 2021, p. 5*).

Hence, in addition to climate risks, communities are increasingly exposed to the dangers of air pollution due to increasing traffic congestion, unregulated construction activities and mismanaged solid waste. Further, these risks impact different communities in variable degrees. Vulnerable communities, informal settlement dwellers living in weak structures with poor access to services, or in areas with poor vegetation or open spaces remain more exposed or sensitive to risks and adverse health impacts.

1.3 Climate & Air Pollution Risks and Vulnerability Assessment

WRI's spatial vulnerability assessment framework therefore focuses on analyzing climate risk and air pollution trends in the city, and understanding differential vulnerabilities based on socio-economic aspects and access to infrastructure or essential services. It is built on three aspects: i) Climate Risk Analysis – that assesses regional and local risk due to climate change and other geographic or topographic factors; ii) Socio-Economic Analysis – that assesses demographic distribution in the city using the Government of India Census 2011 data at census ward and city-district levels; and iii) Accessibility Analysis – that assesses the distribution of services and amenities in the city to identify underserved areas and neighborhoods that are more disadvantaged during extreme weather events and disasters. By highlighting the differential vulnerabilities, the objective of this assessment is to assist city decision makers to target specific actions, spatially, temporally and for specific communities.

The vulnerability assessment includes a summary of these three aspects, where each aspect is framed by a set of indicators and parameters. Each subsection includes a description of the aspect, with a summary of the indicators. Indicators are described by their definition and a rationale for why these were selected. The definition alludes to the various parameters identified for the assessment, and the rationale broadly relates each indicator with aspects of exposure and sensitivity that create (or worsen) conditions of vulnerability. Next, each indicator is introduced by describing the various parameters assessed, with a table listing the parameters, their direct or inverse relationship to vulnerability (defined as positive or negative respectively), methods used and data sources. Following this, key analysis and findings are included to present the overall trends for each indicator. Additional analyses, maps and correlations are included as references in the annexure.

Figure 2: Framework of Vulnerability Assessment Illustrating the Three Aspects and Respective Parameters

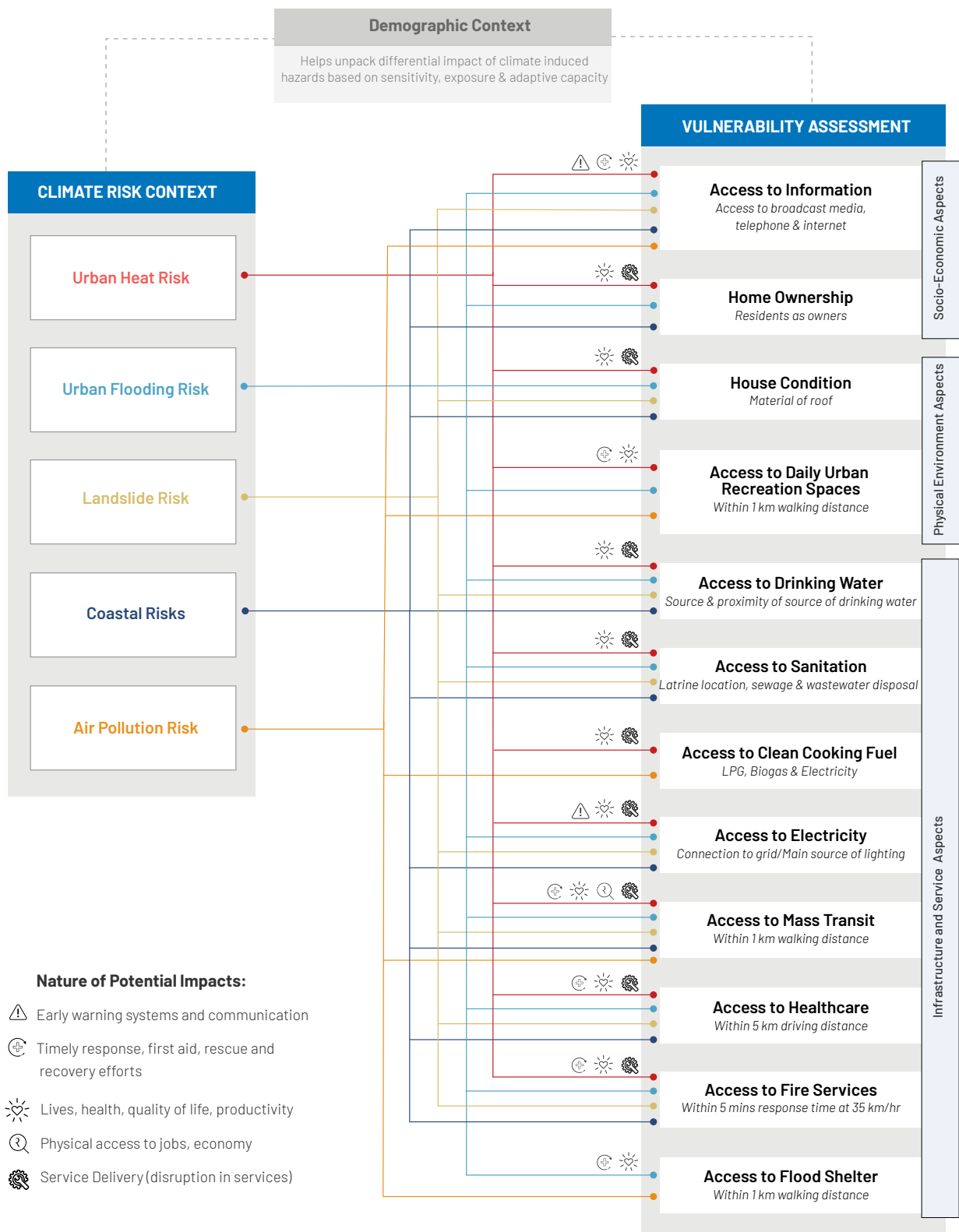




Image Credit: Jensie De Gheest




Chapter 2:



Climate Risk Context

The Climate & Air Pollution Risk Context analysis is an attempt to understand risk exposure in different areas of Mumbai city using monitored weather data from sources like the Indian Meteorological Department (IMD), BMC’s Automatic Weather Sta-

tion (AWS), data from air quality stations, coastal data from the Indian National Center for Ocean Information Services (INCOIS) and satellite imagery for various parameters. Five indicators are being assessed for the climate risk context of Mumbai city as described in Table 1.

Table 1 | Climate Risk Context Indicators

Indicator	Definition	Rationale for Selection
 <p>Urban Heat Risk</p>	<p>Urban heat risk is defined by three parameters – temperature trend, extreme heat events and spatial heat exposure – to identify areas in the city that are more vulnerable.</p>	<p>Annual temperature trends establish overall heat exposure, which is experienced differentially based on heat island effect, and socio-economic and demographic differences within neighborhoods.</p> <ul style="list-style-type: none"> • Exposure: Heat stress is further exacerbated based on housing type, indoor light and ventilation, building material, and extent of humidity creating pockets of heat traps. • Sensitivity: Poor communities living in poorly ventilated, dense housing types, with compromised access to essential services like affordable cooling options, remain most sensitive.
 <p>Urban Flooding Risk</p>	<p>Urban flooding risk is defined by analyzing two parameters – extreme rainfall events (ERE) and flood risk determined by overlaying waterlogging hotspots with the city’s stormwater drainage network and flood shelters – to determine the spatial variation of waterlogging and flooding across the city.</p>	<p>Conditions of waterlogging and flooding in cities affect infrastructure, property, and personal assets (to the least), and lives, livelihoods, and public health concerns at large.</p> <ul style="list-style-type: none"> • Exposure: Flood risk is experienced differentially across the city. Low-lying areas are more exposed to frequent water logging and experience flooding during every ERE. • Sensitivity: Poor communities, living in informal housing, are more sensitive during ERE and incur frequent losses (lives, livelihoods, assets and health).
 <p>Landslide Risk</p>	<p>Landslide risk is defined by the number of landslides (frequency) that determine ‘landslide prone’ areas in the city. These areas are most vulnerable during ERE.</p>	<p>Prolonged rainfall, instability of soil structure, geological conditions and slope failure increase the frequency of landslides.</p> <ul style="list-style-type: none"> • Exposure: Communities found living in/near landslide prone areas are more exposed. • Sensitivity: Several informal settlements live in landslide prone areas, making them more sensitive than those living in formal housing.

Indicator	Definition	Rationale for Selection
 <p data-bbox="256 483 363 551">Coastal Risks</p>	<p data-bbox="469 271 746 674">Coastal risks are defined by four parameters – storm surge and tidal variation, sea surface temperature (SST) patterns, coastline change, and mangrove area assessment – to identify the threats posed to coastal margins of the city.</p>	<p data-bbox="831 271 1465 412">Increase in sea surface temperature contributes to intensification of cyclones and storms, compounding the coastal erosion/sedimentation causing damage to entire coastal ecosystem.</p> <ul data-bbox="831 421 1465 748" style="list-style-type: none"> • Exposure: Limited knowledge on extent of damage caused by extreme waves and winds can aggravate loss of life and property, primarily for those situated in the immediate vicinity of the city’s coastline. • Sensitivity: Natural variability of coast makes it challenging to determine impact of any external stimuli. Therefore, the risk for communities dependent on sea/mangroves for their livelihood make them more sensitive to any changes in the coastline behavior.
 <p data-bbox="220 1059 384 1126">Air Pollution Risk</p>	<p data-bbox="469 837 746 1317">Air pollution risk is defined by two parameters – air pollutant concentration over 10 years, and air pollutant hotspot analysis – to determine the temporality and spatial concentration of different air pollutants, including PM2.5, PM10, Nitrogen Dioxide (NO₂), Sulphur Dioxide (SO₂), Carbon Monoxide (CO) and Ammonia (NH₃).</p>	<p data-bbox="831 837 1417 972">Areas of high concentration of air pollutants in the city are more vulnerable; spatial variability of different pollutants leads to different interventions to improve air quality.</p> <ul data-bbox="831 981 1417 1218" style="list-style-type: none"> • Exposure: Those living or working in close proximity to polluting sources are more exposed. • Sensitivity: Socio-economic factors such as housing condition, i.e., poor ventilation, use of non-LPG cooking fuel, or occupation i.e., transport operators, traffic police, construction labor etc. determine greater sensitivity.



Urban Heat Risk

ASSESSMENT

The assessment of urban heat risk is done by analyzing non-spatial and spatial parameters (Table 2). Non-spatial parameters include air temperature, relative humidity, and heat index (a combination of air temperature and dewpoint temperature), using IMD data between 1973-2020, from the Santacruz monitoring station. Annual, seasonal and monthly

trends of these parameters were analyzed to demonstrate an overall trend of increasing temperatures. The spatial analysis of heat risk uses Land Surface Temperature (LST)² data from LandSat 8 (USGS) that helps identify local areas more exposed to heat stress, also known as Heat Island Effect³.

CONTRIBUTIVE PARAMETERS

Table 2 | Urban Heat Risk – Assessment Parameters and Attributes

Parameter	Vulnerability	Methods Used	Data Source
1. Temperature Trend Analysis	Positive relation	Annual air temperature anomalies, annual and monthly timeseries for air temperature, and change-point detection	IMD station data for Mumbai, Santacruz station between 1973 and 2020
2. Extreme Heat Events	Positive relation	<ul style="list-style-type: none"> Inter-annual heat index trend between 1973 and 2020 Heatwaves based on the departure or deviation from the normal air temperature 	
3. Land Surface Temperature Anaysis	Positive relation	Comparison with land use type, roofing material, and vegetation index	LandSat 8 (USGS), October 2017 - 2019

KEY FINDINGS

1. Temperature Trend Analysis

It presents an overall warming trend for Mumbai city across 47 years. This section includes find-

ings from annual, seasonal, monthly and hourly air temperature timeseries.

1A. Annual Air Temperature Anomalies¹

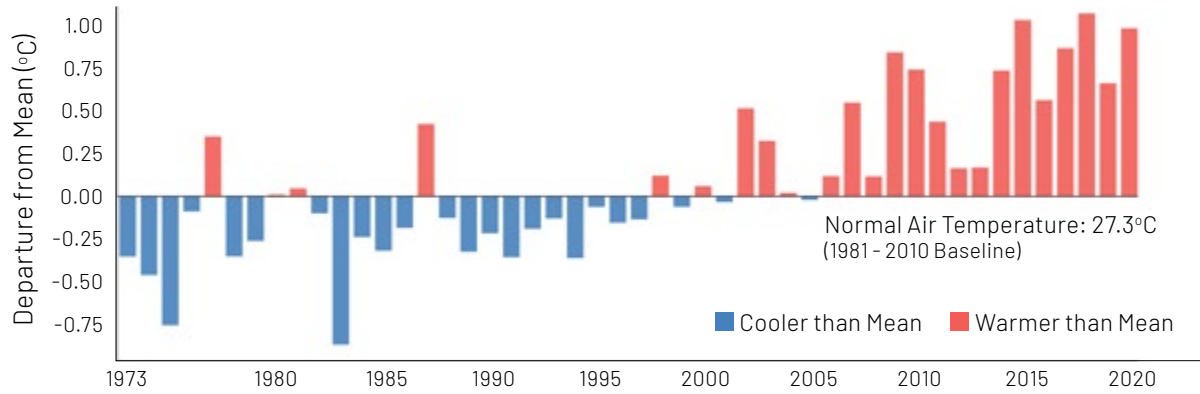
Increase in frequency of warmer years observed, with three out of the last five years showing a departure of more than 1°C from the baseline average air temperature (1973-2020). Between 1973 and 2020, 24 years were warmer than the

baseline average air temperature (27.3°C). Except for 1999, 2001 and 2005, every year post-1998 has been a warm year with 2015, 2018, and 2020 being the warmest (departure of above 1°C) on record as shown in Figure 3.

2 - LST is the radiative skin temperature of the land derived from solar radiation. LST measures the emission of thermal radiance from the land surface where the incoming solar energy interacts with and heats the ground, or the surface of the canopy in vegetated areas. Land Surface Temperature. Science Direct. Elsevier. www.sciencedirect.com/topics/earth-and-planetary-sciences/land-surface-temperature

3 - Heat islands are urbanized areas that experience higher temperatures than outlying areas. Structures such as buildings, roads, and other infrastructure absorb and re-emit the sun's heat more than natural landscapes such as forests and water bodies. Urban areas, where these structures are highly concentrated and greenery is limited, become "islands" of higher temperatures relative to outlying areas. Heat islands can contribute to a range of environmental, energy, economic, and human health effects. Heat Island Effect, Learn About Heat Islands. United States Environmental Protection Agency. www.epa.gov/heatislands/learn-about-heat-islands

Figure 3 | Annual Air Temperature Anomalies between 1973 and 2020

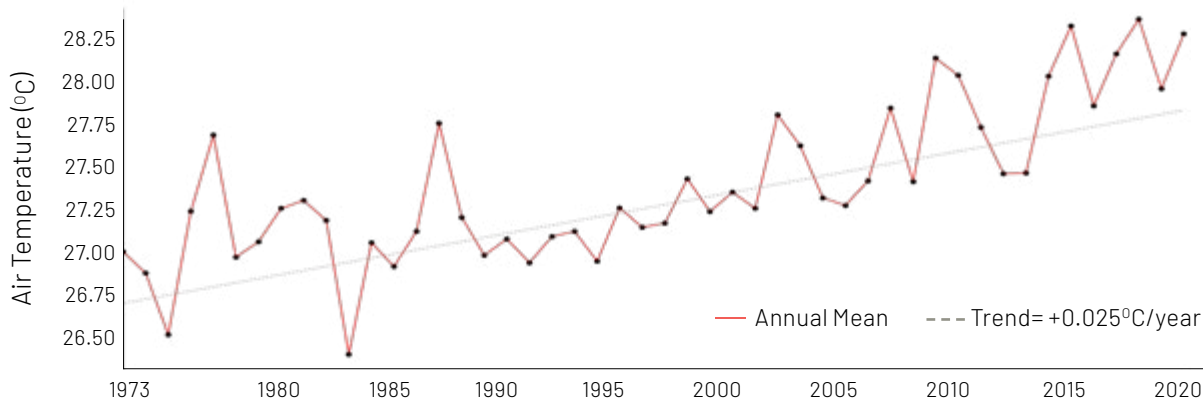


1B. Trend Analysisⁱ

Increasing trend of annual air temperatures observed with 0.25°C rise per decade between 1973 and 2020. The overall air temperature trend highlights warming related to global climate change, whereas the trend of increase in late evening and night-time temperature (Korade & Dhorde, 2016) points to a much more localized phenomenon

associated with city-scale urbanization and development. The long-term trends of increasing night-time and evening temperatures correspond well with the concept of urban expansion, whereas the rise in post-monsoon and winter temperature trends point to the post-monsoon heat phenomenon.

Figure 4 | Inter-annual Air Temperature Trend between 1973 and 2020

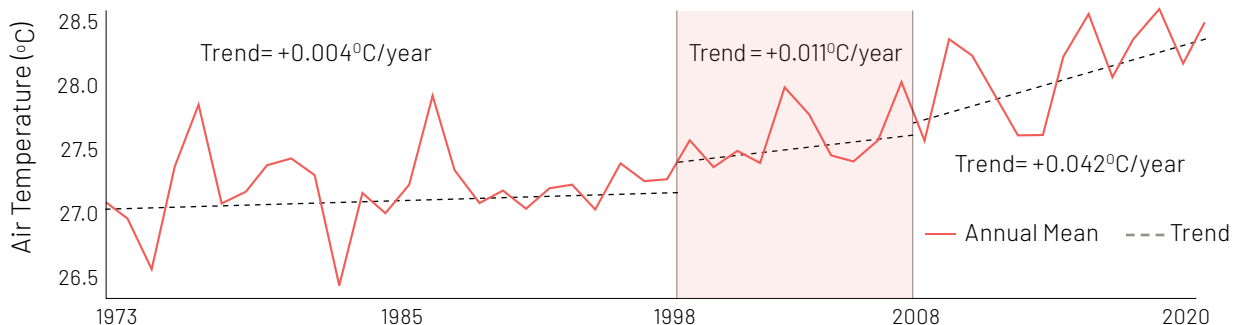


1C. Change Point Detectionⁱⁱⁱ

Change-point analysis indicates that air temperature timeseries exhibit a statistically significant shift in

trend between mid-to-late-1990s and early-2000s as shown in Figure 5.

Figure 5 | Statistically Significant Shift in Mean Annual Air Temperature Based on Change-point Analysis between 1973 and 2020



Source for Figures 3, 4, 5: Meteorological data from IMD Santacruz station

2. Extreme Heat Events

These are identified as instances when the recorded temperature is beyond the threshold for heat waves as defined by the IMD or global standards for maximum human adaptive capacity of 35°C^{IV}. For coastal areas exposed to higher relative humidity, annual

heat index trends help determine the impact of temperature and humidity on the human body. This section includes findings from annual ‘heat index’ analysis and frequency of heatwaves per year.

2A. Heat Index Classification^V

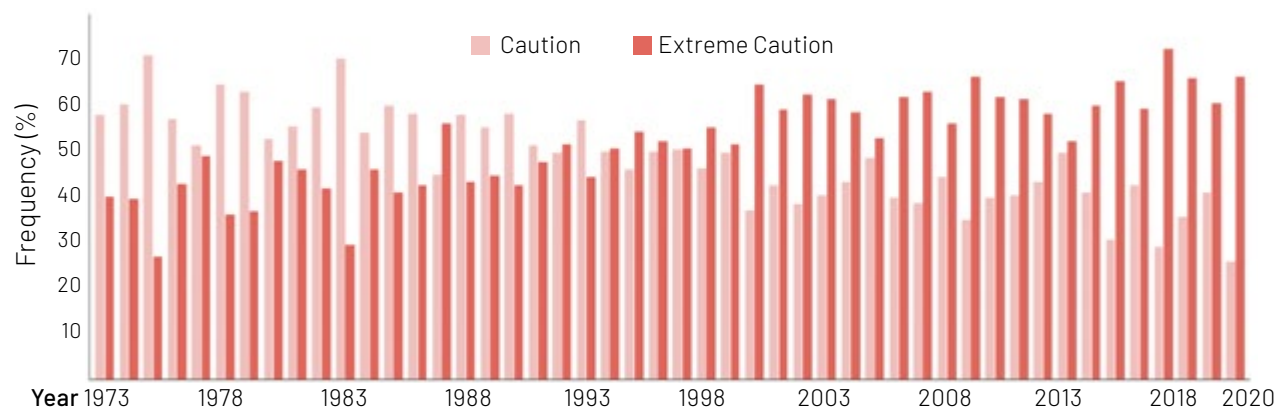
Since the mid-nineties, a transition from caution to extreme caution events has been observed with over 200 days annually classified as extreme caution events.

Heat Index classification takes into consideration both the air temperature and relative humidity and provides an indication of how warm the human body feels. As the moisture content in the air (relative humidity) increases, the capacity of a human body to cool down via evaporation of perspiration decreases. If the air temperature and relative humidity increase, heat index too increases. The heat index or the apparent/felt temperature for the IMD station in Santacruz, Mumbai falls under two categories – caution and extreme caution⁴ – based

on National Weather Service (NWS) classification (Figure 6).

The inter-annual heat index trend shows that number of days under caution category have declined at roughly the same rate as the number of days with extreme caution have increased over the years. This likely indicates a transition from caution to extreme caution. Several factors, including urbanization and a warming trend observed in the post-monsoon months could have triggered this transition over the years. Any given day is more likely to be classified as extreme caution in 2020 compared to 1973, especially in the March-May and October-November period.

Figure 6 | Inter-annual Variation in Frequency of Caution and Extreme Caution Events between 1973 & 2020



Source: WRI India; Derived using IMD meteorological data for Santacruz Station

2B. Heatwaves^{VI}

Based on IMD’s heatwave definition, between 1973 and 2020, 10 heatwaves and two extreme heatwave events were observed. The years in which a heatwave event was observed are 1977, 1981, 1985, 1989, 1995, 2005, 2009, 2013, 2014 and 2018. Extreme heatwaves were observed in 2004

and 2011. The analysis shows that from 1973-2020, more than half of the observed heatwave events (7 of the 12) have occurred in the last 15 years while one third of them have been frequently observed in the last 10 years.

4 - National Weather Service under NOAA has classified Heat Index into four categories: a) Caution (26-32°C), b) Extreme Caution (32-41°C), c) Danger (41-54°C) and d) Extreme Danger (above 54°C) to identify its differential adverse impact on human body.

3. Land Surface Temperature (LST) Analysis

The analysis is focused on mapping certain areas in the city which experience increased risk due to heat reflected from the earth's surface wherever it is in contact with sunlight. Paved surfaces like concrete terraces, metal roofs and roads reflect more heat, creating heat islands, while natural landscapes with vegetation and waterbodies absorb heat reducing the prevalent temperature. To establish the extent of risk,

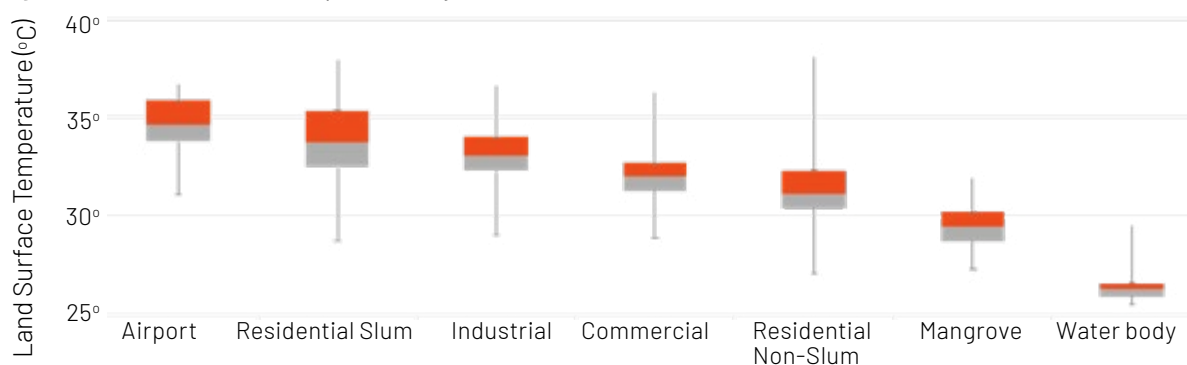
the mean LST for the month of October when temperature is comparable to extensive summer peaks including the higher relative humidity, is mapped for Mumbai city (Annexed as Figure 32 & Figure 33). Correlations with (1) land use and land cover type, (2) roofing material and, (3) vegetation cover are also assessed to understand areas that are more exposed to heat stress given their limited adaptive capacity.

3A. LST Correlations with Land Use Type

Built up surface temperatures are significantly higher with temperatures in informal settlements observed to be nearly 5°C warmer than neighboring residential areas. As per the LST map (Refer Annexure - Figure 32 & Figure 33), the areas with higher density of informal housing and severe lack of vegetation record much higher temperatures

(almost 6-8°C higher) than areas with lower slum density and high vegetation cover. Industrial and commercial land uses with large built-up footprints like the airport, industrial estates and malls have a significantly higher surface temperature than blue-green areas (forests, lakes and mangroves).

Figure 7 | Land Surface Temperature by Land Use and Land Cover in Mumbai



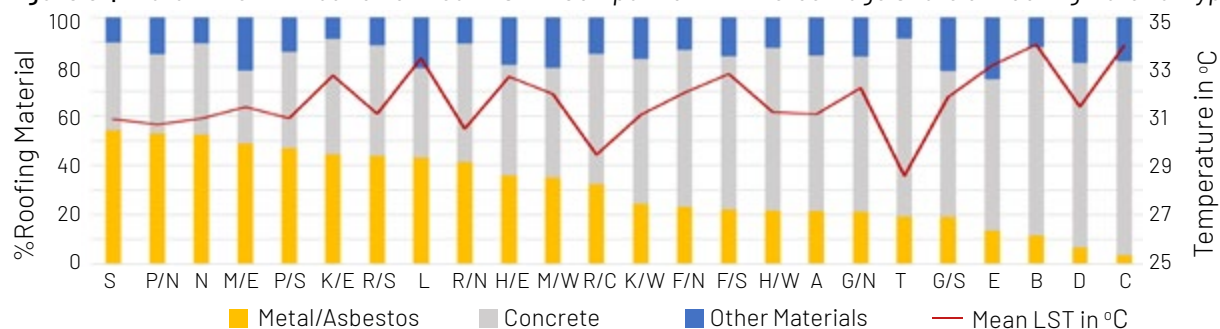
Source: WRI India; Derived using LandSat 8 (USGS) for October month between 2017 and 2019

3B. LST Correlations with Roofing Material

Surface temperatures vary with the type of roofing material as higher temperature trends are observed with metal/asbestos roofing in the low-income housing and industrial areas. Wards with higher density of slum housing or industrial warehouses,

have higher average LST. These wards are majorly located in the central and northern parts of the city. Wards with a fewer presence of metal and asbestos roofed structures have moderate to low LST and are mostly located in the southern parts of the city.

Figure 8 | Ward-wise Distribution of Mean LST in Comparison with Percentage Share of Roofing Material Type



Source: WRI India; Census 2011; LandSat 8 (USGS) for October month between 2017 and 2019

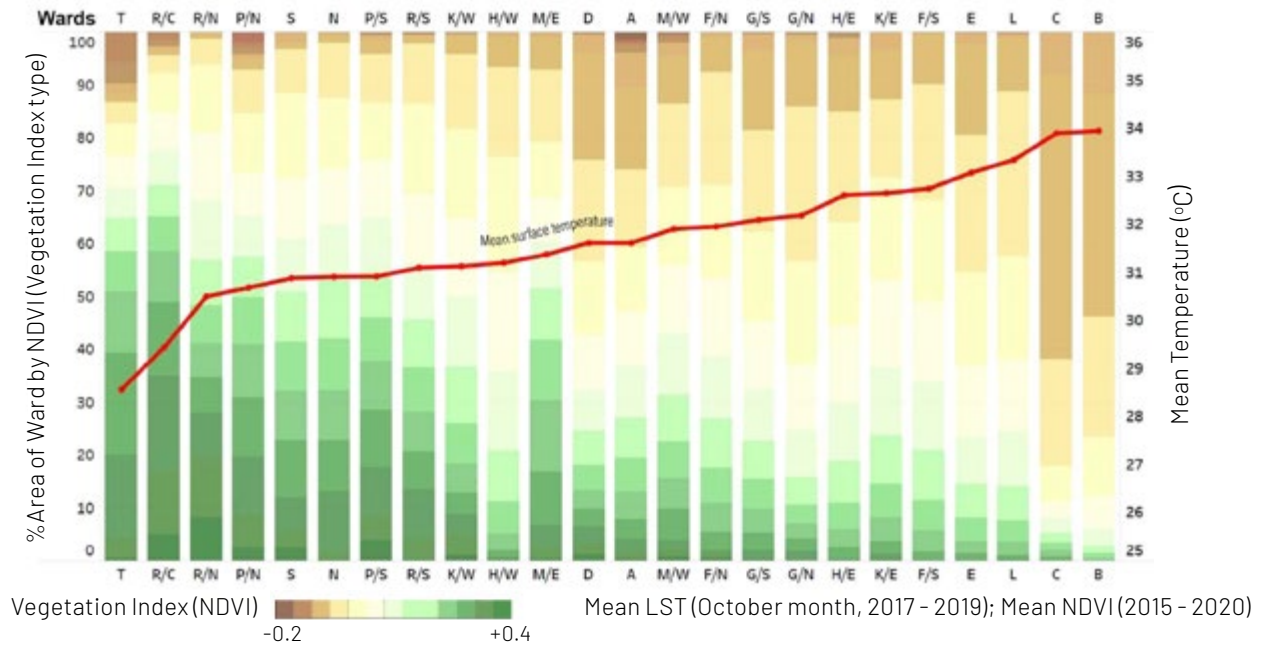


3C. LST Correlations with Vegetation Index

Surface temperatures indicate a negative relationship with green cover (NDVI), with higher temperatures observed in areas with lower green cover. Wards and areas in the north, north-western and eastern parts of the city with higher vegetation

index, (around +0.4) have a comparatively lower LST, while wards and areas in Central Mumbai and some parts of South Mumbai with a lower vegetation index (around -0.2) have a comparatively higher land surface temperature.

Figure 9 | Ward-wise Distribution of Mean LST in Comparison with Mean NDVI Share (% Area)



Source: WRI India; Modified Copernicus Sentinel Data between 2015 and 2020; LandSat 8 (USGS) for October month between 2017 and 2019





Urban Flooding Risk

ASSESSMENT

The assessment of urban flooding risk is based on analyzing two parameters: extreme rainfall events and flood risk (mapped spatially) described in Table 3. Extreme rainfall events (ERE) analysis is carried out using precipitation data from BMC’s automatic weather stations to assess the interannual variation of these events, their intensity, and spatial concentrations in the city over a 10-year period.

The analysis is based on the timeseries data of the June-July-August (JJA) months based on data from 37 stations. The flood risk analysis is done based on three data points from BMC’s disaster management department: waterlogging/flooding hotspots data⁵, flood shelters and the spatial coverage of the city’s storm water drainage network. This assessment helps identify areas most prone to flooding and waterlogging that need attention.

CONTRIBUTIVE PARAMETERS

Table 3 | Urban Flooding Risk – Assessment Parameters and Attributes

Parameter	Vulnerability	Methods Used	Data Source
1. Extreme Rainfall Events	Positive relation	Ten-year time series to measure the frequency, intensity, & duration of Extreme Rainfall Events(ERE)	BMC’s AWS data between 2011 and 2020
2. Flood Risk Analysis	Positive relation	Overlaying three geospatial data points to determine vulnerability to flood risk: <ul style="list-style-type: none"> • BMC’s flooding and waterlogging hotspots • BMC’s flood shelter locations • Spatial coverage of the storm water drainage (SWD) network within BMC boundaries 	LandSat 8 (USGS), October 2017 - 2019

KEY FINDINGS

1. Extreme Rainfall Events (ERE)

The criteria used for classification of an ERE is based on the intensity of daily accumulated rainfall. Intensity is used to determine the probability of a single rainfall event that can overwhelm the drainage capability of hydraulic structures in a particular locality. IMD’s classification scheme for 24-hour (daily) accumulated rainfall intensity is used to study ERE from three categories – heavy, very heavy, and extremely heavy rainfall events (IMD, 2021). Most ERE are expected to be one-off events which

last only a day. The lifetime of an ERE is important from the perspective of disaster preparedness. For example, a very heavy rainfall event that lasts for four consecutive days is more likely to result in flooding than a one-off extremely heavy event. The duration of an ERE is studied on five different time intervals – an event that lasts only a single day, or consecutively for two, three, four and five days. Figure 10 details cumulative counts of ERE reported at all 37 stations in Mumbai between 2011 and 2020.

5 - Flood hotspots include roughly last three years (2018-2020) of geolocated coordinates capturing the complaints by the residents and observations made on site by the ward officers where frequent waterlogging or flooding have been reported as per BMC records.



Figure 10 | Duration of Extreme Rainfall Events

Category/Duration	1 Day	2 Days	3 Days	4 Days	5 Days
Heavy	2,203	291	47	7	1
Very Heavy	2,006	311	77	21	8
Extremely Heavy	1,385	281	74	4	0

1A. Intensity of Extreme Events^{vii}

Based on daily rainfall timeseries data from 37 stations over the last 10 years, Mumbai experiences, on average, six heavy (64.5 – 115.5 mm), five very heavy (115.6 – 204.4 mm), and four extremely heavy (> 204.5 mm) rain events per year. Each year, around 9.5%, 8.7%, and 5.8% of all monsoon rainfall is classified as heavy, very heavy,

and extremely heavy, respectively. (Figure 11). The four-year period between 2017 and 2020 has seen a steady increase in the extremely heavy rainfall events. Spatially, most ERE tend to occur as localized clusters in central and western areas like Worli-Dadar, Kurla and Andheri (Figure 12).

Figure 11 | Frequency of Extreme Rainfall Events (ERE) between 2011 and 2020

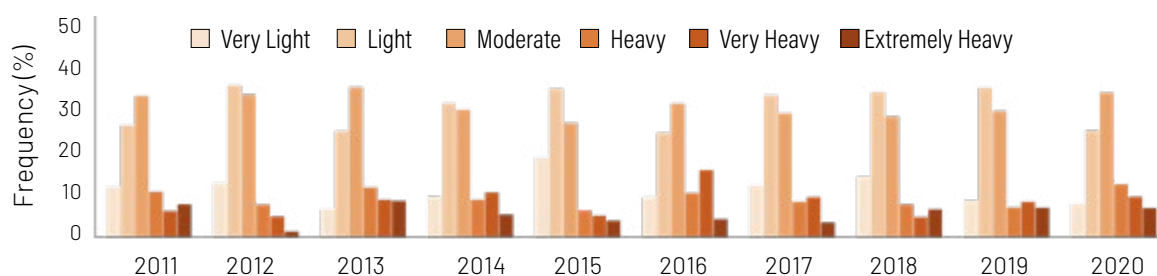
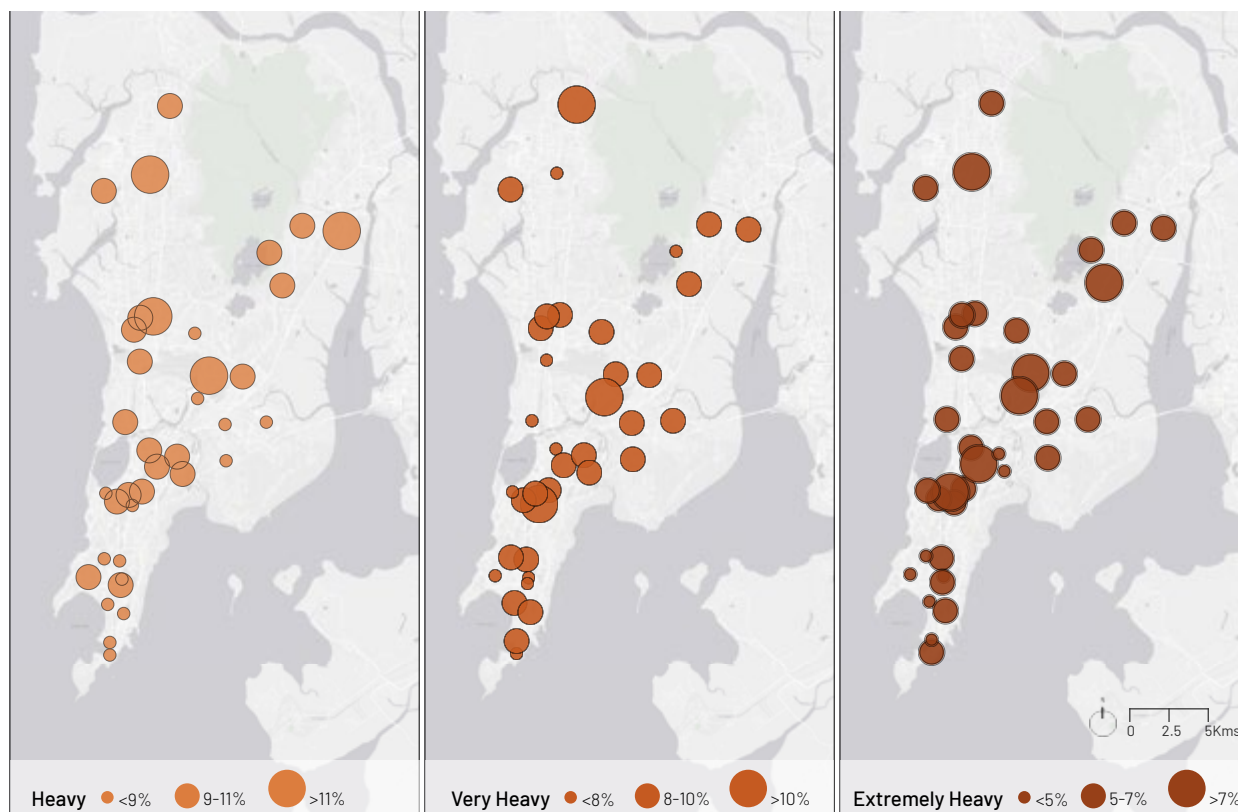


Figure 12 | Inter-annual Spatial Variation in Frequency of Different Rainfall Events between 2011 and 2020



Source for Figures 10, 11, 12: Rain gauge data from BMC AWS Network

1B. Duration of Extreme Rainfall Events

Analysis shows that most ERE tend to last only a single day (Figure 10). But 14% of all heavy ERE in the last decade were not one-off events. Similarly,

17% of very heavy, and 21% of extremely heavy ERE lasted more than a day.

2. Flood Risk Analysis

This parameter is used to spatialise the flood risk. Correlating flooding hotspots with flood shelter locations and informal settlements, differential impact can be identified. Evaluating the stormwater

drainage network in relation with the topography, built landscape and surface material helps understand the drainage condition and surface runoff scenario.

2A. Flooding Hotspots

A relatively higher concentration of flooding hotspots, based on waterlogging/ flooding data from BMC, in South and Central Mumbai can be observed. Overlaying these hotspot locations with informal settlements helps us identify overlapping

risks and vulnerable communities to streamline action on ground. Within BMC, 31.3% area of informal settlements is at risk of floods as it is within a 250m buffer of these flooding hotspots (Refer Annexure Figure 37).

2B. Flood Shelters

A considerable number of flood shelters are available, corresponding to the locations of flooding hotspots. Similar to the distribution pattern of flooding hotspots, flood shelters are also present throughout the city, with highest concentrations in the central and southern portions, in areas around Dadar, Byculla, Girgaum Chowpatty and Grant Road. They are also located to the north and northeast, around Bandra, Ghatkopar, Andheri, Mulund and Borivali.

Flood shelters are available in the vicinity of slums and informal settlements, except for a few locations to the northwest and northeast areas around Mankhurd. Considering a walkable distance of 1km, 76% of BMC's population has access to these shelters. However, this access may effectively reduce during a flood event⁶ to 46.5% (Refer to Chapter 4: Vulnerability Assessment - 12. Access to Flood Shelters and Figure 62 in the Annexure for details).

2C. Stormwater Drainage (SWD) Network Coverage

According to currently available data, the areas in the north, northwestern and central parts of the city appear to have a relatively sparse network compared to its south (Refer Annexure Figure 35).

For a comprehensive assessment on efficacy of the SWD network, a thorough carrying capacity report⁷ of the latest network in place is required.

6 - Primary assumption for the analysis reinforces the observed facts that heavy downpour mostly inundates and blocks vehicular and pedestrian access. For this purpose, immediate 250m from BMC's flood/ waterlogging hotspots has been considered as the area at risk.

7 - Carrying capacity of SWD network must be synced with the natural contours and the landcover/ landscape and determined based on land use and built density. Data regarding condition of drains is useful to determine temporal conditions such as silting and choking of drains. This enables effective planning of actions pre-monsoon to avoid frequent water logging. Data on outfall conditions is critical to determine drainage patterns. Studying the drainage network with surface treatment and material will offer opportunities to improve percolation and creation of retention ponds to reduce and slow down the surface runoff.



Landslide Risk

ASSESSMENT

The analysis comprises assessment of locations of the landslide prone areas within Mumbai in terms of their spatial distribution and proximity to slum

settlements that are more vulnerable to loss of lives and assets.

CONTRIBUTIVE PARAMETERS

Table 4 | Landslide Risk - Assessment Parameters and Attributes

Parameter	Vulnerability	Methods Used	Data Source
Landslide Prone Areas	Positive relation	<ul style="list-style-type: none"> Spatial mapping of landslide prone areas Correlation of landslide prone areas with distribution of slum settlements 	Geolocations of landslides observed - BMC, Disaster Management Department

KEY FINDINGS

Landslide Prone Areas

These areas, mostly the foothills in case of Mumbai, have loose soil/ rock, extreme slope, and instable tectonic conditions, making them further vulnerable to any hydro-geological hazard. During heavy rain-

fall, foothills, and consequently informal settlements along unstable slopes or at the foothills, tend to be at the risk of landslides due to saturation with water and their limited adaptive capacity.

Spatial Mapping of Landslide Prone Hotspots

Figure 36 in the Annexure shows areas marked as hotspots or most vulnerable to landslides, based on BMC data. These include locations observed

to have instable soil structure and geological conditions, and prone to slope failure during routine assessments.

Overlaying Landslide Prone Areas with Informal Settlements

The informal settlements⁸ located along the slopes of the hills/hillocks or foothill regions are prone to landslide events. . These are mostly located towards the north, near Borivali and western flanks of the Sanjay Gandhi National Park, and to the northeastern part of the city, near Mulund and Kanjurmarg, along the eastern flank of the National Park. Slums to the central part of the city, around Ghatkopar and the airport are also highly

prone to landslide events caused by sudden heavy rainfall episodes or slope failures. Pockets of slum areas near Andheri and few in the southeastern part are also affected by landslides. Largely, slum settlements across Mumbai are not affected by landslides as they are located on flat ground. Refer to Figure 36 in the Annexure for overlay of informal settlements with landslide prone locations.

8- Derived from BMC's Land use and other maps in the Development Plan 2034



Coastal Risks

ASSESSMENT

Coastal risk assessment in Mumbai involves examining sea surface temperature patterns along with the measurements from tidal gauges to investigate temporal patterns in tides and short-term effects such as storm surges. Analyzing storm surges are critical as a heated sea surface can create more cyclonic storms

as well as impact the city's storm water drainage system's ability to move water due to the increased sea height. Coastal risk assessment also includes long term coastline change analysis at different tidal phases (1990 - 2020) and the transformation in mangrove areas that act as natural cushions against violent storm surges.

CONTRIBUTIVE PARAMETERS

Table 5 | Coastal Risks - Assessment Parameters and Attributes

Parameter	Vulnerability	Methods Used	Data Source
1. Sea Surface Temperature Pattern	Positive relation	Trend analysis of annual average Sea Surface Temperature (SST) - Day and Nighttime	MODIS - AQUA Sea Surface Temperature Data Annual Average Year 2003-2020
2. Storm Surge and Tidal Variation	Positive relation	<ul style="list-style-type: none"> Trend analysis of annual sea level variation Maximum sea level variation during the active storm period 	<ul style="list-style-type: none"> Astronomical tidal motion, INCOIS Radar tide gauge data from JNPT Port (2011-2021) Preliminary reports & meteorological information related to all cyclone events by the Cyclonic Weather Division, IMD (2011- updated till June 2021)
3. Mangrove Area Assessment	Positive relation	Spatio-temporal analysis of mangrove cover loss & regeneration	LandSat 5, LandSat 8 (USGS) Year 2008-2010 and 2018-2021
4. Coastline Change	Positive relation	Examination of erosion and deposition, emergence and submergence of the coastline using satellite imagery	LandSat 5, LandSat 8 (USGS) Year 1990 and 2020

KEY FINDINGS

1. Sea Surface Temperature Pattern

Sea Surface Temperature (SST) is an important physical property which impacts biological processes, flora and fauna in coastal regions. SST is one of the key factors in the formation of tropical cyclones (TC), with a requirement of at least 26°C (Dare & John, 2011) for TC to develop. While various factors are required for TC development, SST is widely considered as a leading factor for examining the TC climatology, especially the maximum intensity that a TC can attain

in a given environment (Thanh, Cuong, Hien, & Kieu, 2019). As established by several researches, the Arabian Sea's surface temperature is observed to have increased (Kumari, Jayappa, Thomas, & Gupta, 2021), (Bharti, et al., 2020), and (Nandkeolyar, Raman, Kiran, & Ajai, 2013) in the last two decades. This can also be a tentative cause for the increase in cyclone events in the Arabian Sea (Refer to Storm Surge and Tidal Variation Analysis section).

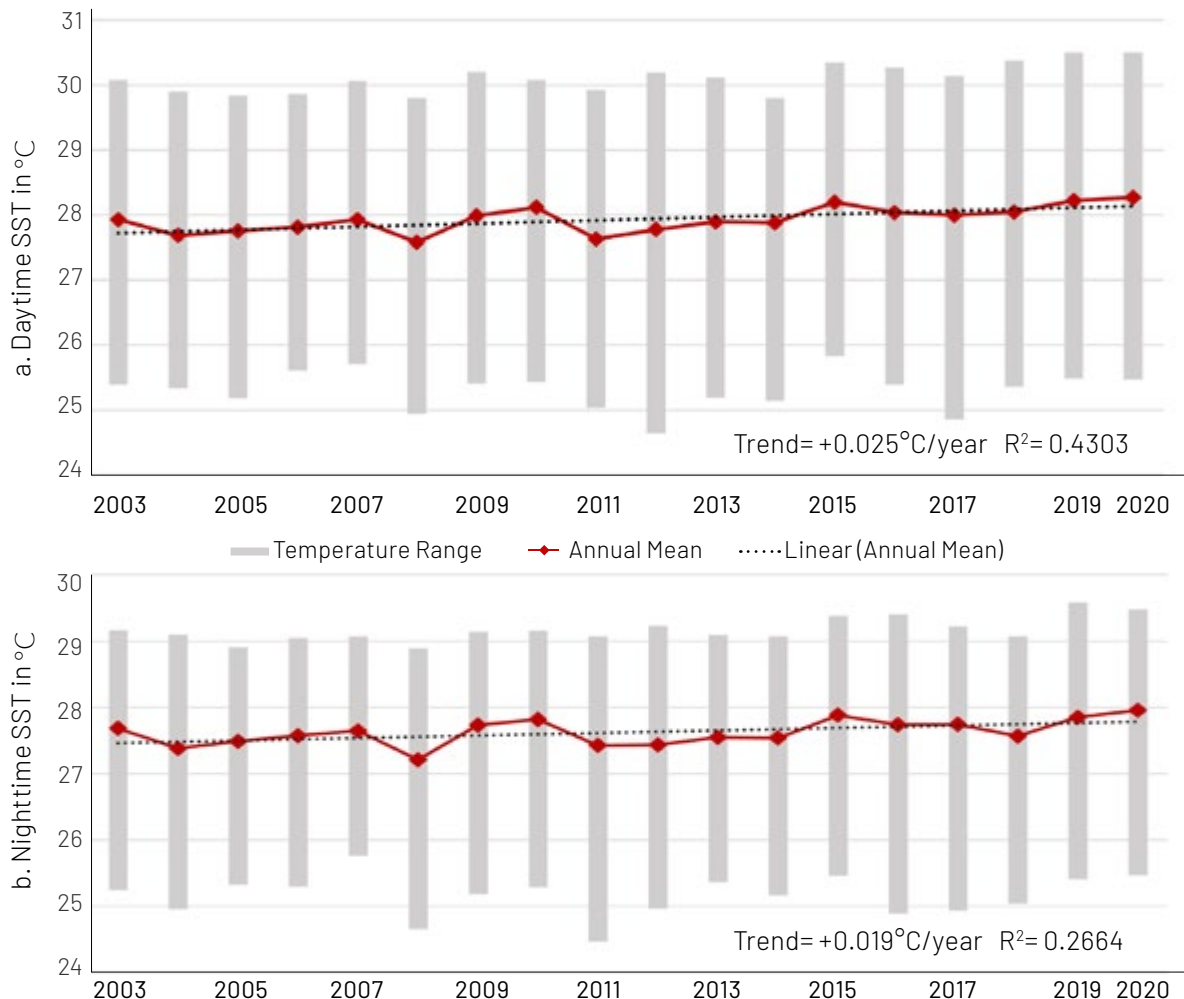


1A. Annual Mean Sea Surface Temperature^{VIII}

A slight steady increase of 0.025°C per year for Daytime SST and 0.019°C per year for Nighttime SST can be observed as illustrated in Figure 13. The analysis of annual average SST demonstrates the varying range (difference between minimum and maximum observed)

of SST across all the grid points in the entire Arabian Sea. (Refer to the methodology in the Endnote VIII for details). For both daytime and nighttime, between 2003 and 2020, there is an absence of a statistically significant trend in sea level variations.

Figure 13 | (a) Daytime (b) Nighttime, Average Annual Sea Surface Temperature between 2003 and 2020



Source: WRI India; MODIS - AQUA Sea Surface Temperature Data (LPDAAC - NASA), Annual Average 2003 - 2020

2. Storm Surge and Tidal Variation

The objectives of this analysis include estimation and comparison of annual trend of sea level variations from radar and float sensors, and examination of sea level variations caused by storm surge events. The analysis is conducted using tide height data recorded only from radar and float sensors due to gaps in pressure sensor data. Storm surge events

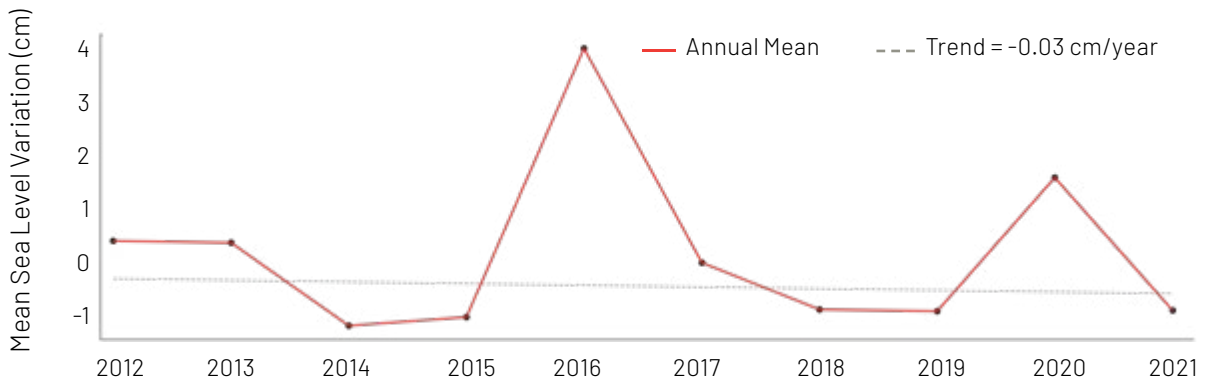
that coincide with high tides result in high sea level variations. A storm surge event results in an exceptional rise of water level due to the impact of strong winds associated with a storm. During this period when the storm is active, the maximum sea level variation is used as an indicator of the amount of sea level change or surge due to the storm event.

2A. Annual Trend Analysis of Sea Level Variation^{ix}

Analysis of annual sea level trend estimated for the period between 2012 and 2021 shows

an absence of a statistically significant trend in sea level variations.

Figure 14 | Annual Sea Level Trends from Radar Tide Gauge Sensor between 2012 and 2021



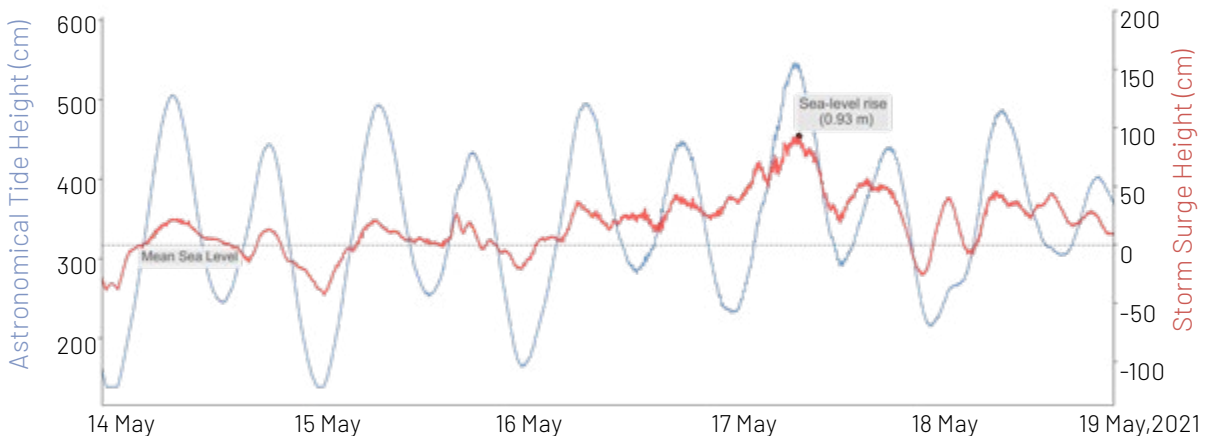
Source: WRI India; INCOIS Radar tide gauge data from JNPT Port

2B. Sea Level Variation during the Active Storm Period*

The year 2019 saw the highest number of cyclones in the region. Storm surge events that coincide with high tide formation are more likely to contribute to higher sea level increase. This is highlighted by Cyclone Kyarr-2019 and Cyclone Tauktae-2021 (refer to the detailed results in the Endnote X), both

of which reached their highest potential during a high tide. Figure 15 illustrates the sea level rise associated with Cyclone Tauktae at 0.93m. According to the IMD, between 2011 and 2021 (updated till June), Mumbai and other areas along the Arabian Sea were subjected to 18 storm events.

Figure 15 | Storm Surge associated with Cyclone Tauktae, May 2021



Source: WRI India; INCOIS Radar Tide Gauge Data from JNPT Port

3. Mangrove Area Assessment^{XI}

There is a significant transformation of mangroves since the year 2008, with most of the mangrove cover increasing which can be attributed to the efforts made by the state forest department (Prasad, Prasad, & Dutt, 2010) to protect the mangrove areas. Thane Creek, as observed in Figure 17 in the Coastline Change section, has been shrinking due to expansion of mangroves towards the north and east⁹ due to siltation. However, the

analysis is limited to BMC boundary and does not include the east or north of the creek. Based on satellite imagery analysis of BMC area (not including Thane creek), from the year 2008 to 2021, 325 ha of dense mangrove cover changed to sparse mangrove cover or has been converted to intertidal mudflats due to excessive erosion and sedimentation as illustrated in the Figure 16; and for around 305 ha of mangroves the density has increased.

9 - The reports suggest, in Thane, the land under mangroves has increased by 0.7 km² and in Mumbai suburbs by 0.3 km² (Tol, 2019).

Figure 16 | Mumbai Mangrove Area Assessment, Year 2008-2010 vs 2018-2021



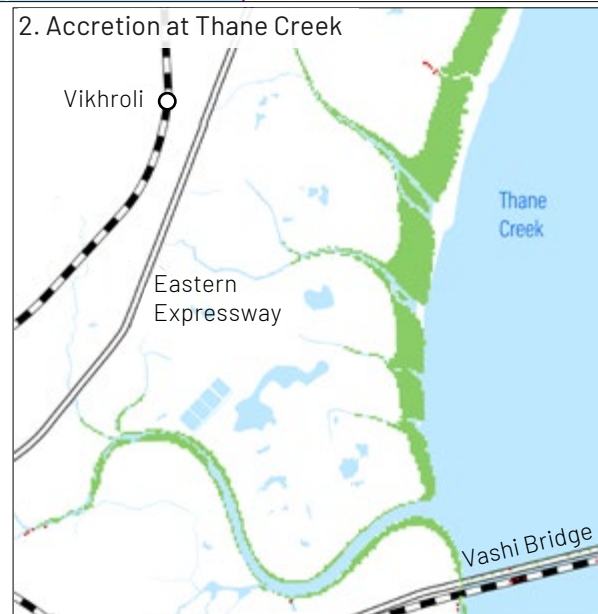
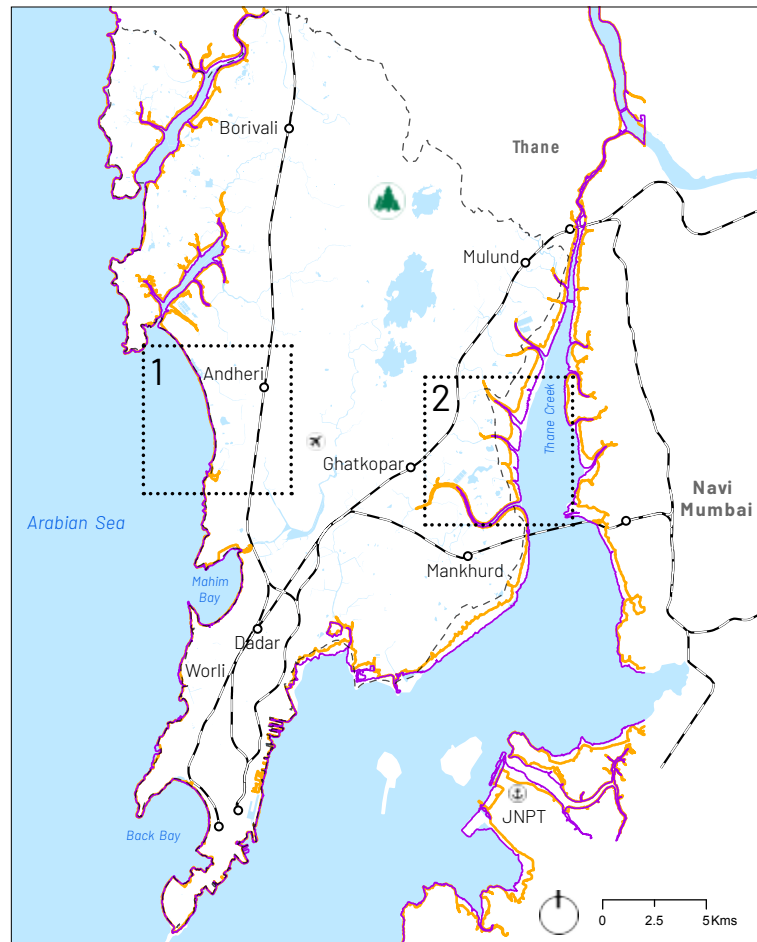
- | | | | |
|--|---|---|--|
| ■ Increased Mangrove Density | BMC Boundary | Railway Line | ✈ Airport |
| ■ Decreased Mangrove Density | 🌳 National Park | ○ Station | ⚓ Sea Port |

Source: WRI India; LandSat 5 & LandSat 8(USGS) for years 2008, 2010, 2018, 2021

4. Coastline Change^{XII}

The coastline comparison between the years 1990 and 2020 shows that the Thane Creek on the eastern side has been shrinking as also observed by the Mangrove and Marine Biodiversity Conservation Foundation of Maharashtra (2021). The creek is converting into mudflats and mangroves in the last three decades – more than 14 km² of coastline has seen mud deposition. On the western side, there are certain cases of extension of land into the sea through land reclamations (ex: Bandra). The overall coastline in Southern Mumbai has not changed much because of the presence of tetrapods¹⁰, stone blocks which comprise the sea wall as demonstrated in Figure 17. However, along the northwestern coast, which is not protected, or in areas with no cases of reclamation, the sea has been eroding and accreting. Even in the northwestern side of Mumbai, the creeks led by Malad Creek are shrinking due to extension of mangroves and flats like that of Thane Creek.

Figure 17 | Mumbai Coastline Change, Year 1990 vs 2020



- Coastline 1990
- Coastline 2020
- Coastline Accretion
- Coastline Erosion

- Highway
- Railway Line
- Airport
- Sea Port
- Station

Source: WRI India; LandSat 5 & LandSat 8 (USGS)

10 - The total length of the sea wall at Mumbai is about 3340 m and is protected by tetrapods and stones in some reaches. Central Water and Power Research Station, Pune. <http://cwprs.gov.in/WriteReadData/file/coastal-opn-others/MARINE%20DRIVE%20SEA%20WALL.pdf>



Air Pollution Risk

ASSESSMENT

The air pollution risk assessment includes a temporal analysis of the concentration of various air pollutants and hotspot analysis based on data received from BMC, CAAQMS and SAFAR monitoring stations along with satellite imagery. The pollutants assessed include Particulate Matter (PM_{2.5} and PM₁₀), Nitrogen Dioxide (NO₂), Sulphur Dioxide (SO₂), Carbon Monoxide (CO) and Ammonia (NH₃) with reference to their individual permissible limits as per National Ambient Air Quality (NAAQ) Standards prescribed by CPCB listed in Table 6. Analyzing the indoor air pollution scenario for the entire city is also part of the detailed assessment. Figure A.3^{xiii} in the endnotes illustrates spatial distribution of air pollution monitoring stations maintained by different agencies and the resolution of data used.

Table 6 | Annual and Daily Permissible Limits for Various Air Pollutants as per the National Ambient Air Quality (NAAQ) Standards, CPCB

Pollutants	NAAQ CPCB Permissible Limit	
	Annual	Daily
Particulate Matter (PM) 2.5	40 (µg/m ³)	60 (µg/m ³)
Particulate Matter (PM) 10	60 (µg/m ³)	100 (µg/m ³)
Nitrogen Dioxide (NO ₂)	40 (µg/m ³)	80 (µg/m ³)
Sulphur Dioxide (SO ₂)	50 (µg/m ³)	80 (µg/m ³)
Ammonia (NH ₃)	100 (µg/m ³)	400 (µg/m ³)
Carbon Monoxide (CO)	1.78 (8 hours' average)(ppm)	

The concentrations observed for PM_{2.5} in the city (refer to Figure 25 & Figure 38) make it one of the most perilous pollutants in the city predominantly generated from construction and roadside dust and marginally due to vehicular emissions. Therefore, analysis includes timeseries for monthly, daily, and hourly PM_{2.5} concentrations as illustrated in Figure 40 & Figure 41 in the Annexure. Due to the incongruent nature of data and to keep analytical coherence, the PM_{2.5} timeseries is limited to the years 2019 and 2020.

CONTRIBUTIVE PARAMETERS

Table 7 | Air Pollution Risk – Assessment, Parameters and Attributes

Parameter	Vulnerability	Methods Used	Data Source
1. Air Pollutant Concentrations	Positive relation	<ul style="list-style-type: none"> Annual averages of air pollutants across monitoring stations using SAFAR, BMC and CAAQMS data, by type of pollutant Monthly and Hourly variation of PM_{2.5} between June 2019 to May 2021 	<ul style="list-style-type: none"> SAFAR Mumbai data, July 2015 to March 2021 (Annual averages derived from Monthly data) BMC Stations data, April 2010 to March 2021 (Annual averages) CAAQMS data, May 2019 to June 2021 (hourly)

Parameter	Vulnerability	Methods Used	Data Source
2. Air Pollutant Hotspot Analysis	Positive relation	Mapping spatial concentration of critical pollutants in Mumbai based on satellite imagery analysis and SAFAR and CAAQMS data	<ul style="list-style-type: none"> • ESA Copernicus Sentinel 5P, June 2019 to May 2020 • SAFAR & CAAQMS data, June 2019 to May 2021
3. Indoor Air Pollution Analysis	Positive relation	Socio-economic analysis of cooking fuel usage by households in Mumbai correlated with secondary literature	<ul style="list-style-type: none"> • Census 2011 • National Sample Survey, 2013-2014 • Human Index Survey, 2012

KEY FINDINGS

1. Air Pollutant Concentrations

The temporal analysis of different air pollutant levels (annual averages) for Mumbai city has been carried out to assess the city level and individual monitor-

ing station variations using data from nine stations under SAFAR, seven stations under BMC and nine stations under CAAQMS, CPCB.

1A. Annual Average Concentrations of PM2.5 & PM10

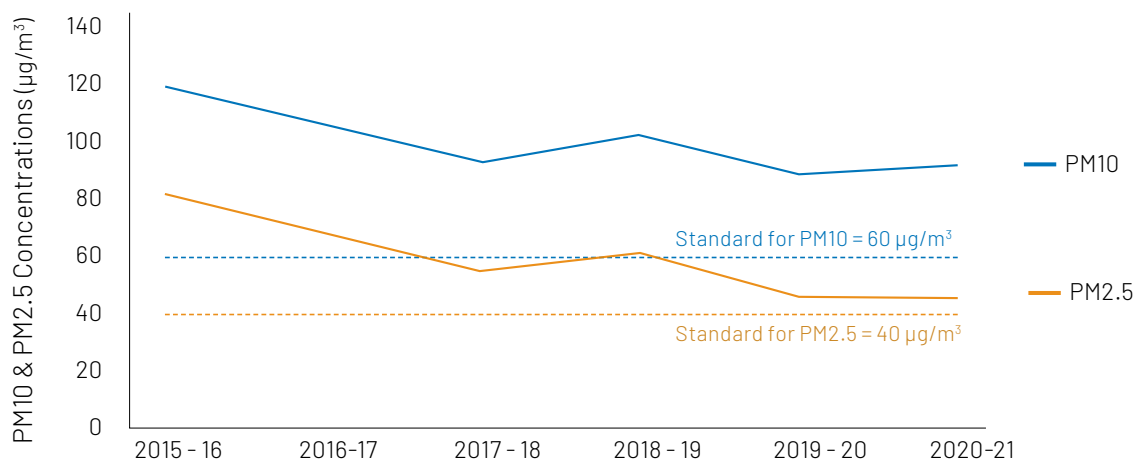
The average annual concentrations of PM2.5 and PM10 have declined over the past few years but remain above the NAAQ standards. The hazardous (Walvekar, Gurjar, & Nagpure, 2019) concentrations range from 1.5 times to twice the permissible limits between 2015 to 2019, making them critical pollutants for Mumbai city. Individual monitoring stations – Bandra Kurla Complex, followed by Mazgaon, Andheri and Malad emerge as areas

of high concentration based on SAFAR data as illustrated in Figure 38 in the Annexure.

Observations During Lockdown

In the year 2020-21, the city recorded a significantly lower annual average concentration level of PM10 at 91 $\mu\text{g}/\text{m}^3$ and PM2.5 at 46 $\mu\text{g}/\text{m}^3$ which could be attributed to the COVID-19 pandemic related lockdown and restrictions.

Figure 18 | Average Annual Concentrations of PM10 and PM2.5 from July 2015 to March 2021



Source: 9 Monitoring Stations - SAFAR, Mumbai; NAAQ Standards, CPCB

1B. Annual Average Concentrations of NO₂, SO₂ and NH₃

The consistently growing concentration levels of Nitrogen Dioxide (NO₂) attests it to be a major air pollutant, unlike Ammonia (NH₃) and Sulphur Dioxide (SO₂). NO₂ is also categorized as a lethal air pollutant which degrades air and water quality by contributing to ground-level ozone concentrations and by polluting water bodies/ coastal waters¹¹.

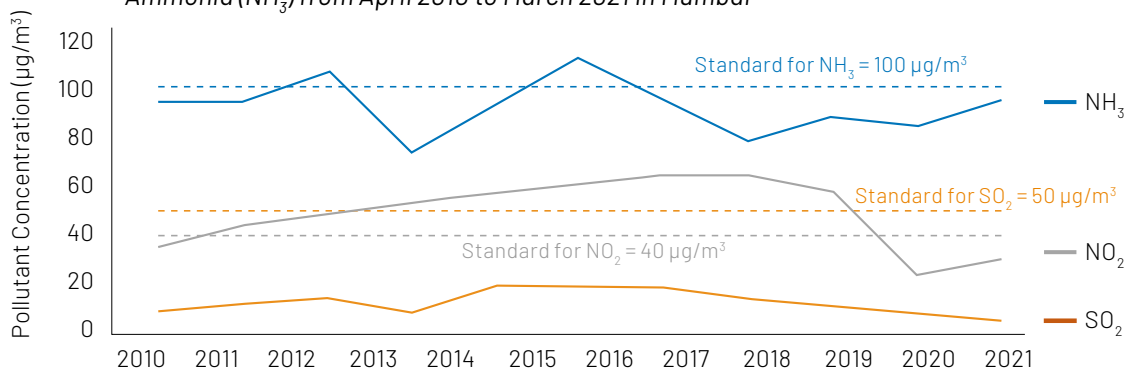
The concentration of NO₂ shows a steady rise from 35.71 µg/m³ in the year 2010 to 58.25 µg/m³ in 2018, higher than permissible limits prescribed in the NAAQ standards as shown in Figure 19, specifically in Maravli, Khar and Andheri as shown in Figure 20. The annual average concentrations of

NH₃ has remained below NAAQ permissible limits of 100 µg/m³ through most of the period from 2010 - 2021, except in 2012 and 2015 when it recorded peaks above permissible standards. The SO₂ concentrations throughout the analysis period was recorded below NAAQ permissible limits of 50 µg/m³.

Observations during Lockdown

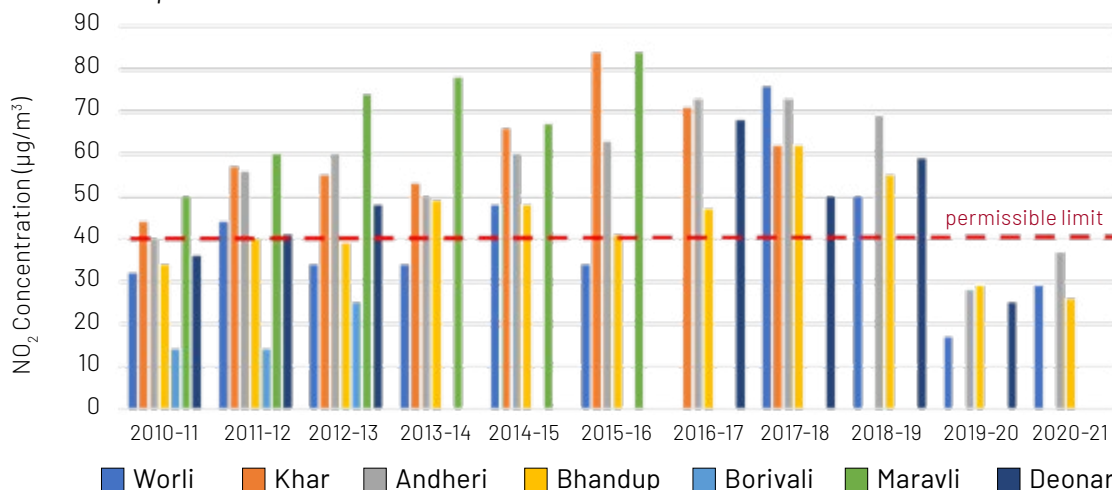
Similar to PM10 and PM2.5, the year 2020 has seen relatively lesser concentrations of all three aforementioned air pollutants, probably owing to the lockdown curbs.

Figure 19 | Annual Average Concentrations of Sulphur Dioxide (SO₂), Nitrogen Dioxide (NO₂) and Ammonia (NH₃) from April 2010 to March 2021 in Mumbai



Source: 7 BMC monitoring stations, Mumbai; NAAQ Standards, CPCB

Figure 20 | Station-wise Annual Average Concentrations of NO₂ at Fixed Monitoring Stations from April 2010 to March 2021



Source: SAFAR; NAAQ Standards, CPCB

11 - Nitrogen dioxide is soluble in water, reddish-brown in colour, and a strong oxidant. NO₂ results from combustion processes such as those used for heating, transport and power generation. Exposure to nitrogen dioxide can irritate airways and aggravate respiratory diseases. NO₂ is an important ozone precursor, a pollutant closely linked to asthma and other respiratory conditions. (World Health Organisation. Air Quality and Health, type of pollutants, 2021. <https://www.who.int/teams/environment-climate-change-and-health/air-quality-and-health/health-impacts/types-of-pollutants>)

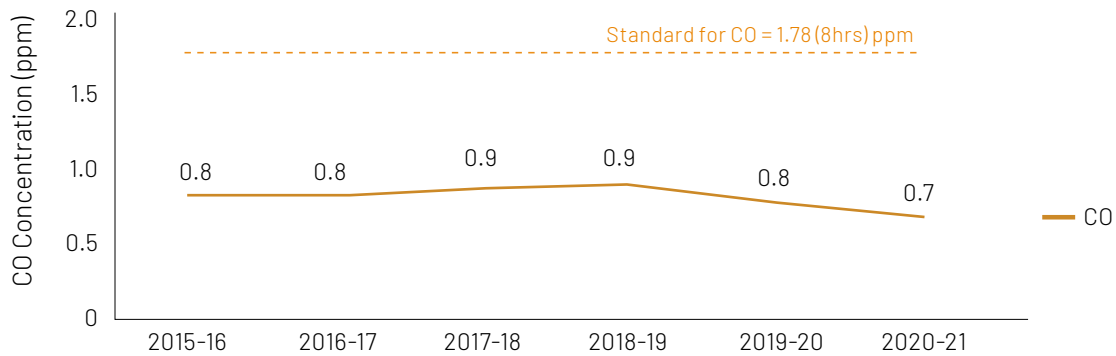
1C. Concentration of Carbon Monoxide (CO)

The average annual concentration of Carbon Monoxide (CO) in Mumbai is nearly half of the NAAQ permissible limits across all years. Thus, CO is not one of the major pollutants for Mumbai.

Observations During Lockdown

CO levels have remained roughly constant with a slight decrease in 2019 and 2020, probably influenced by the COVID-19 induced lockdown.

Figure 21 | Annual Average Concentrations of Carbon Monoxide (CO) in Mumbai from July 2015 to March 2021



Source: 9 Monitoring stations, SAFAR, Mumbai; NAAQ Standards, CPCB

1D. Monthly, Weekly and Hourly Variation of PM2.5

The monthly and hourly variations¹² in PM2.5 have been computed using hourly mean PM2.5 data recorded at the nine CAAQMS monitoring stations in Mumbai from June 2019 to May 2021. Monthly variation using mean weekday and weekend data of PM2.5 concentrations has been derived using daily averages for PM2.5 as shown in the Annexure Figure 40 & Figure 41. For hourly season-wise comparison, 3D timeseries using hourly average through each month has been shown in Figure 23 below. The analysis demonstrates the following:

- How the concentration of the pollutant differs by season (month of the year), and by hour of day – i.e.

peak and off-peak hours.

- Interlinkages of these concentrations with different activities during the day, week, and festivals, etc. affect the pollutant concentration. Variation in pollutant levels can also be observed through pre and post pandemic-induced lockdown¹³ when traffic congestion and other activities were at a minimum.

- The two stations – Bandra and Colaba – are selected as indicative cases of different areas in the city (from Mumbai City district to Mumbai Suburban) to compare and understand varying city-wide concentration levels based on land use type.

Monthly Variations

Higher concentrations of PM2.5 were observed during the winter months than the rest of the year, and relatively lower concentrations during the monsoon. The concentration of PM2.5 starts increasing post monsoon (September) and continues

to be high till February, in both pre-lockdown and post-lockdown phases¹³ as shown in the 2D time series, Figure 40 and Figure 41, in the annexures.

12 - Hourly-monthly 3D timeseries for PM2.5 is represented by mean PM2.5 concentration for the entire month. Therefore, all the data gaps, i.e., the daily averages that are reflected as gaps in the 2D timeseries is well accounted in the 3D timeseries. Both 2D and 3D timeseries for PM2.5 are to be read in tandem to understand the variations.

13 - PM2.5 concentrations at various resolutions between (pre-lockdown) June 2019 – May 2020 vs (post-lockdown) June 2020 – May 2021

Weekly Variations

As shown in Figure 40 and Figure 41 in the annexures, at most stations the maximum daily mean concentration for both weekdays and weekends ranges from 120-180 $\mu\text{g}/\text{m}^3$ for a major part of the analysis period (June 2019 to May 2021), which is almost two to three times higher than the daily permissible limit. This is except in Colaba where the weekday and weekend peaks have reached as high as 600 $\mu\text{g}/\text{m}^3$, 10 times higher than the daily permissible limit as shown in the same 2D timeseries.

• Tentative Impact of Different Activities

On an average, based on pre and post COVID-19 lockdown scenarios, concentration of PM_{2.5} is higher on weekdays than on weekends with some winter months recording higher concentrations on weekends due to festivities in that season. Figure 22 and Figure 23 illustrate variations in

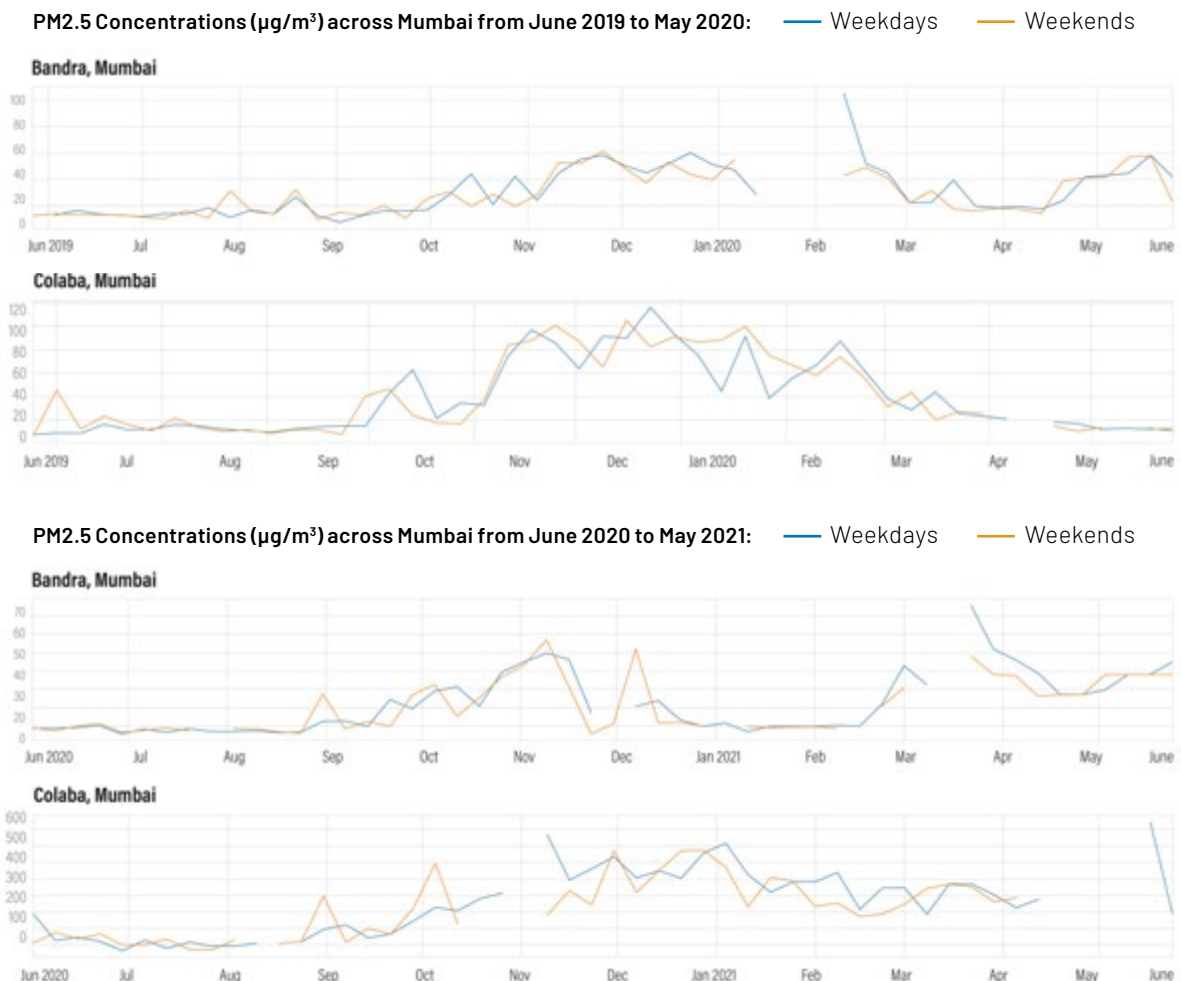
the observed PM_{2.5} concentration at Bandra and Colaba which can be attributed to their land use type. Bandra, a mixed-use residential and commercial hub, observes higher PM_{2.5} concentration compared to the evident spikes monitored at the Colaba station which is dominated by residential and service sector use.

• Observations During Lockdown

The highest average annual concentration across all stations recorded during lockdown was 100 $\mu\text{g}/\text{m}^3$ which is 2.5 times higher than permissible annual limits (refer to Figure 25 for details).

However, there are instances of a greater number of weekday and weekend spikes during September, October, December and January after the lockdown when curbs were relaxed and more outdoor activities led to an increase in road traffic.

Figure 22 | 2D Timeseries of Weekly Average Concentrations of PM_{2.5} for Bandra and Colaba Monitoring Stations from: a) June 2019 to May 2020 and b) June 2020 to May 2021



Source: 2 monitoring stations - CAAQMS; CPCB June 2019 to May 2021; NAAQ Standards, CPCB

Hourly Variation

For all the stations, during an average day, the concentration of PM_{2.5} increases after midnight, most likely due to freight movement; and during peak traffic hours from 8 am to 12 pm, and from 5 pm onwards.

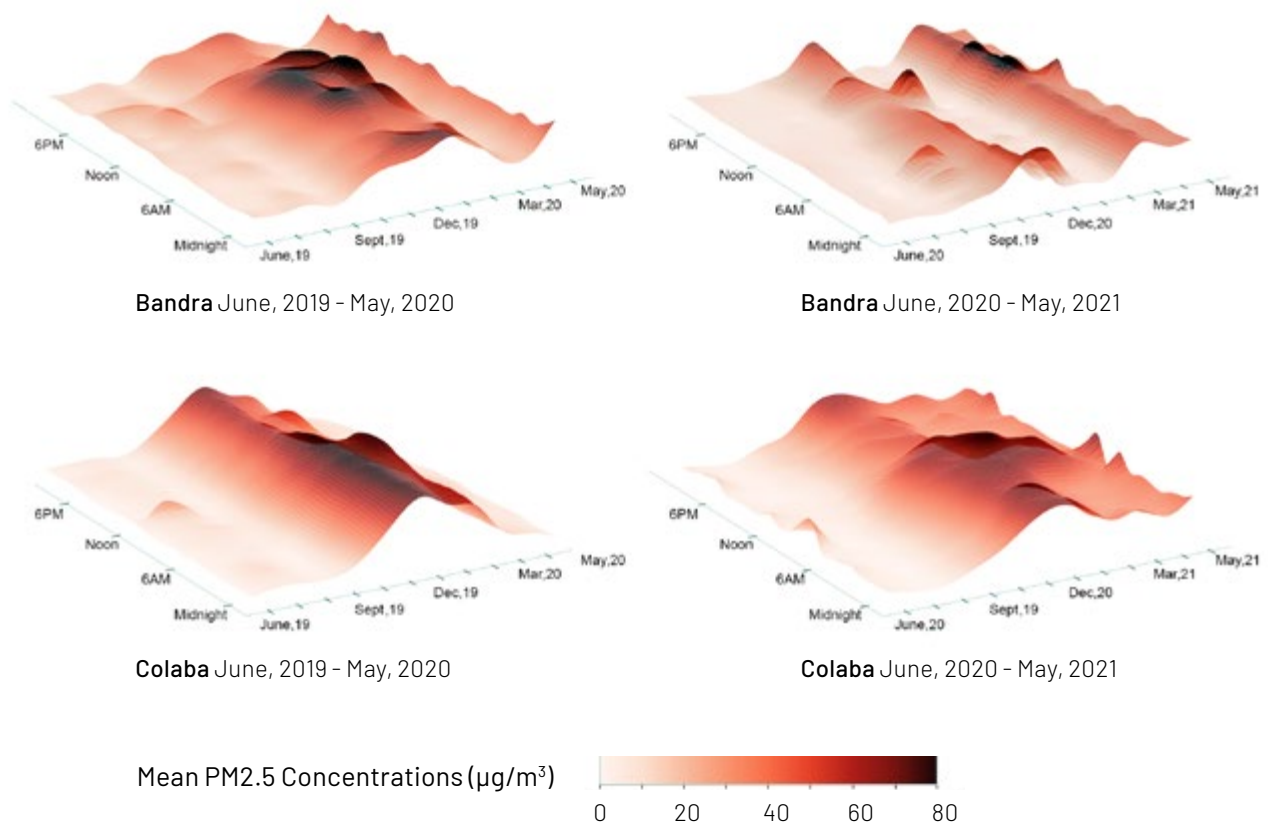
• Tentative Impact of Different Activities

As shown in Figure 23, at both Bandra and Colaba, PM_{2.5} concentrations are lower during the wee hours (between midnight and 5 am) of the day.

• Observations During Lockdown

In 2019, the overall concentration is higher during the winter months, nearly twice the permissible limits compared to 2020. Starting September 2020, with the post lockdown relaxations, a steady increase PM_{2.5} levels can also be observed till the New Year before curbs owing to the COVID-19 second wave.

Figure 23 | 3D Timeseries of Hourly Average Concentration of PM_{2.5} for Bandra and Colaba Monitoring Stations, Mumbai, June 2019 to May 2021



Note: Both hourly-monthly 3D timeseries and weekly-monthly 2D timeseries for PM_{2.5} concentrations are to be read in tandem to understand the variations in PM_{2.5} levels.

Source: 2 Monitoring Stations - CAAQMS; CPCB June 2019 to May 2021

2. Air Pollutant Hotspot Analysis

The critical hotspots of NO₂, CO and SO₂ have been identified for the period from June 2019 to May 2020 using the annual average value of Copernicus Sentinel 5P (TROPOMI) data. For PM_{2.5}, the

critical hotspots have been identified for the period from June 2019 to May 2021, using the data from CAAQMS monitoring stations.

2A. Carbon Monoxide (CO) Concentration (June 2019 to May 2020)

The concentration of CO is found mostly in two areas – around Mulund and the south-eastern belt of the city around Mankhurd. The concentration

based on vertical column density of CO ranges from 36 – 41 (millimoles/m²) in Mumbai.

2B. Nitrogen Dioxide (NO₂) Concentration (June 2019 to May 2020)

NO₂ is mostly concentrated in the central and southeastern parts of the city, near the airport and near the Deonar landfill site, industrial areas, and the Tata Power Plant, Trombay at 145 (micromoles/m²). The concentration based on vertical

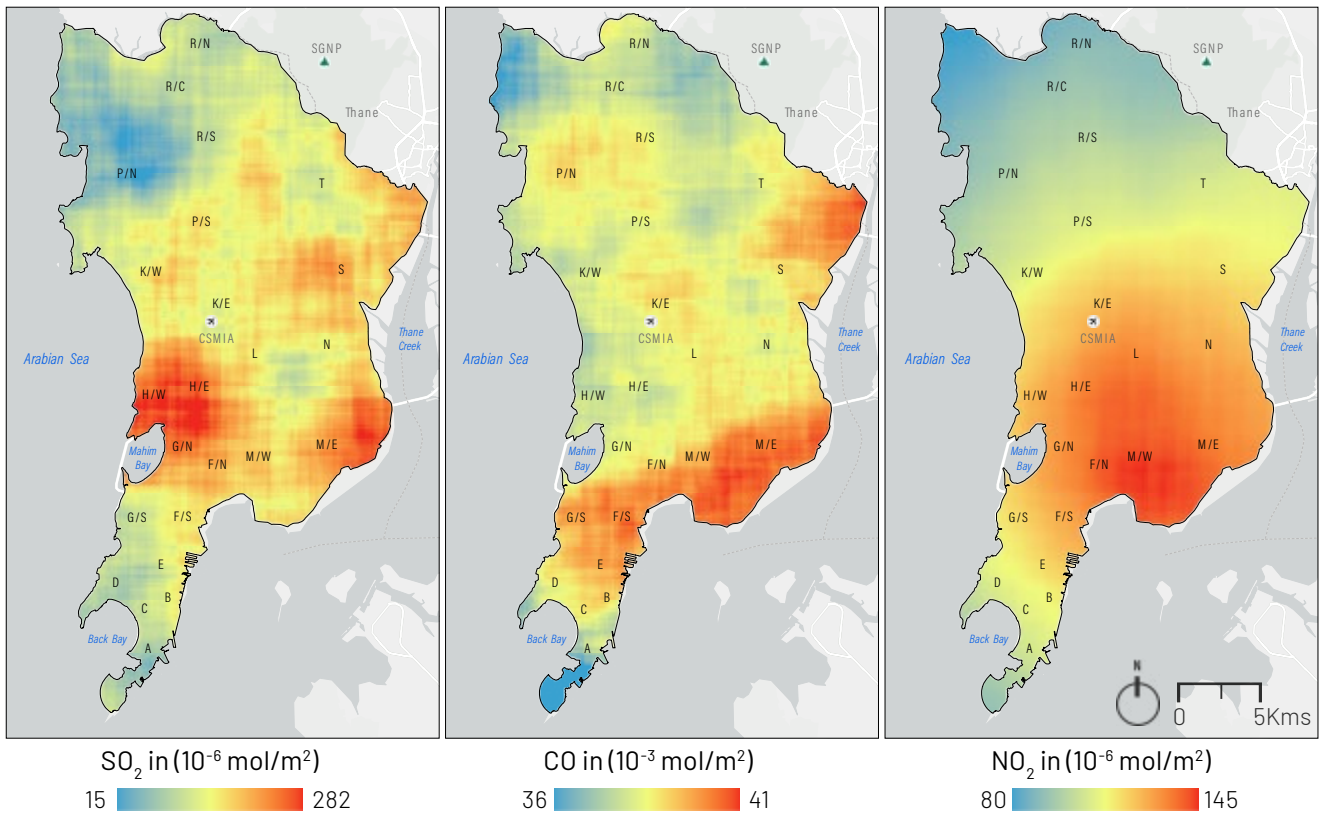
column density of NO₂ ranges from 80 – 145 (10 micromoles/m²) in Mumbai. Wards to the north and northwest have minimum concentration of NO₂ around 80 (micromoles/m²).

2C. Sulphur Dioxide (SO₂) Concentration (June 2019 to May 2020)

High concentrations of SO₂ at around 282 (10⁻⁶ mol/m²) is observed to the eastern side of the M/E Ward around Mankhurd and in H/E Ward and H/W Ward to the west. Lowest concentrations of the pollutant are found to the northwest in P/N

Ward, which primarily comprises tourism centres, and is devoid of settlements and regular traffic flow. The overall concentration based on vertical column density of SO₂ ranges from 15 – 282 (micromoles/m²) in Mumbai.

Figure 24 | Total Vertical Column Density of SO₂, CO, & NO₂ – Mean of June 2019 to May 2020



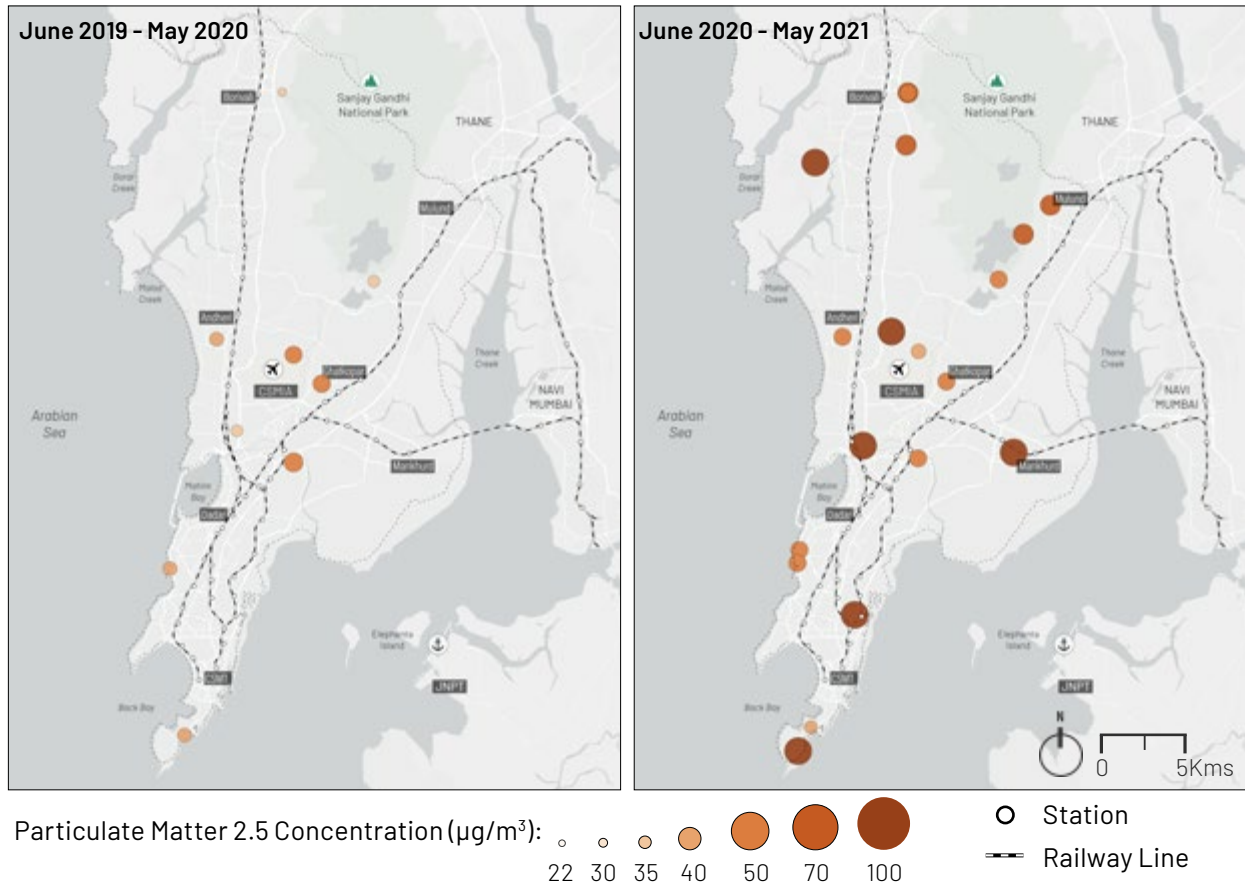
Source: WRI India using Copernicus Sentinel 5P(TROPOMI)

2D. PM_{2.5} Concentration (June 2019 to May 2020)

Major concentrations of PM_{2.5} (annual average) had been observed in the central part of the city around the airport, Kurla, Andheri and Sion where the concentration ranged between 27 - 44 µg/m³ during 2019 – just on the border of the

NAAQ permissible annual standards. In 2020, the same stations recorded average concentrations of PM_{2.5} between 22 - 100 µg/m³, nearly double the permissible annual limits.

Figure 25 | Annual Average Concentration of PM2.5 from June 2019 to May 2021



Source: 9 monitoring stations - CAAQMS, CPCB; 9 monitoring stations - SAFAR from June 2019 to May 2021

3. Indoor Air Pollutant Analysis

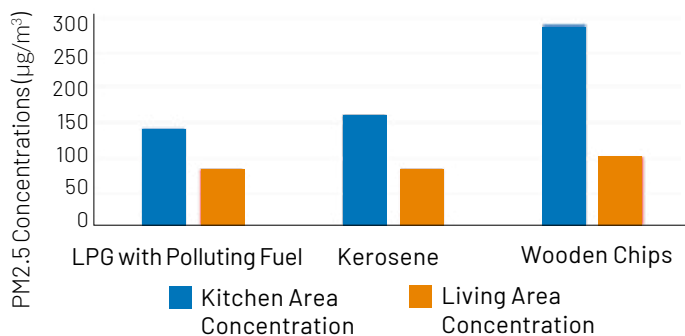
The major contributor to indoor air pollution is burning of fossil fuels, largely generated during domestic activities such as cooking and heating water.

Globally, 4.5 million premature deaths every year are attributed to exposure to the burning of fossil fuels, with over 1 million occurring in South Asia in 2018 (World Bank, 2021).

3A. Indoor Air Pollution and Cooking Fuel^{XIV}

India's Census 2011 states that firewood is consumed by only 2% of the households in Mumbai in comparison to kerosene and LPG. Refer to ward-wise access to clean cooking fuel, Figure 57 in the annexure for details. However, based on WRI analysis¹⁴ from 2021, these 2% households are exposed to maximum indoor concentration of PM2.5 from the kitchen area, which is twice the exposure of PM2.5 concentration levels from kitchens fueled by kerosene and LPG.

Figure 26 | Indoor PM2.5 Concentrations by Type of Fuel Use in Mumbai



Source: Nagpure et al., 2022

14 - Nagpure et al., 2022. The air pollution emissions and health risks associated with household cooking fuels in India.

Chapter 3:

Demographic Context

Mumbai is one of the most densely populated mega cities in the world, with a population of 12.44 million (according to Census 2011), and a population density of 28,426 persons/km². The decadal population growth rate has dropped since 1991, from 38.07% (1981) to 20.41% (1991), with a marginal increase to 20.68% (2001) and a drastic drop to 3.87% (2011). Subsequently, the percentage of slum residents in Mumbai decreased from 52.52% (2001) to 41.85% (2011), though spatial coverage of slum areas has increased according to the Census 2011 and Development Plan 2034. Population projections (based on academic research models) estimate that the Mumbai Metropolitan Region (MMR) will be the world's largest urban agglomeration by 2050, at 42.4 million people (Daniel Hoornweg & Kevin Pope, 2014).

The city's workforce largely comprises male workers. The worker participation rate in Mumbai has remained consistent since 1961 at around 35-40%,

with male worker participation at 55-61%. But female worker participation doubled from 8.81% (1961) to 16.38% (2011). Despite this, there is a large gap between the male and female workforce. According to the Census 2011, 44.2% of Mumbai's population is identified as 'migrant', of which 62.7% have come from other states, 55.8% are male, and 30.4% cite employment as their reason for migration. A recent study by the International Institute for Environment & Development (IIED) (Bharadwaj, Hazra, Reddy, Das, & Kaur, 2021) to understand and estimate climate migration studies across three states in India highlighted the fact that at least one member of the household has migrated to big cities in Maharashtra, Gujarat or the National Capital Region. A majority were males, who migrated seasonally, once or twice a year due to droughts or floods which affected their existing livelihoods, forcing them to find jobs in the informal sector in other cities. With more than 40% of Mumbai's population living in slums and about 65% employed



Image Credit: Zeber2010

in the informal sector (Bhowmik, 2010) negative impacts of climate-induced hazards are exacerbated in these vulnerable communities. This also suggests that exposure to and experience of climate risks are highly varied across the city and across different socio-economic groups.

This section presents the demographic context which can help understand the potential disproportionate effects of climate change suffered by different socio-economic groups. Mapping 'differential vulnerabilities' to climate hazard risks in the city

helps demonstrate the sensitivity of the population and the variation based on the demographic diversity and its manifestation spatially in the city. The data used for this analysis is disaggregated by gender, age, income, and social profiles, allowing city officials to map varied risks and differential vulnerabilities across neighborhoods (Rangwala, Elias-Trostmann, Burke, Wihanesta, & Chandra, 2018) to help identify the priority actions. Unpacking the socio-economic context helps understand and spatialize differing exposure levels and resilience capacities.

Table 8 | Demographic Context Indicators

Indicator	Definition	Rationale for Selection
Literacy	Literacy indicator comprises overall effective ¹⁵ literate population, effective female literate population and access to education. Educational institutions constitute an essential service, and physical access to schools have been considered based on pedestrian accessibility standards within 1 km.	Literacy is crucial for building awareness regarding climate induced hazards and building resilience capacities for preparedness, response activities during a disaster event. Higher literacy levels (with the assumption that easy access to schools offers an opportunity for improved enrolments) enable development of better adaptive capacities by enhancing the opportunity to access stable jobs thereby increasing socio-economic stability and decreasing one's sensitivity to shocks and strains. Knowledge of saving mechanisms, etc. are observed to be better in educated individuals/ families.
Gender Imbalance	Gender imbalance is calculated as sex ratio.	Disproportionate impact on women and girls with increased care-giving tasks post disaster, unequal access to resources and services, crucial role of women in disaster response.
Social Composition	Percentage of Scheduled Castes (SC) and Scheduled tribes (ST) population is estimated to understand the extent of social vulnerability on the basis of caste.	Caste also serves as an equity indicator to identify underserved neighborhood SC and ST population potentially have higher exposure, higher sensitivity and lower adaptive capacity

ASSESSMENT

The framework incorporates a range of diverse indicators related to demographic characteristics to represent complex dimensions of socio-economic vulnerability. Using Census 2011 population series

data, ward level assessment and mapping are carried out to evaluate the dynamics of literacy, gender, and social composition in the city.

15 - Based on the Census definition of 'Effective' literacy, only population aged 7 years and above is considered for this analysis. Chapter 6, "State of Literacy", Pg 99, Provisional Population Totals, Paper 1 of 2011 India Series

CONTRIBUTIVE PARAMETERS

Table 9 | Demographic Context – Assessment Parameters and Attributes

Indicator	Parameter	Methods Used	Data Source
Literacy	Effective Literacy Rate	(Total literate population aged 7 and above/Total population aged 7 and above)*100	Ward level: Census 2011 - Primary Census Abstract ¹⁶
	Effective Female Literacy Rate	(Total female literate population aged 7 and above/Total female population aged 7 and above)*100	
	Access to Educational Institutions	Population coverage computed within 1km of walking distance using service area polygons around school locations ^{xv}	Education Department BMC, Census 2011
Gender Imbalance	Sex Ratio	(Total female population)/ (Total male population)*1000	Ward level: Census 2011 - Primary Census Abstract ¹⁶
Social Composition	Percentage of SC and ST population	(Total SC population + Total ST population)/ (Total Population)*100	

KEY FINDINGS

Based on Census 2011, Greater Mumbai has the highest literacy rate (81%) and highest female literacy rate (77.7%) among all districts in MMR. While M/E Ward has the lowest effective literacy rate of nearly 83% along with the lowest effective female literacy rate at 78%, R/C Ward has the highest effective literacy of more than 93% and T Ward has the highest effective female literacy at 91.3% (Refer Annexure 1 Figure 42 and Figure 43).

At least 95.5% of Mumbai's population has access to a school within 1 km. Mumbai has 405 aided schools, 710 unaided schools and 1,136 municipal schools. Ratio of aided, unaided and municipal schools is 1:1.8:2.8. Madh, Andheri East, Mahul are some of the underserved areas with limited access to schools within 1 km (Refer Annexure 1 Figure 44).

The sex ratio in Greater Mumbai is 853, lower than the state average of 925 and the national average of 940. The lowest sex ratio of 695 is observed in C Ward in south Mumbai and Ward R/C has the highest sex ratio of 944 females to 1,000 men (Refer Annexure 1 Figure 45). Mumbai City and Mumbai Suburban district have 832 and 862 females per 1,000 males, respectively.

Data shows that city areas under the BMC have fewer persons belonging to the Scheduled Castes and Scheduled Tribes, compared to the MMR. SCs and STs constitute 7.5% of Mumbai's population. M/W Ward has the highest concentration of SCs and STs at 19% and C Ward has the lowest concentration at 1.6% (Refer Annexure 1 Figure 46).

16 - Mumbai & Mumbai Suburban, Maharashtra, Primary Census Abstract Data Tables. Office of the Registrar General & Census Commissioner, India. Census India-2011; <https://censusindia.gov.in/pca/pcadata/Houselisting-housing-Maha.html>



Image Credit: Rajas Chitnis

Chapter 4: Vulnerability Assessment


Climate-induced risks such as urban heat, flooding, landslides, and coastal risks and increasing exposure to various air pollutants in the city are jointly seen as hazards or drivers of vulnerability. Vulnerability to climate and air pollution-induced risks is carried out across three aspects: socio-economic, physical built environment, and infrastructure and services. The Figure 2 presents the interlinkages of the climate risk context to demographics of the city and the vulnerability aspects listed above.

The overall demographic context provides a background to understand how vulnerabilities are experienced differentially even within a neighborhood (that is equally exposed geographically) or a household (that is equally impacted) based on demographic differences of age, gender, occupation, education and so on. Incorporating social equity, areas with different income levels and potential exposure to information are included in the analysis under socio-economic aspect that spatializes such areas at risk of intensified climate disaster impact.

Poor living conditions such as dilapidated house condition/temporary material for roofs and wall/ limited access to amenities is a routine stress factor for many who live in underserved, informal settlements in the city. They are differentially more vulnerable to climate risks since their ability to recover from extreme events or absorb financial or life loss is substantially narrow. The physical environment aspect helps understand these varied impacts.


Self-reliant neighborhoods with access to amenities within 15-20 minutes enhances the quality of living while making a city more resilient. The aspect of infrastructure and services illustrates provision and physical access to essential services on a regular day and potentially compromised access during a disaster event. Varying levels of access to physical, infrastructural, and service contribute to contrasting adaptive capacity. When access to essential services is impacted, it makes households vulnerable for everyday functioning and impacts their ability to cope during and bounce back after a disaster. In this analysis, 'access' is limited to physical access and/or provision.

Table 10 | Vulnerability Assessment Indicators


Indicator	Definition	Vulnerability to Climate Induced Hazards
Socio-Economic Aspects		
 <p>1. Access to Information</p>	<p>This indicator is measured as a function of ownership of phone (landline, mobile and both), computer with internet, television and/or radio/transistor. Access to these assets contribute assured access to information, significantly reducing the vulnerability.</p>	<ul style="list-style-type: none"> • Ownership of information and telecommunication devices offers the opportunity to access regular live news updates, broadcast warning alerts, evacuation instructions as well as preparedness information in the event of a disaster. Information access enables awareness and better adaptive capacity, reducing vulnerability to disasters and slow onset events. • Communication with a higher percentage of population before and during such events can help authorities and communities be better prepared, efficiently manage evacuation plans and effectively carry out rescue operations.

Indicator	Definition	Vulnerability to Climate Induced Hazards
 <p>2. Home Ownership</p>	<p>Home ownership is understood based on the census data that indicates households which own the house they live in.</p>	<ul style="list-style-type: none"> • Home ownership increases one’s willingness to invest in improvements to increase safety (against increasing climate risks like heat and extreme rainfall events) and resilience of property and associated assets. • In case of other associated losses like job loss, income loss due to health impacts, and asset losses (like vehicles or electronics), having a safe living space to come back to is critical to retain a sense of social security and decreased vulnerability.
Physical Environment Aspects		
 <p>3. House Condition</p>	<p>Roof is the primary built envelope of the house with highest area exposed. House condition is defined as a function of the roofing material. Based on census categories, households with predominant roofing material which can be deemed as “Temporary”¹⁷ are considered vulnerable.</p>	<p>Housing units with temporary roofing materials are relatively exposed to a greater risk during extreme weather events such as heavy rainfall, flooding, or heat stress, due to their limited structural strength. The cost of putting together a roof may not be viable for economically weaker households, making them more vulnerable.</p>
 <p>4. Access to Daily Urban Recreation Spaces</p>	<p>Daily urban recreation spaces include public parks, sports grounds and maidans affiliated to government or private institutions such as schools. Based on the location, scale and type, these spaces serve as recreation spaces or lung spaces at a neighborhood and city level. Service radius for each type of recreation space has been defined based on capacity, scale and location, with larger areas defined for bigger city level parks (Refer to the endnote XVIII).</p>	<ul style="list-style-type: none"> • Open spaces provide much needed space for play, active health, and mental relief. • These spaces act as catchment zones during heavy rainfall events reducing the risks associated with urban flooding. Green open spaces are also crucial to reduce effects of urban heat. During disaster events, open spaces serve as grounds for evacuation, rescue and recovery. • During slow onset events like extreme summers or heat waves, well-shaded open spaces can offer poor and more exposed communities (like those living in informal settlements) essential respite from extreme indoor heat stress. Populations with limited access to open spaces are at higher risk, and more vulnerable.

17 - Following roof material types based on Census classification are considered as “Temporary” due to their limited structural strength: Grass/ Thatch/ Bamboo/ Wood/Mud etc., Plastic/ Polythene, Handmade Tiles, Stone/ Slate, and Galvanized Iron /Metal/ Asbestos sheets. etc.

Indicator	Definition	Vulnerability to Climate Induced Hazards
Infrastructure and Service Aspects		
 <p>5. Access to Drinking Water</p>	<p>Access to water distribution network is calculated as a function of source of drinking water and its proximity.</p>	<ul style="list-style-type: none"> • While source is considered as a proxy for quality of water, sources of water outside or away from premises are vulnerable to climate risks such as flooding, water logging, pollution etc. • During or after a disaster, households dependent on alternate water sources such as tankers or community taps are vulnerable since physical access via roads may be impacted. • During a heat wave or on days of extreme heat, households with limited access to piped water are vulnerable to health impacts. During times of water cuts in the city, these households do not receive tanker water or other sources, or procurement is very expensive, thereby restricting access to many. • Access to reliable and potable water is crucial for public health. Limited access to drinking water increases health hazards and exacerbates vulnerabilities during climate-induced disasters.
 <p>6. Access to Sanitation</p>	<p>Access to sanitation infrastructure and services is evaluated as a function of latrine availability, sewage disposal methods and wastewater disposal methods. Limited access has a differential gender impact, making women and children more vulnerable.</p>	<ul style="list-style-type: none"> • Latrines within the premises offer better hygiene, safety, ease of use and access for all. Households lacking this are dependent on public toilets, exposing people to health risks, and ease-of-use issues, especially for women, children, and special needs population. These conditions are exacerbated during extreme events when physical access is hindered, increasing vulnerabilities. • Unhygienic methods of sewage and wastewater disposal can pose serious health hazards, pollute surface, and groundwater, exacerbate air pollution and can worsen living conditions during climate induced hazards such as flooding.
 <p>7. Access to Clean Cooking Fuel</p>	<p>Access to cooking fuel is defined by the use of non-polluting fuels, including LPG, electricity, and biogas.</p>	<ul style="list-style-type: none"> • Several low-income households continue to rely on firewood and kerosene for cooking purposes. Use of such polluting cooking fuels increases harmful exposure and deteriorates indoor living conditions. • Indoor air pollution is as critical as outdoor air quality. Current trends of deteriorating air quality coupled with indoor air pollution increases health risk and make populations more vulnerable. Those living in smaller homes with kitchens not separated from living quarters are most at risk. • Households dependent on wood for cooking, have to travel far or depend on the limited local natural resources available. Thus, those responsible for collecting fuelwood are more exposed to outdoor climate events.

Indicator	Definition	Vulnerability to Climate Induced Hazards
 <p>8. Access to Electricity</p>	<p>Access to electricity is estimated based on the main source of lighting.</p>	<p>Electricity as a main source of lighting represents connection to a safe and stable grid. Such a metered electricity connection reduces the risks of illegal connections, and ensures ability to resume connectivity post disasters once the grid is restored. Access to electricity improves adaptive capacity of households.</p>
 <p>9. Access to Mass Transit</p>	<p>Access to mass transit network is measured by evaluating pedestrian access to mass transit stations within 1 km, which has been defined as an optimal distance for a person to access such a station by foot.</p>	<ul style="list-style-type: none"> • Access to mass transit enables access to jobs and resources which can help improve household income. Women and children have access to safe and affordable networks for better access to jobs and education, and therefore increased adaptive capacity and reduced vulnerability. • During flood events, waterlogged streets hinder physical access to mass transit stations, disrupting regular access to mobility networks, access to basic amenities and impacting livelihoods. • Populations that are dependent on mass transit to access jobs and for personal needs are deeply impacted due to loss of working hours, reduced productivity, loss of income and inability to access basic needs or health and emergency services. • Vulnerability of poor households and captive users is further exacerbated during such events.
 <p>10. Access to Healthcare</p>	<p>All public and private hospitals with in-patient facilities are considered. Access is defined as vehicular access within 5km from a health center.</p>	<ul style="list-style-type: none"> • Ensuring access to urban health amenities constitutes a basic essential service. Access to medical care is crucial to improving living standards and becomes even more critical during disaster events. Better access improves adaptive capacity by enabling timely medical assistance. • Vulnerability of population concentrations with limited access is further exacerbated during heat waves, flooding or landslides, which may lead to higher mortalities or long-term health risks.
 <p>11. Access to Fire Services</p>	<p>Access to emergency services is defined as the response time taken by emergency personnel to reach the incident location. Based on review of international best practices and feasible response times in India, standard response time developed by RMSI for urban areas in India has been considered at 5 minutes.</p>	<ul style="list-style-type: none"> • Prompt emergency services with adequate coverage across the city increases adaptive capacity and ensures timely emergency response to vulnerable areas. • Residents of high-density, informal settlements are most at risk during fire emergencies (since risk of spread is highest due to high densities) and for rescue operations during a flood or other disasters.

Indicator	Definition	Vulnerability to Climate Induced Hazards
 <p>12. Access to Flood Shelters</p>	<p>Proximity and easy pedestrian access to flood shelters is critical during flood events for timely evacuation.</p> <p>And 1 km has been identified as an optimal distance for a person to access a flood shelter by foot, especially during heavy rains and flooding events.</p>	<ul style="list-style-type: none"> • In floodprone cities such as Mumbai, access to flood shelters is pivotal to ensure safety of lives, effective evacuation and emergency response measures. Better access to flood shelters increases adaptive capacity enabling effective evacuation/ emergency response measures. • Underserved populations living away from flood shelters are more vulnerable during flood events due to compromised road access. People living in temporary structures in dense informal settlements are more vulnerable as there is a danger of the structure collapsing, giving lesser time to react.

ASSESSMENT

Provision of services at a household level and physical access to services has been evaluated for the accessibility indicators. Using Census 2011 data, ward level assessment and mapping has been carried out to evaluate provision and access to essential utility services such as water, sanitation, electricity and clean cooking fuel. Based on street network analysis, pedestrian access to services such as mass transit, education, flood relief shelters and open spaces in the city has been evaluated. Vehicular access to emergency infrastructure such as health facilities and fire stations has been computed using standard response travel times.

Census 2011 population has been appropriated to the recent built-up pixels (gridded population)¹⁸ extracted from satellite imagery to approximate population density with access and limited access. In this report, gridded population with walkable/ vehicular access to a utility/ infrastructure within defined thresholds are referred to as serviced

population (Refer to the Figure 31). In order to examine and quantify the extent of climate risk – both spatially and numerically – an overlay analysis has been incorporated in the vulnerability assessment that superimposes spatial layers of areas with climate risks. Based on inferences from Climate Risk Context Section, of the various geo-hydrological hazards, urban heat and urban floods pose an intimidating threat due to their frequent recursive occurrences in Mumbai and implications over other hazards that can cause serious infrastructure and service provision failures. Therefore, the analysis considers overlay of spatial distribution of both urban heat¹⁹ and flood risk²⁰ areas with ‘serviced and unserved population’ or ward areas with comparatively lesser access to amenities. This yields a quantifiable figure spatially located, either by number of persons at risk or ward percentage area exposed to certain climate risk, for evidence-based mitigation and adaptation measures.

18 - Based on residential built-up area in each ward, the Census 2011 pop has been apportioned and population density has been estimated at 100m spatial resolution. The socio-economic data and access to water and sanitation is from Census 2011 and the status of these indicators may have changed over the last decade.

19 - As defined by the Indian Meteorological Department (IMD) or global standards for maximum human adaptive capacity of 35°C, urban heat risk is assumed for areas with LST ≥ 35°C.

20 - Using a buffer of 250m from the flood hotspots. For details refer to Impact Analysis Section, Hazard Risk Impact Analysis, methods used for impact on services.

Socio-economic Aspects



1. Access to Information

ASSESSMENT

Using Census 2011 house listing and housing data, ward level assessment and mapping are carried out to evaluate access to assets that are crucial for preparedness, response during disaster, and relief measures post-disaster.

Given the potential change in asset ownership over the last decade and non-spatial nature of this data set, this assessment does not correlate it to any specific hazard. It used an indicative statistic with the assumption that ownership of these devices, in general, improves one's adaptive capacity to a climate induced hazard.

CONTRIBUTIVE PARAMETERS

Table 11 | Access to Information^{xvi} – Assessment, Parameters and Attributes

Parameter	Vulnerability	Methods Used	Data Source
Households owning Radio/Transistor	Negative relation	(Total households having each of the specified assets / Total households)* 100	Ward level: Census 2011 – Availability of Assets ²¹
Households Owning Landline, Mobile or Both			
Households Owning PC with Internet			
Households Owning TV			

KEY FINDINGS

Ward-wise assessment of asset ownership shows that M/E Ward has the lowest percentage of households owning Television (75.3%) and Computer with internet (7.7%) while the average in Mumbai is 85.3% and 20.1%, respectively. B Ward has the lowest percentage of households owning radio/transistor (17.5%) while the average in Mumbai is 36.2% (Refer Annexure Figure 47).

Similarly, M/E Ward has the lowest percentage of households owning landline (6.2%) and both landline and mobile (8.6%) while the average is Mumbai is 9.3% and 24%, respectively. D Ward has the lowest percentage of households owning mobiles (40.2%) while the average in Mumbai is 61.7% (Refer Annexure Figure 48).

21 - Table H-14 – Table on Houses, Household Amenities and Assets, Mumbai & Mumbai Suburban, Maharashtra. Houselisting and Housing Census. Office of the Registrar General & Census Commissioner, India. Census India-2011. https://censusindia.gov.in/2011census/HLO/HL_PCA/Houselisting-housing-Maha.html



2. Home Ownership

ASSESSMENT

Higher ownership and secure tenure increases the competency to undertake adaptation measures thereby reducing the extent of vulnerability. Using Census 2011 house listing and housing data, ward level assessment and mapping are carried out to evaluate the house ownership status in the city. This analysis is limited to house ownership, i.e., using

the Census data, and does not take into account rental policy and tenure mechanisms in the city due to their dynamic (different forms and regulations) and non-spatial nature. This metric of home ownership is examined as an indicative statistic at the ward and city level without making specific correlations to any climate induced hazard.

CONTRIBUTIVE PARAMETERS

Table 12 | Home Ownership – Assessment Parameters and Attributes

Parameter	Vulnerability	Methods Used	Data Source
Percentage of Own Houses ^{xvii}	Negative relation	(Total households having ownership of the property they reside at/ Total households)* 100	Ward level: Census 2011 – Ownership Status ²¹

KEY FINDINGS

On an average, nearly 74% of Mumbai’s population live in their ‘own’ houses. C Ward has the lowest percentage at 54%, and R/C Ward has

the highest percentage of households, at more than 82%, living in ‘own’ houses (Refer Annexure Figure 49).

Physical Environment Aspects



3. House Condition

ASSESSMENT

Using Census 2011 house listing and housing data, ward level assessment and mapping are carried out to evaluate the percentage households by each ward with predominant roofing material as Grass/ Thatch/ Bamboo/ Wood/Mud etc., Plastic/ Polythene, Handmade Tiles, Stone/ Slate,

and Galvanized Iron /Metal/ Asbestos sheets. etc. The assumption is that these temporary²² roofing materials make a household more vulnerable to climate induced hazards due to their limited physical stability.

22 - Based on census data, the households having the following roofing material have been clubbed under households with temporary roofing as these materials are most vulnerable to impact of extreme weather events such as heavy rainfall, flooding or heat stress. Roof material type: Grass/ Thatch/ Bamboo/ Wood/Mud etc., Plastic/ Polythene, Handmade Tiles, Stone/ Slate, and Galvanized Iron/Metal/ Asbestos sheets etc.

CONTRIBUTIVE PARAMETERS

Table 13 | House Condition – Assessment Parameters and Attributes

Parameter	Vulnerability	Methods Used	Data Source
Percentage of Households with Temporary Roofing Material	Positive relation	(Total households having predominant roofing material categorized as temporary/ Total households)* 100	Ward level: Census 2011 – Material of Roof ²¹
Illustrative Case of Vulnerability to Climate Induced Hazard			
Urban Heat Risk¹⁹	Positive relation	Area with $\geq 35^{\circ}\text{C}$ LST overlaid on total ward area	WRI Analysis; LandSat 8 (USGS)
Urban Flood Risk²⁰	Positive relation	250m buffer zone overlaid on wards with highest share of ‘temporary’ roof households	WRI Analysis; Disaster Management Department, BMC

KEY FINDINGS

On an average, 45.7% of Mumbai’s population lives in houses with temporary roofing material. C Ward has the lowest percentage at 10.8% and S Ward has the highest at 63.6%. Nearly 20% of the population in S Ward is potentially exposed to heat stress, with over 25% potentially exposed to

the risk of flooding. The ward also has the highest percentage of Mumbai’s slum population and the majority – 147 out of 160 – of the ward’s landslide prone locations overlap with slums. Potential overlap of these risks can exacerbate vulnerabilities. (Refer Annexure Figure 50).



4. Access to Daily Urban Recreation Spaces

ASSESSMENT

Recreation spaces, often the open public greens, act as cushions to floods and temperature dampening resources at both neighborhood and

city levels. Proximity to such breathing spaces reduces long term exposure to both air pollution and high surface temperatures.

CONTRIBUTIVE PARAMETERS

Table 14 | Access to Daily Urban Recreation Spaces – Assessment Parameters and Attributes

Parameter	Vulnerability	Methods Used	Data Source
Access to Various Types and Scales of Daily Urban Recreation Spaces	Negative relation	Proximity and per capita space are used to evaluate access to recreation spaces. Daily urban recreation spaces include children’s park, neighborhood park, institutional playgrounds, maidans and district park. Service area polygons differ based on park capacity and using network analysis, ped shed service areas have been created using defined standard best practices ^{XVIII} . Ped shed of 0.25 km was considered for children’s park, 0.5 km for neighborhood park and 1 km for district park, institutional playgrounds and maidans.	Mumbai Development Plan (DP 2034), Google Maps, Census 2011

Illustrative Case of Vulnerability to Climate Induced Hazard			
Urban Heat Risk¹⁹	Positive relation	Area with $\geq 35^{\circ}\text{C}$ LST overlaid on the gridded population density having limited access to daily urban recreation space (unserved population)	WRI Analysis; LandSat 8 (USGS)
Urban Flood Risk²⁰	Positive relation	A 250 m buffer zone overlaid to gridded population density, having access to daily urban recreation space (served population)	WRI Analysis; Disaster Management Department, BMC

KEY FINDINGS

While 59.8% of Mumbai's population has access to at least one type of daily urban recreation space within the defined threshold values, 40.2% does not have access to any daily urban recreation space within 1 km (Refer Annexure Figure 51).

The total area of daily urban recreation spaces across Mumbai is 7.6 km² and the served population has 0.8 m² of daily urban recreation space per capita. But during a flood event, the population in Mumbai with access to a daily urban recreation space can potentially reduce from 59.8% to 36.8%.

M/W Ward has the highest percentage of population with access (79%) but it is potentially reduced to 38.7% during a flood event.

At least 18.1% of Mumbai's population who do not have access to a daily urban recreation space within the defined thresholds (unserved population) are also exposed to heat stress ($\geq 35^{\circ}\text{C}$), exacerbating their vulnerability due to the overlapping risks. M/E Ward has the highest percentage of population (20.1%) exposed to such overlapping risks.

Infrastructure and Service Aspects



5. Access to Drinking Water

CONTRIBUTIVE PARAMETERS

Table 15 | Access to Drinking Water – Assessment Parameters and Attributes

Parameter	Vulnerability	Methods Used	Data Source
Source of Drinking Water	Negative relation	Percentage of households having provision of treated tap water as main source ^{xix}	Ward Level: Census 2011 – Main source of drinking water and location of drinking water source ²¹
Proximity of Drinking Water Source	Negative relation	Area with $\geq 35^{\circ}\text{C}$ LST overlaid on the least served ward's area (ward having least proximity to source and lowest access to treated water)	
Illustrative Case of Vulnerability to Climate Induced Hazard			
Urban Heat Risk¹⁹	Positive relation	Area with $\geq 35^{\circ}\text{C}$ LST overlaid on the least served ward (ward having least proximity to source and lowest access to treated water)	WRI Analysis; LandSat 8 (USGS)

KEY FINDINGS

With regard to source of drinking water, 94.4% of households (HHs) have provision of treated tap water (Refer Annexure Figure 52). Evaluating proximity of drinking water source, 79.2% of HHs have water source within premises (Refer Annexure Figure 53).

M/E Ward ranks lowest on both parameters, with the highest percentage of its households not having

access to treated tap water (17.2%) and not having a water source within their premises (46.4%). Further, 11.8% of this ward's area is exposed to the risk of heat stress ($\geq 35^{\circ}\text{C}$). Potential overlap of service deficit and exposure to heat stress will exacerbate the vulnerability and pose a serious health hazard, potentially reducing productivity and thereby income of households.



6. Access to Sanitation

CONTRIBUTIVE PARAMETERS

Table 16 | Access to Sanitation – Assessment Parameters and Attributes

Parameter	Vulnerability	Methods Used	Data Source
Latrine Availability	Negative relation	Percentage of households having latrine facility within premises	Ward Level: Census 2011 – Number of households having latrine within premises, Flush/pour latrine, Pit latrine, Night soil disposed into open drain, Service latrine ²¹
Unhygienic Sewage Disposal Methods	Negative relation	Percentage of households following unhygienic sewage disposal methods including open pit latrines, open drains, removal by humans, etc.	
Unhygienic Wastewater Disposal Methods	Negative relation	Percentage of households with wastewater outlets connected to open drainage or no drainage	
Illustrative Case of Vulnerability to Climate Induced Hazard			
Urban Flood Risk²⁰	Positive relation	A 250m buffer zone overlaid on the least serviced ward (ward having least proximity to latrine, highest unhygienic sewage disposal, and highest unhygienic wastewater)	WRI Analysis; Disaster Management Department, BMC

KEY FINDINGS

Assessing latrine availability, it was found 58.3% of HHs have a latrine within the premises (Refer Annexure Figure 54). A total of 2.8% of HHs follow unhygienic sewage disposal methods (Refer Annexure Figure 55), while 18% of HHs dispose wastewater in an unhygienic manner (Refer Annexure Figure 56).

M/E Ward ranks lowest on all three parameters,

with highest percentage of its households not having a latrine within premises (64.2%), following unhygienic sewage disposal methods (4.1%) and unhygienic wastewater disposal methods (47.9%). Further, 13.1% of this ward's area is exposed to the risk of flooding. Potential overlap of service deficit and exposure to risk of flooding will exacerbate the vulnerability and pose as a serious health hazard.



7. Access to Clean Cooking Fuel

ASSESSMENT

Using Census 2011 house listing and housing data, ward level assessment and mapping are carried out to evaluate the percentage households by each ward using LPG, biogas or electricity for cooking purposes. Choice of cooking fuel at first impacts indoor air quality, hence this indi-

cator has not been mapped against a specific climate induced hazard. It is used as an indicator to represent quality of living environment and identify wards with population that are generally more vulnerable given their exposure to a more polluted indoor space.

CONTRIBUTIVE PARAMETERS

Table 17 | Access to Clean Cooking Fuel – Assessment Parameters and Attributes

Parameter	Vulnerability	Methods Used	Data Source
HH Access to Clean Cooking Fuels	Negative relation	Percentage of households using clean cooking fuels ^{xx}	Ward Level: Census 2011 – Type of fuel used for Cooking ²¹

KEY FINDINGS

Clean cooking fuels are used by nearly 79% of Mumbai’s households (Refer Annexure Figure 57).



8. Access to Electricity

ASSESSMENT

Census 2011 house listing and housing data has been used for ward level assessment and mapping, to evaluate the percentage of households with electricity as the main source of lighting. Assuming that access to electricity is connection to a state-provided grid, it is evident that a major-

ity of Mumbai’s households fare well on this indicator. Hence, most households in Mumbai are not vulnerable due to lack of power/electricity and thus this section does not make specific correlations with any climate induced hazard.

CONTRIBUTIVE PARAMETERS

Table 18 | Access to Electricity – Assessment Parameters and Attributes

Parameter	Vulnerability	Methods Used	Data Source
Access to Electricity	Negative relation	Percentage of households having electricity as main source of lighting ^{xxi}	Ward Level: Census 2011 – Main Source of Lighting ²¹

KEY FINDINGS

A total of 97.3% of HHs have electricity as main source of lighting (Refer Annexure Figure 58).



9. Access to Mass Transit

CONTRIBUTIVE PARAMETERS

Table 19 | Access to Mass Transit – Assessment Parameters and Attributes

Parameter	Vulnerability	Methods Used	Data Source
Access to Mass Transit Stations Including Monorail, Metro and Suburban Rail	Negative relation	Access is computed by overlaying microgrids within 1 km walking distance to each station. Each microgrid is ranked based on its walkability access to transit stations. ^{XXII}	OSM, Google Maps, Metro Project reports, Census 2011
Illustrative Case of Vulnerability to Climate Induced Hazard			
Urban Flood Risk²⁰	Positive relation	A 250 m buffer zone overlaid to gridded population density with access to mass transit stations (served population)	WRI Analysis; Disaster Management Department, BMC

KEY FINDINGS

Around 60.5% of Mumbai’s population lives within 1 km of either of the three mass transit modes. Ratio of population share served by the three modes – Mono, Metro, Suburban rail – within the serviced area is 12 : 76.9 : 37.3 (individual coverages include populations served by more than one mode). Ghatkopar, Marol, Kanjurmarg, Lower Parel, CST, Colaba (previously underserved and now connected by the upcoming Metro line 3), Dadar etc. are well connected areas, with access to more than one mass transit mode. Areas such as Govandi, Deonar (underserved population concentration more than 2,500 ppha), Saki Naka, do not have access to a mass transit station within 1km. Areas including Madh and Gorai only have access to ferries and lack the possibility of being connected to the other existing mass transit modes (Refer Annexure Figure 59).

During a flood event, Mumbai’s population which can access a mass transit station within 1 km is potentially reduced from 60.5% to 36.6%. Ward B, 99.2% of whose population (the highest in the city) has access to such stations, is potentially reduced to 55.4%. Ward M/E, which ranks lowest with only 25.4% of its population having access, is potentially further reduced to 17%, making the population more vulnerable, especially the captive users.



Image Credit: Atharva Tulsi



10. Access to Healthcare

CONTRIBUTIVE PARAMETERS

Table 20 | Access to Healthcare – Assessment Parameters and Attributes

Parameter	Vulnerability	Methods Used	Data Source
Access to In-patient Facilities	Negative relation	Population coverage within 5km drivetime service area polygons around health care locations ^{XXIII}	BMC Health Department, Google API, Census 2011
Illustrative Case of Vulnerability to Climate Induced Hazard			
Urban Heat Risk¹⁹	Positive relation	Area with $\geq 35^{\circ}\text{C}$ LST overlaid on the gridded population density with limited access to urban health amenities (unserved population)	WRI Analysis; LandSat 8 (USGS)
Urban Flood Risk²⁰	Positive relation	250 m buffer zone overlaid on the gridded population density having access to urban health amenities (served population)	WRI Analysis; Disaster Management Department, BMC

KEY FINDINGS

It was seen 98.9% of Mumbai's population has access to an in-patient healthcare facility (government, civic and private run) within 5 km. In total, Mumbai has 71 government and civic run hospitals with a total bed count of 18,797. Mumbai also has 1,521 private hospitals with a total bed count of 34,889. The population-to-bed ratio within the serviced area is 3.4 beds per 1,000 people. For every bed in a government or civic run hospital, Mumbai has 1.85 private hospital beds (Refer Annexure Figure 60 and Endnotes XXIII). Madh and Versova are the only areas with limited access to hospitals.

In the event of a flood, Mumbai's population with access to a healthcare facility within 5km is potentially reduced from 98.9% to 63.9%. Wards C and

F/N rank the highest as 100% of their population have access to a healthcare facility, but this is potentially reduced to 78% and 33% respectively during a flood event. This reduction in level of access during a flood event can potentially impact timely medical aid, especially for the poorer population (due to limited financial resources and dependency on public transport).

Moreover, 14.1% of Mumbai's population who do not have access to a healthcare facility within the defined thresholds (unserved population) are also exposed to heat stress ($t_{35}^{\circ}\text{C}$), exacerbating their vulnerability due to the overlapping risks. G/N Ward has the highest percentage of population (2.5%) exposed to such overlapping risks.



11. Access to Fire Services

CONTRIBUTIVE PARAMETERS

Table 21 | Access to Fire Services – Assessment Parameters and Attributes

Parameter	Vulnerability	Methods Used	Data Source
Access to Fire Stations	Negative relation	Population coverage within 5-7 min drivetime service area polygons around fire station locations ^{XXIV}	Disaster Management Department, BMC; Google API
Illustrative Case of Vulnerability to Climate Induced Hazard			
Urban Heat Risk¹⁹	Positive relation	Area with $\geq 35^{\circ}\text{C}$ LST overlaid to the gridded population density with limited access on fire services (unserved population)	WRI Analysis; LandSat 8 (USGS)
Urban Flood Risk²⁰	Positive relation	A 250m buffer zone overlaid to gridded population density with access to fire services (served population)	WRI Analysis; Disaster Management Department, BMC

KEY FINDINGS

A total of 47.4% of Mumbai’s area which houses 78.6% of the population has access to fire stations within five minutes. Mumbai has 39 fire stations including mini stations. Andheri SEEPZ, Vikhroli, Kanjurmarg, Khar-Danda, Borivali West, Gorai are some of the high density underserved areas that lie beyond the five-minute response time (Refer Annexure Figure 61).

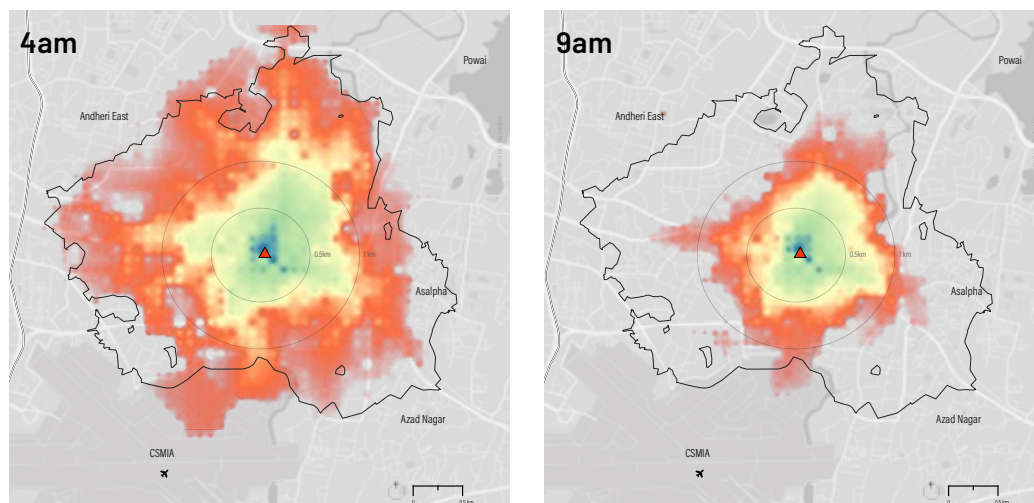
The level of access also varies temporally through the day based on traffic and road conditions. Based on temporal analysis²³, an example as seen in Figure 27, the area that can be reached by a fire tender from Marol Fire Station within five minutes reduces from 1.9km² at 4am to 1.1km² at 9am, a 42% reduction in terms of service area, thereby increasing the potential risk.

In case of a flood event, Mumbai’s population served by all the fire stations within a response time of five minutes is potentially reduced from 78.6% to 47.2%. Ward C, which has the most people – 100% of its ward population – living within a five-minute response time, sees that potentially reduced to 78% in a flood, increasing time required for rescue and recovery efforts and, thereby, increasing vulnerability.

Moreover, 12.9% of Mumbai’s population who are not serviced by the fire services within the standard five-minute response time (unserved population) are also exposed to heat stress ($\geq 35^{\circ}\text{C}$), exacerbating their vulnerability due to the overlapping risks. S Ward has the highest percentage of population (14.5%) exposed to such overlapping risks.

23 - Using Google distance API for 30.07.2021 considering the pessimistic scenario results on vehicular speeds have been derived. The aforementioned date has been chosen based on the last few years’ usual distribution of rainy days through monsoon season. The same illustrative case can be considered for any other date to understand variation in traffic due to natural and man-made activities.

Figure 27 | Temporal Analysis showing Change in Serviced Area under Different Traffic Conditions during a Day



Service Area Buffers based on Response Time (in minutes): ■ 1 ■ 2 ■ 5 ■ 7
▲ Fire Station ✈ Airport 2.5 km Service Area Buffer assuming 30 km/hr Average Speed

Note: In this case of Marol Fire Station, located in Andheri East, area covered under the Standard Reponse Time of five minutes is highest at 4am. During morning peak hour traffic, at around 9am and evening peak hour traffic at around 6pm, this serviced area is drastically reduced due to increased traffic congestion.

Source: WRI India; Google Distance Matrix API



12. Access to Flood Shelters

CONTRIBUTIVE PARAMETERS

Table 22 | Access to Flood Shelters – Assessment Parameters and Attributes

Parameter	Vulnerability	Methods Used	Data Source
Access to Flood Shelters	Negative relation	Population coverage computed within 1 km of walking distance using service area polygons around flood shelters ^{XXV}	Disaster Management Department, BMC, Census 2011
Illustrative Case of Vulnerability to Climate Induced Hazard			
Urban Flood Risk²⁰	Positive relation	A 250m buffer zone overlaid to gridded population density having access to flood shelters (serviced population)	WRI Analysis; Disaster Management Department, BMC

KEY FINDINGS

Nearly 43% of Mumbai’s area, which houses 75.9% of the city’s population, has access to a flood shelter within 1 km walking distance. While the city has 868 flood shelters, Deonar, Mahul, Kandivali East, Saki Vihar Road in Powai, Four Bungalows in Andheri, and Versova are some of the underserved high-population density areas that do not have access to a flood shelter within 1 km (Refer Annexure Figure 62).

In the event of a flood, Mumbai’s population with access to a flood shelter within 1 km walking distance is potentially reduced from 75.9% to 46.5%. Ward C ranks the highest, with 99.9% of its population living within 1km walking distance from a flood shelter, but this is potentially reduced to 77.5% during a flood. Similarly, Ward M/E, which ranks the lowest with only 31.5% of population having access to a flood shelter, experiences a further reduction to 13.3% in such an event, exacerbating the vulnerability.



Image Credit: Joel Steevan

Chapter 5:

Impact Analysis

A logical precursive step to a climate change adaptation plan is to estimate and analyze the extent of disruption likely to be caused by the hazards in the city. Impact assessments solicit expected damage caused to individuals, communities, the city's economy, infrastructure, and the natural environment. For risk quantification, the study follows an illustrative approach to estimate population exposed, livelihoods affected, and potential disruption of critical services in the city due to an exemplar climate hazard.

Flooding has been a major challenge for Mumbai. Increasingly heavy rains and the resultant 170

landslides, floods and collapsed homes have claimed more than 400 lives in the last decade (Srivastava, 2021). Based on the Hazard Risk Analysis, in the last five years, the number of "very heavy" to "extreme" rainfall events has nearly doubled. Flooding cripples the city's infrastructure, especially the transport services, derailing the country's financial capital. While such phenomena of disruption are witnessed as a result of all climate induced hazards, this section uses flooding as a demonstrative case. The following table elaborates the impacts of flooding across three dimensions – lives, livelihoods and services – along with the methods used in the study to mensurate the same.

Table 23 | Impact Analysis

Phenomenon	Rationale	Method
Impact on Lives	Compromised human habitat puts the lives of individuals at risk, especially those living in the immediate vicinity or in the impact area of a disaster. The urban marginal communities – Urban Poor – are more vulnerable due to their limited adaptive capacity and higher sensitivity to such events.	Using a 250 m radius as buffer around the flood hotspots ²⁴ , population density (Census 2011) is mapped to spatially estimate the distribution of the population exposed to the risk of flooding.
Impact on Livelihoods	Climatic variables tend to have both direct and indirect impact on the economy of the city. For instance, during a heat wave, resultant health impacts lead to loss of productive hours, absence from jobs, that not only impact a household's income but also significantly affects the daily GDP. For instance, civic bodies spend millions to repair cracked roads due to extreme heat, or potholes due to rains. They also lose a significant share of daily GDP or revenue due to the halt caused to economic activities in the city by the climate anomalies.	Potential loss of daily jobs based on concentration and size of the employment provided by various commercial or industrial establishments falling within 500 m of the flood hotspots ²⁴ .

24 - Flood hotspots include last three years of data capturing complaints by the residents and observations made on site by the ward officers according to BMC records.

Phenomenon	Rationale	Method
Impact on Services	Climate change impacts access to various essential, lifesaving, and livelihood-oriented services, exacerbating the risks during a climate hazard event. For example, waterlogged streets during a flood hinders physical access of ambulances, access to temporary evacuation shelters and other essential services, affects transit systems and damages the city's infrastructure. A large section of the population is primarily dependent on mass transport to access daily needs such as water, sanitation, food supplies and other services. Events of flooding disrupt and cordon the access to these essential civic amenities, making these populations more vulnerable.	Using a buffer of 250 m from the flood hotspots ²⁰ , mass transit stations with jeopardized access are mapped to spatially reflect the differential impact of floods on physical access to daily critical urban services.

Impact on Lives

KEY FINDINGS

Around 35% of Mumbai's population lives within 250 m from the flood hotspots exposing them to the highest risk of floods. Ward F/N has the highest percentage of population exposed to the risk of flooding (250 m buffer from flood hotspots²⁴), as high as 67% of the ward population.

Most of the informal settlements are located along the low-lying areas such as canals or water channels, riverbanks, railway lines, dumping sites etc. There-

fore, communities living in these settlements are more exposed to the risks associated with flood hazards. As per Mumbai DP 2034, there are more than 5.2 million people living in such areas. Wards P/N and S have the highest percentage of population living in informal settlements and a high number of flooding hotspots, making these wards the most vulnerable. Refer to the Endnote XXVI for detailed summary of population exposed to flood risks and Figure 28 for spatial distribution of population at flood risk.

Impact on Livelihoods

KEY FINDINGS

With frequent spells of heavy rainfall, the city has been witnessing extensive waterlogging. These recurrent waterlogging events also limit the means to access business centers impacting the daily wage/ industrial jobs the most (UNICEF, 2021). Based on Directory of Establishments' 2015 data, 73% of Mumbai's small & large industrial and commercial establishments are located within 500m of flood hotspots, exasperating the risk caused by flooding to their businesses. And 69% of the employees who work at these establishments may experience hindered access due to physical disconnect caused by waterlogging in the area. Refer to Figure 29 for spatial distribution of daily jobs that are likely to be

at risk due to flood events.

Based on a 2013 study that ranked major coastal cities on their associated flood risks, Mumbai is placed fifth in the world with annual losses to the economy mounting to USD284 million (Hallegatte, Green, Nichollas, & Corfee-Morlot, 2013). Several researchers have projected these annual losses from flooding and heavy rain events to reach USD6.1 billion per year by 2050 (Picciariello, Colenbrander, Bazaz, & Roy, 2021). Most of these losses are uninsured and borne by individuals or small businesses (Patankar & Patwardhan, 2016) leading to increased and differential vulnerability.

Impact on Services

KEY FINDINGS

Heavy rainfall and flooding affect the transport infrastructure in a city by impacting its safety, operation costs, travel time and regularity of service. This further disrupts access to most essential and critical civic services. Based on the flood hotspot influence zone analysis, 33%²⁵ of Mumbai's mass transit network – including its lifelines of the suburban rail network, Metro line and Monorail – are heavily impacted by inundation limiting physical access²⁶ to transit stations.

As witnessed in the year 2005, railway services including local trains, all major roads, and the airport were waterlogged, bringing the city to a standstill. The Mumbai airport, built on reclaimed land from the Mithi river, was inundated for three days and no flights operated for more than 30 hours (Singh, 2018). Heavy rainfall increases travel time by road from roughly 8% to 140% in some road sections (Soni & Chandel, 2020), making it challenging to provide emergency response and recovery initiatives.

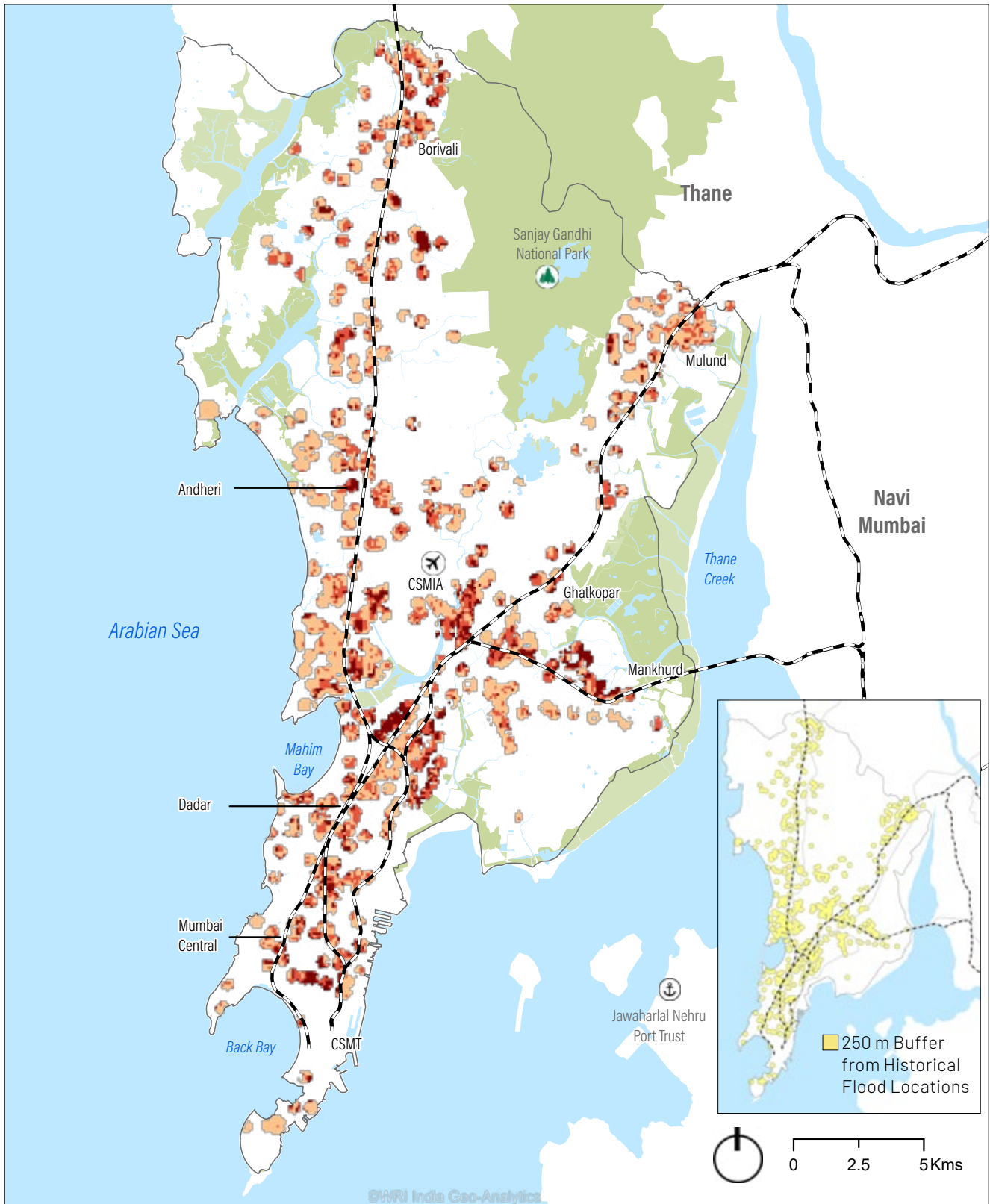


Image Credit: Alfarnas Solkar

25 - $(\text{Number of transit stations within 250 m of flood hotspots} / \text{Total number of transit stations}) * 100$

26 - Primary assumption for the analysis reinforces the widely observed fact that heavy downpour can inundate and block vehicular and pedestrian access

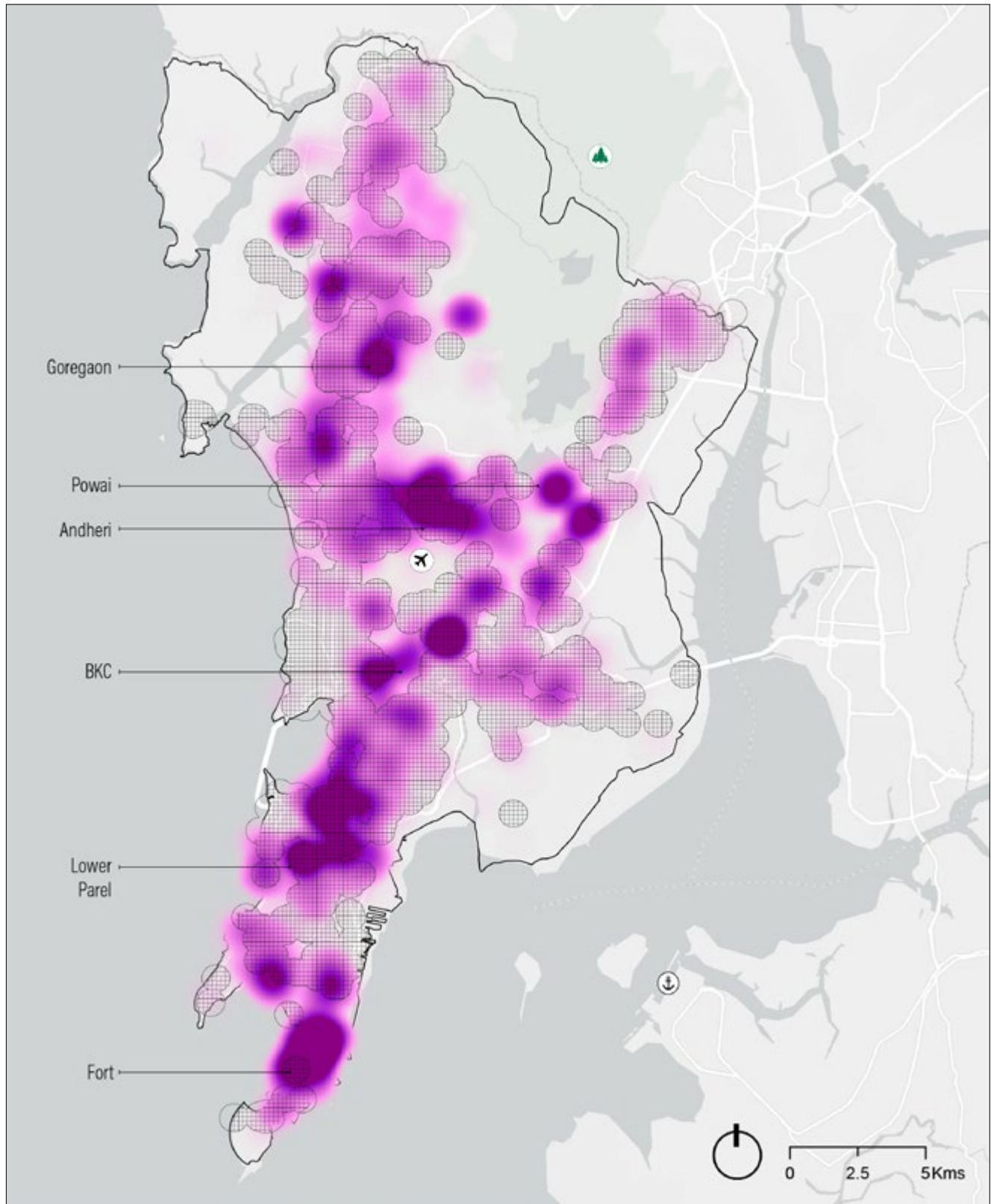
Figure 28 | Population Potentially at Risk due to Floods



Population within Flood Zone (250 m):	 5-500	 500-1,000	 1,000-13,800	 Waterbody	 BMC Boundary	✈ Airport
	(Population per Ha)	 Railway Line	 Green Cover	🌳 National Park	⚓ Sea Port	

Source: WRI India using Historical Flood Locations from BMC; Census 2011; OpenStreetMap

Figure 29 | Impact on Employment Hubs due to Floods

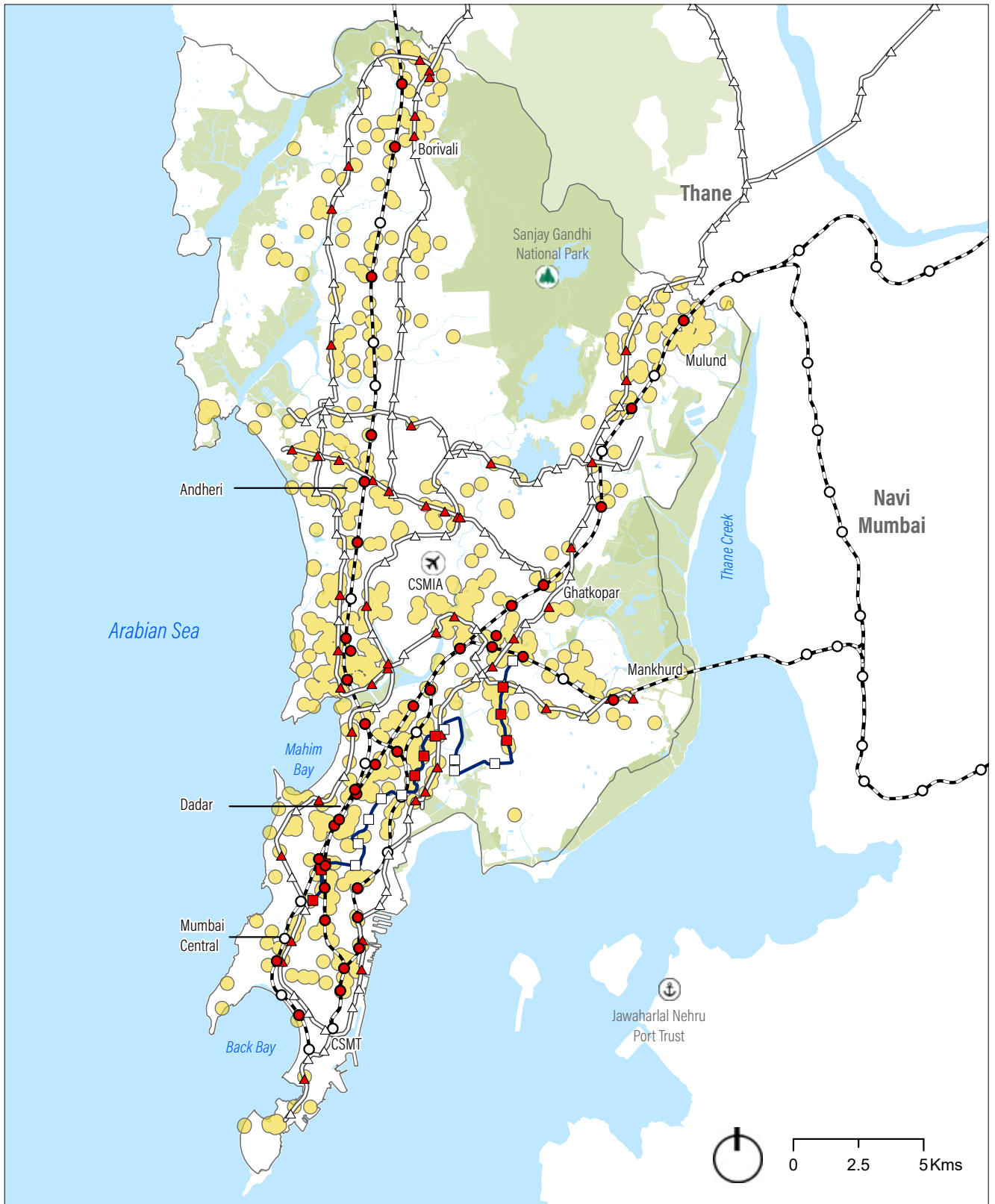


Number of Formal Jobs within 1 km: 0 7000

Flood Buffer Zone within 250 m
 BMC Boundary
 ✈ Airport
 ⚓ Sea Port
 🌲 National Park

Source: WRI India using Historical Flood Locations from BMC; Directory of Establishments (Sixth Economic census, MOSPI)

Figure 30 | Mass Transit Stations with Limited Physical Access during Floods



- | | | | | | |
|---------------------------------|--------------------|-----------------|--|-----------------|------------|
| Transit Station at Risk: | ● Railway Station | — Railway Line | □ Waterbody | □ BMC Boundary | ✈ Airport |
| | ■ Monorail Station | — Monorail Line | ■ Green Cover | ■ National Park | ⚓ Sea Port |
| | ▲ Metro Station | — Metro Line | ■ 25m Buffer from Historical Flood Locations | | |

Source: WRI India; MMRCL; OpenStreetMap

Chapter 6:

Conclusion

Mumbai's geography and scale, rate and pattern of urbanization exposes it to several climate-induced hazards. Analysis reveals that changing and uncertain patterns of rainfall, deteriorating coastal ecology and development choices have made flooding a recurrent major challenge. Over 30% of Mumbai's population lives within the influence of (within 250m radius buffer) BMC-reported flooding hotspots. Ward F/N has the highest number of flooding hotspots (54) and over 60% of its population is exposed to the risk of flooding, making it the most vulnerable area to flood hazards. Also, only 50% of the households in this ward have a latrine available within their premises, aggravating this deficit by hindered access to safe and hygienic sanitation services during a flood event.

Urban heat not only in summer but also post-monsoon is another big challenge for Mumbai owing to the rise in relative humidity post monsoon, increasing built density, choice of building materials, reducing green cover in the city. Ward M/E is the most vulnerable to heat stress with over 38% of its population exposed to a surface temperature greater than 35°C. This ward is also one of the three in the city with the highest number of houses with temporary roofing such as polythene or asbestos, over 45% of households don't have a drinking water source within their premises and only about 35% households have a latrine within their premises, greatly intensifying the risk.

Table 24 | Ward-wise Summary - Climate & Air Pollution Risks and Vulnerability Assessment

	Indicator	Parameter	Most Vulnerable Administrative Ward	Least Vulnerable Administrative Ward	BMC Average
Climate Risks	Urban Heat	Population impacted by urban heat risk ¹⁹	M/E - 40.08%	A - 0.92%	14.46%
	Urban Flooding	Population impacted by flood - 250 m buffer	F/N - 66.8%	P/N - 15.4%	35.3%
Demographic Context	Literacy	Effective literacy rate	M/E - 83.3%	T - 93.2%	89.7%
		Effective female literacy rate	M/E - 78%	R/C - 91.3%	86.4%
		Access to education	G/S - 93.6%	C - 100%	96.8%
	Gender Imbalance	Sex ratio	C - 695	R/C - 944	852
	Social Composition	% SC and ST population	M/W - 19%	C - 1.6%	7.5%

Indicator	Parameter	Most Vulnerable Administrative Ward	Least Vulnerable Administrative Ward	BMC Average	
Socio-Economic Aspects	Access to Information	Household access to radio/transistor	B - 17.5%	R/C - 55.7%	36.2%
		Household access to TV	M/E - 75.3%	R/C - 92.4%	85.3%
		Household access to PC with internet	M/E - 7.7%	H/W - 39.8%	20.1%
		Household access to landline	M/E - 6.2%	H/W - 14.6%	9.3%
		Household access to mobile	D - 40.2%	L - 75.7%	61.7%
		Household access to landline and mobile	M/E - 8.6%	D - 44.7%	24%
	Home Ownership	% Population living in own house	C - 54.1%	R/C - 82.7%	73.7%
Physical Environment Aspects	House Condition	Households living in houses with temporary roofing material	S - 63.6%	C - 10.8%	45.7%
	Access to Daily Urban Recreation Spaces	Population having access to daily urban recreation spaces on a regular day	T - 39%	M/W - 79%	59.8%
		Population having access to daily urban recreation spaces during a flood event	T - 13.1%	N - 54.3%	36.8%
		Unserviced population also exposed to risk of heat stress ¹⁹	M/E - 20.1%	R/C - 0.7%	18.1%
Access to Drinking Water	Households with access to tap water from treated source	M/E - 82.8%	C and D - 98.3%	94.4%	
	Households with tap within premises	M/E - 53.6%	C - 98.4%	79.2%	

Indicator	Parameter	Most Vulnerable Administrative Ward	Least Vulnerable Administrative Ward	BMC Average
Access to Sanitation	Households with latrine within premises	M/E - 35.8%	C - 93.4%	58.3%
	Households following unhygienic sewage disposal methods	M/E - 4.06%	F/N - 1.7%	2.8%
	Households following unhygienic wastewater disposal methods	M/E - 47.9%	C - 1.26%	18%
Access to Clean Cooking Fuel	Households with access to LPG, biogas, electricity	M/E - 54.3%	R/C - 91.3%	78.6%
Access to Electricity	Households with electricity as main source of lighting	M/E - 95.3%	C - 99.7%	97.3%
Access to Mass Transit	Population having access to mass transit within 1 km on a normal day	M/E - 25.4%	B - 99.2%	60.5%
	Population having access to mass transit within 1km during a flood event	H/W - 10.9%	C - 66%	36.6%
Access to Healthcare	Population having access to healthcare services on a regular day	P/N - 95.8%	F/N and C - 100%	98.9%
	Population having access to healthcare services during a flood event	F/N - 32.5%	N - 82%	63.9%
	Unserviced population exposed to risk of heat stress ¹⁹	G/N - 2.5%	A, B, C, D, E, F/N, F/S, G/S, H/E, H/W, L, M/E, P/N, P/S, R/C, R/N, S, T - 0%	14.1%
Access to Fire Services	Population having access to fire rescue services on a regular day	S - 38.9%	C - 100%	78.6%

Infrastructure and Service Aspects

Indicator	Parameter	Most Vulnerable Administrative Ward	Least Vulnerable Administrative Ward	BMC Average	
Infrastructure and Service Aspects	Access to Fire Services	Population having access to fire rescue services during a flood event	H/W - 15.4%	C - 77.6%	47.2%
		Unserviced population exposed to heat stress ¹⁹	S - 14.5%	A, B, C, D, E, F/N, K/W - 0%	12.9%
	Access to Flood Shelters	Population having access to flood shelters on a regular day	M/E - 31.5%	C - 99.9%	75.9%
		Population having access to flood shelters during a flood event	M/E - 13.3%	C - 77.5%	46.5%

Table 24 presents all the indicators and identifies the most and least vulnerable ward against the average of each indicator for Greater Mumbai. Among the 24 administrative wards in Greater Mumbai, Ward M/E ranks lowest across most socio-economic, infrastructure provision and physical access parameters which may result in greater vulnerability in that area. It has the highest percentage of households depending on polluting cooking fuels (over 45%) such as firewood, coal, cow dung, kerosene etc., without taps within premises (46.4%), without a latrine within premises (64.2%) and depending on unhygienic wastewater disposal mechanisms (47.9%). Further exacerbating this vulnerability, it has the lowest percentage population having access to a mass transit station (25.4%) and a flood shelter (31.5%) within 1km. And the population with access to a flood shelter is potentially further reduced to 13.3% during a flood event. With a large section of Mumbai's population living in underserved neighborhoods, climate and air pollution related risks can be catastrophic for the city.

Drawing from the framework according to Figure 2, Figure 31 details and quantifies the correlation between different climate hazard risks against access to various critical urban services in the context of Greater Mumbai. The correlations are measured in three ways – i) disruption in services (shown as a potential reduction in serviced population due to exposure to a specific hazard risk), ii) population concentrations with exacerbated vulnerability (unserved population

exposed to a specific hazard risk) and iii) potential risk in most vulnerable wards (percentage area of ward with lowest level of provision of services exposed to a specific hazard risk). The color of the value corresponds to the specific hazard risk.

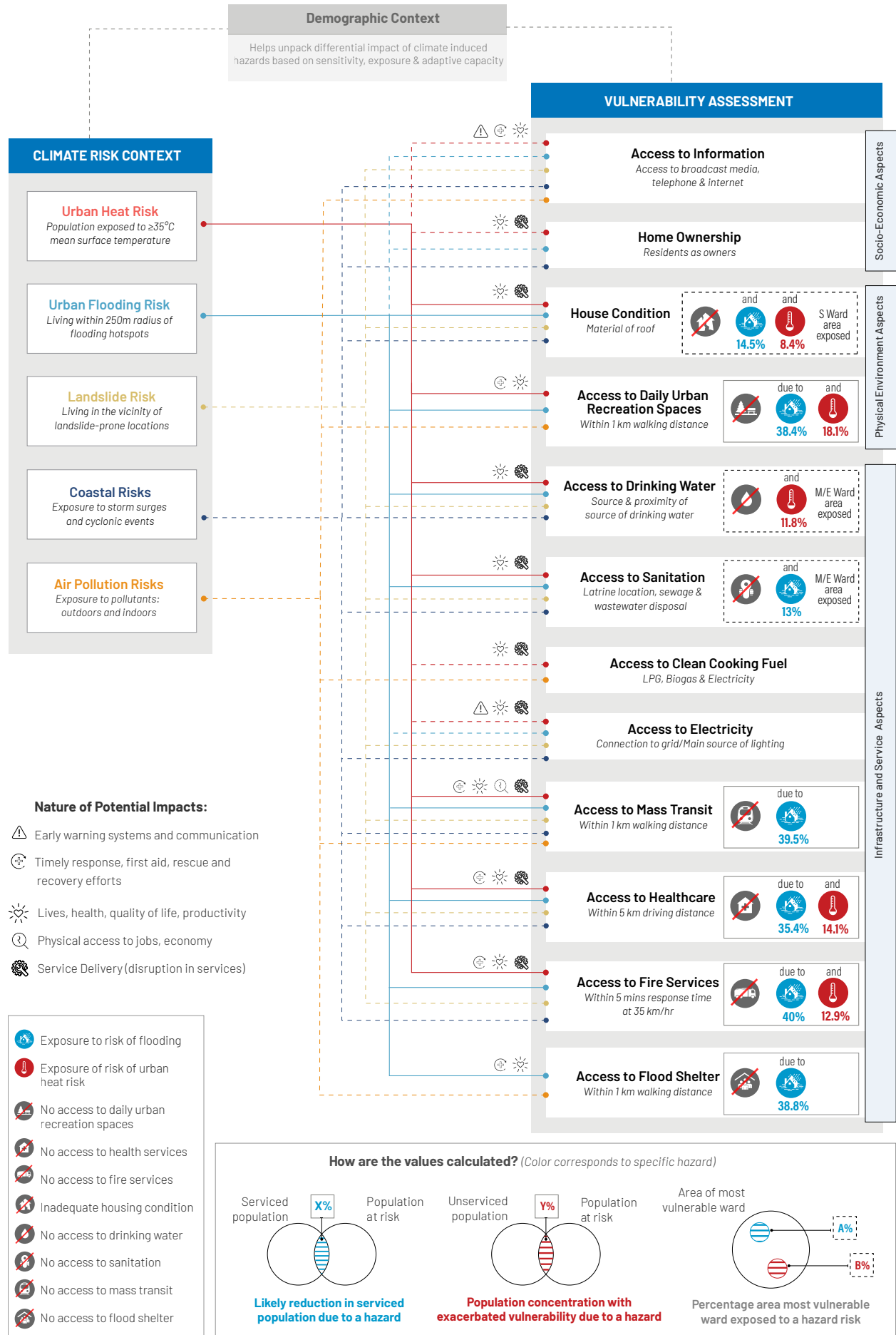
Across different aspects and indicators, we observe more than 30% potential reduction in services (access to mass transit, healthcare, daily urban recreation space, fire services and flood shelter) during a flood event and between 10% and 15% of Mumbai's underserved population (limited or no access to daily urban recreation spaces, healthcare, fire services based on defined thresholds) exposed to an overlapping risk of heat stress, intensifying the risk.

Way Forward

The demographic and socio-economic study to assess Mumbai's vulnerability is largely based on Census 2011 data, which is outdated and may not adequately represent the city's vulnerability to climate induced disasters. A deeper assessment of vulnerability parameters and community resilience capacities is recommended to bridge capacity gaps and ensure dignity of infrastructure and services, and thereby reduced vulnerability for Mumbai's residents.



Figure 31 | Mumbai's Vulnerability Assessment



References

Bharadwaj, R., Hazra, S., Reddy, M., Das, S., & Kaur, D. (2021). *Connecting the dots: climate change, migration and social protection*. IIED. London: IIED.

Balakrishnan, K., Ghosh, S., Ganguli, B. S., Bruce, N., & Barnes, D. F. (2013, 08 11). State and national household concentrations of PM_{2.5} from solid cookfuel use: results from measurements and modeling in India for estimation of the global burden of disease. *Environmental health: a global access science*, 12(1), 77. doi:10.1186/1476-069X-12-77

Bharti, V., Jayasankar, J. J., Shukla, S. p., George, G., Ambrose, T. V., Augustine, S. K., Shafeeque, M. (2020). Study on Sea Surface Temperature and Chlorophyll-a concentration along the south-west coast of India. *Indian Journal of Geo Marine Sciences*, 40(1), 51-56. Retrieved from <http://nopr.niscair.res.in/bitstream/123456789/53541/1/IJMS%2049%281%29%2051-56.pdf>

Bhowmik, S. K. (2010). *Hawkers and the urban informal sector: a study of street vending in seven cities*. National Alliance of Street Vendors of India (NASVI). Retrieved from <https://www.wiego.org/sites/default/files/publications/files/Bhowmik-Hawkers-URBAN-INFORMAL-SECTOR.pdf>

Bose, I., Faleiro, J., & Singh, H. (2020). *Climate migrants pushed to the brink - South Asia is unprepared to protect climate migrants, even as it battles the COVID-19 crisis*. Johannesburg: ActionAid.

Daniel Hoornweg & Kevin Pope. (2014, January). *Socioeconomic Pathways and Regional*. Retrieved from <https://shared.ontariotechu.ca/shared/faculty-sites/sustainability-today/publications/population-predictions-of-the-101-largest-cities-in-the-21st-century.pdf>

Dare, R. A., & John, L. M. (2011, 05 09). Sea Surface Temperature Response to Tropical Cyclones. *Monthly Weather Review*, 139, pp. 3798-3808. doi:10.1175/MWR-D-10-05019.1

District Disaster Management Plan. (2019).

Draft Development Plan 2034. (n.d.). *Draft Development Plan 2034, Greater Mumbai*.

Eckstein, D., Künzel, V., & Schäfer, L. (2021). *Global Climate Risk Index 2021*. Bonn: Germanwatch e.V.

Final Regional Plan of Mumbai Metropolitan Region. (2021). MMRDA.

Gupta, K. (2007). Urban flood resilience planning and management and lessons for the future: a case study of Mumbai, India. *Urban Water Journal*, 4(3), 183-194.

Hallegatte, S., Bangalore, M., Bonzanigo, L., Fay, M., Kane, T., Narloch, U., Vogt-Schilb, A. (2016). *Shock Waves - Managing the Impacts of Climate Change on Poverty*. Washington DC: World Bank Group.

Hallegatte, S., Green, C., Nichollas, R. J., & Corfee-Morlot, J. (2013). Future flood losses in major coastal cities. *Nature Climate Change*, 3, pages802–806. doi:<https://doi.org/10.1038/nclimate1979>

Hallegatte, S., Henriot, F., Patwardhan, A., Narayanan, K., Ghosh, S., Karmakar, S., & Patnaik, U. (2010). *Flood Risks, Climate Change Impacts and Adaptation Benefits in Mumbai: An Initial Assessment of Socio-Economic Consequences of Present and Climate Change Induced Flood Risks and of Possible Adaptation Options*. Paris: OECD Publishing.

Hijioka, Y., Lin, E., Pereira, J. J., Corlett, R. T., Cui, X., Insarov, G., . . . Surjan, A. (2014). Asia. In *Climate Change 2014: Impacts, Adaptation, and Vulnerability. Part B: Regional Aspects. Contribution Working Group II to the Fifth Assessment Report of the Intergovernmental Panel on Climate Change* (pp. 1327-1370). Cambridge, United Kingdom: Cambridge University Press.

IDMC. (2020). *Global Report on Internal Displacement*. Internal Displacement Monitoring Centre.

- IMD. (2021). *Standard Operation Procedure: Weather Forecasting and Warning*. India Meteorological Department. New Delhi: Ministry of Earth Sciences. Retrieved from https://mausam.imd.gov.in/imd_latest/contents/pdf/forecasting_sop.pdf
- IMD. (n.d.). *FAQ-Heat Wave*. India Metrological Department. New Delhi: Office of Director General of Meteorology. Retrieved from https://internal.imd.gov.in/section/nhac/dynamic/FAQ_heat_wave.pdf
- IPCC. (2014). *Climate Change 2014: Synthesis Report*. Geneva: IPCC.
- Korade, M. S., & Dhorde, A. (2016). Trends in surface temperature variability over Mumbai and Ratnagiri cities of coastal Maharashtra, India. *Mausam*, 67(2), 455-462. doi:10.54302/mausam.v67i2.1352
- Kulp, S. A., & Strauss, B. H. (2019). New elevation data triple estimates of global vulnerability to sea-level rise and coastal flooding. *Nature Communications*, 10.
- Kumari, P. V., Jayappa, K. S., Thomas, S., & Gupta, A. (2021). Decadal variations of sea surface temperature in the eastern Arabian Sea and its impacts on the net primary productivity. *Spatial Information Research*, 29, 137-148. doi:<https://doi.org/10.1007/s41324-020-00340-y>
- Kuruppu, N. D., Bee, S., & Schaer, C. (2018). Developing the business case for adaptation in agriculture: case studies from the Adaptation Mitigation Readiness Project . In *Private-sector action in adaptation: Perspectives on the role of micro, small and medium size enterprises* (pp. 51-62). UNEP DTU Partnership. Retrieved from <http://www.unepdtu.org/PUBLICATIONS/Perspective-Series-2018>
- LEA Associates. (2016). *Comprehensive Mobility Plan (CMP) for Greater Mumbai*. Mumbai: Municipal Corporation of Greater Mumbai.
- Mangrove and Marine Biodiversity Conservation Foundation of Maharashtra. (2021). *A study regarding the shrinking of Thane Creek*. Mumbai: Mangrove Cell, GoM. Retrieved from https://mangroves.maharashtra.gov.in/Site/SiteInfo/Pdf/Shrinking_Thane_Creek_Mangrove_Foundation_Press_Note.pdf
- Marine Regions. (2022, 01 05). *Marine Gazetteer Place details*. Retrieved from [Marineregions.org: https://www.marineregions.org/gazetteer.php?p=details&id=4268](https://www.marineregions.org/gazetteer.php?p=details&id=4268)
- McKinsey Global Institute. (2020). *Climate risk and response: Physical hazards and socioeconomic impacts*.
- Mehrotra, S., Bardhan, R., & Ramamritham, K. (2018). Urban Informal Housing and Surface Urban Heat Island Intensity: Exploring Spatial Association in the City of Mumbai. *Environment and Urbanization ASIA*, 9(2), 158-177.
- Nandkeolyar, N., Raman, M., Kiran, G. S., & Ajai. (2013). Comparative Analysis of Sea Surface Temperature Pattern in the Eastern and Western Gulfs of Arabian Sea and the Red Sea in Recent Past Using Satellite Data. *International Journal of Oceanography*, 2013, 16. doi:<https://doi.org/10.1155/2013/501602>
- National Weather Service. (2021, 12 30). *Beat The Heat! Heat Safety Tips*. Retrieved from National Oceanic and Atmospheric Administration: <https://www.weather.gov/dlh/beattheheat>
- Nochian, A., Tahir, O. M., Maulan, S., & Rakhshandehroo, M. (2015, December). A comprehensive public open space categorization using classification system for sustainable development of public open spaces. *Alam Cipta - International Journal of Sustainable Tropical Design Research and Practice*, 8, 29-40.
- Patankar, A., & Patwardhan, A. (2016). Estimating the uninsured losses due to extreme weather events and implications for informal sector vulnerability: a case study of Mumbai, India. *Natural Hazards: Journal of the International Society for the Prevention and Mitigation of Natural Hazards*, 80(1), 285-310. Retrieved from https://econpapers.repec.org/article/sprnathaz/v_3a80_3ay_3a2016_3ai_3a1_3ap_3a285-310.htm
- Pettitt, A. (1979). A Non-Parametric Approach to the Change-Point Problem. *Journal of the Royal Statistical Society. Series C (Applied Statistics)*, 28(2), 126-135. doi:[doi:10.2307/2346729](https://doi.org/10.2307/2346729)
- Picciariello, A., Colenbrander, S., Bazaz, A., & Roy, R. (2021). The costs of climate change in India - A review of the climate-related risks facing India, and their economic and social costs. *ODI Literature review*. Retrieved from www.odi.org/en/publications/the-costs-of-climate-change-in-india-a-review-of-the-climate-related-risks-facing-india-and-their-economic-and-social-costs
- Prasad, P. R., Prasad, S. N., & Dutt, C. B. (2010). Analysis of Spatial and Temporal Changes in Mangroves Along Thane Creek of Mumbai(India) Using Geospatial Tools. *The IUP Journal of Environmental Sciences*, IV(3).

- Ranger, N., Hallegatte, S., Bhattacharya, S., Bachu, M., Priya, S., & Dhore, K. (2010). An assessment of the potential impact of climate change on flood risk in Mumbai. *Climate Change*, 104, 139-167.
- Rangwala, L., Elias-Trostmann, K., Burke, L., Wihanesta, R., & Chandra, M. (2018). *Prepared Communities: Implementing the Urban Community Resilience Assessment in Vulnerable Neighbourhoods of Three Cities*. World Resources Institute. Retrieved from https://wriorg.s3.amazonaws.com/s3fs-public/prepared-communities-implementing-urban-community-resilience-assessment.pdf?_ga=2.171878112.1906473220.1553678232-891479216.1535376449
- Rothfus, L. P. (1990). *The Heat Index Equation (or, More Than You ever Wanted to Know about Heat Index)*. NWS Southern Region Headquarters, Scientific Services Division. Fort Worth, Texas: National Oceanic and Atmospheric Administration. Retrieved from NWS Southern Region Headquarters, Fort Worth, TX: https://www.weather.gov/media/ffc/ta_htindx.PDF
- Singh, D. (2018, 08 08). *Mumbai: The 'rain ready' city that floods every year*. Retrieved from Prevention Web: <https://www.preventionweb.net/news/mumbai-rain-ready-city-floods-every-year>
- Soni, A. R., & Chandel, M. K. (2020). Impact of rainfall on travel time and fuel usage for Greater Mumbai city. *World Conference on Transport Research - WCTR 2019*. 48, pp. 2096–2107. Mumbai: Transportation Research Procedia. doi:10.1016/j.trpro.2020.08.269
- Srivastava, R. (2021, 09 30). Flood-prone Mumbai digs deep to turn climate change tide. *Thomson Reuters Foundation News*. Retrieved from <https://longreads.trust.org/item/Mumbai-C40-cities-network>
- Steadman, R. (1979). The assessment of sultriness. Part I: A temperature-humidity index based on human physiology and clothing science. *Journal of Applied Meteorology and Climatology*, 18(7), 861–873. doi:doi.org/10.1175/1520-0450(1979)018<0861:TAOSPI>2.0.CO;2
- TERI. (2014). *Assessing Climate Change Vulnerability and Adaptation Strategies for Maharashtra: Maharashtra State Adaptation Action Plan on Climate Change*. New Delhi: The Energy and Resources Institute.
- Thanh, N. T., Cuong, H. D., Hien, N. X., & Kieu, C. (2019). Relationship between sea surface temperature and the maximum intensity of tropical cyclones affecting Vietnam's coastline. *International Journal of Climatology*, 40(5), 2527-2538. doi:<https://doi.org/10.1002/joc.6348>
- Tol. (2019, 12 31). Maharashtra: 72% rise in mangrove cover in 6 years. *Times of India, Mumbai*. Retrieved from <https://timesofindia.indiatimes.com/city/mumbai/maharashtra-72-rise-in-mangrove-cover-in-6-years/articleshow/73040593.cms>
- UNDESA. (2018). *The World's Cities in 2018*. New York: United Nations, Department of Economic and Social Affairs, Population Division.
- UNICEF. (2021). *Humanitarian Action for Children*. Retrieved from <https://www.unicef.org/appeals>: <https://www.unicef.org/media/87396/file/2021-HAC-India.pdf>
- Walvekar, P. P., Gurjar, B. R., & Nagpure, A. S. (2019). Stack emissions and health risk integrated (SEHRI) model: a tool for stack emissions and health risk modeling. *Air Quality, Atmosphere & Health*, 12, 1483–1493. doi:<https://doi.org/10.1007/s11869-019-00766-w>
- World Bank. (2013). *Turn Down the Heat: Climate Extremes, Regional Impacts, and the Case for Resilience*. The World Bank Group.
- World Bank. (2021). *World Bank Group Climate Change Action Plan 2021–2025: Supporting Green, Resilient, and Inclusive Development*. Open Knowledge Repository. Washington DC: The World Bank Group. Retrieved from <https://openknowledge.worldbank.org/handle/10986/35799>

Annexure

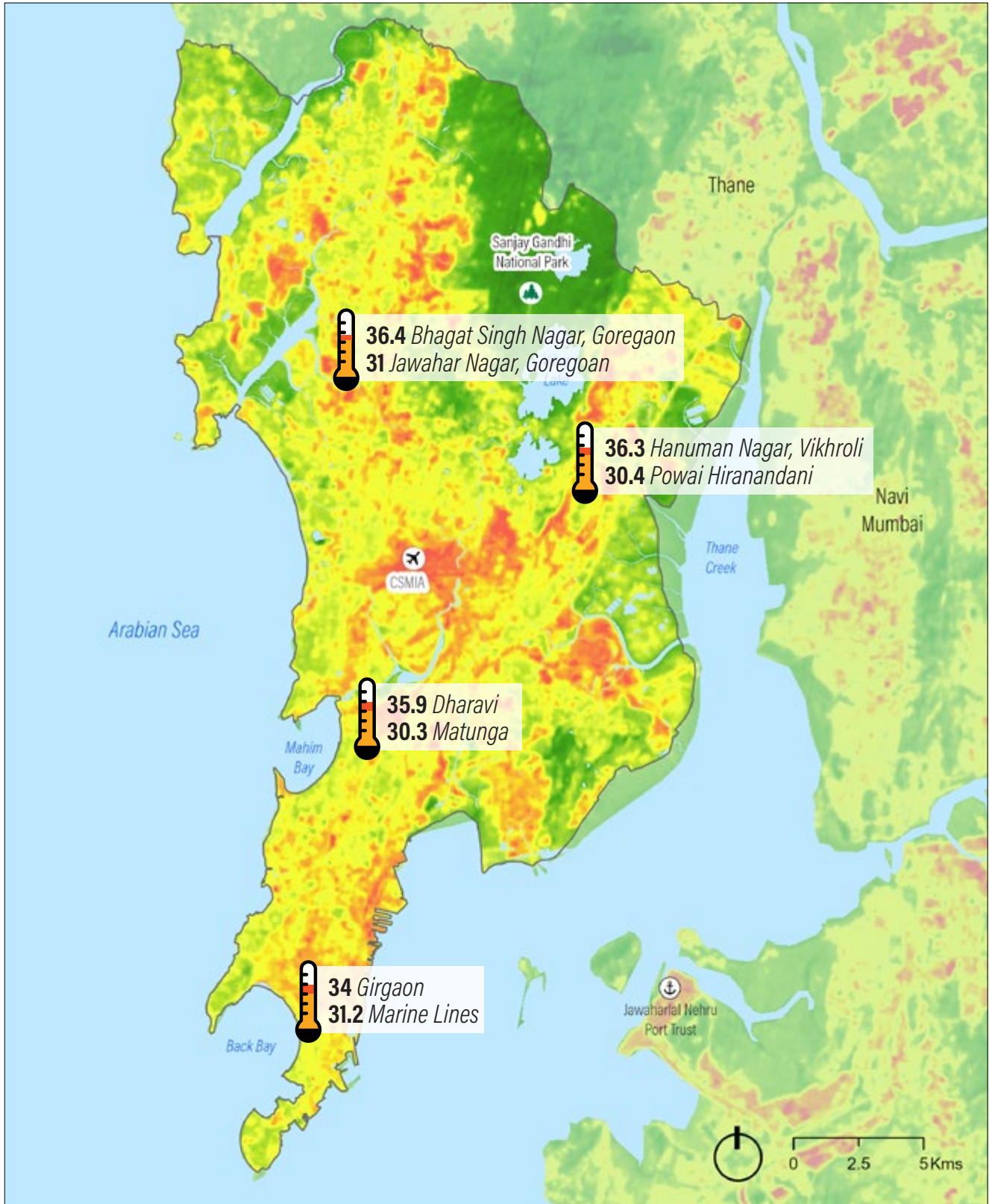
All figures and illustrations

A.1 Climate Risk Context



Image Credit: Aaran Patel

Figure 32 | Mean Land Surface Temperature (October month: 2017-2019)

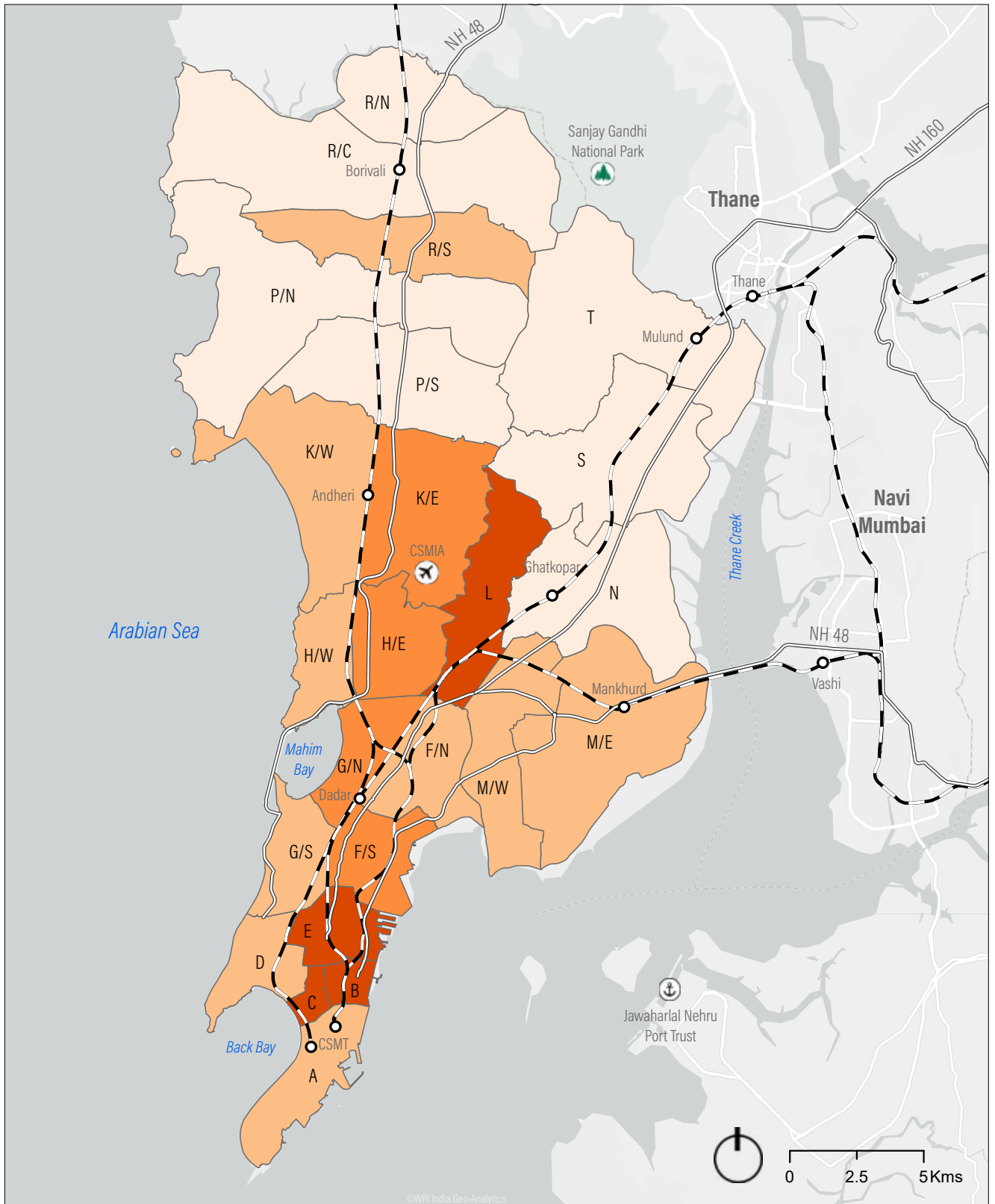


Mean LST: +25°C to +42°C

- Waterbody
- BMC Boundary
- Airport
- National Park
- Sea Port

Source: WRI India derived from LandSat 8(USGS)

Figure 33 | Ward-wise Mean Land Surface Temperature (October month: 2017-2019)



Ward-wise LST in °C: 29-31 31-32 32-33 33-34

BMC Boundary
 Highway
 Airport
🌳 National Park
 Railway Line
 Sea Port

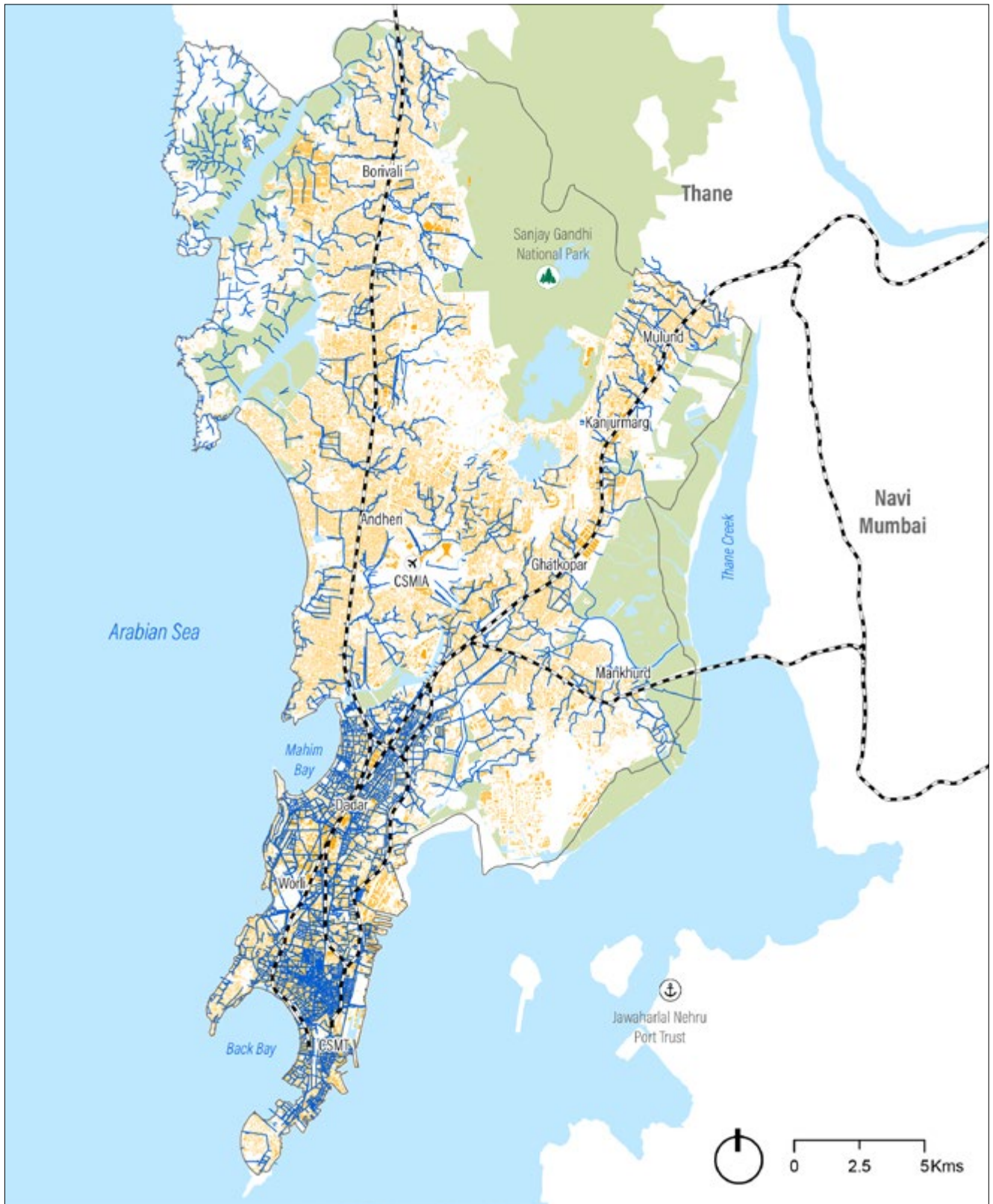
Source: WRI India derived using LandSat 8 (USGS)

Figure 34 | Mean Normalised Difference Vegetation Index (2015-2020)



Source: WRI India; Modified Copernicus Sentinel Data between 2015 and 2020; LandSat 8 (USGS) for October month between 2017 and 2019

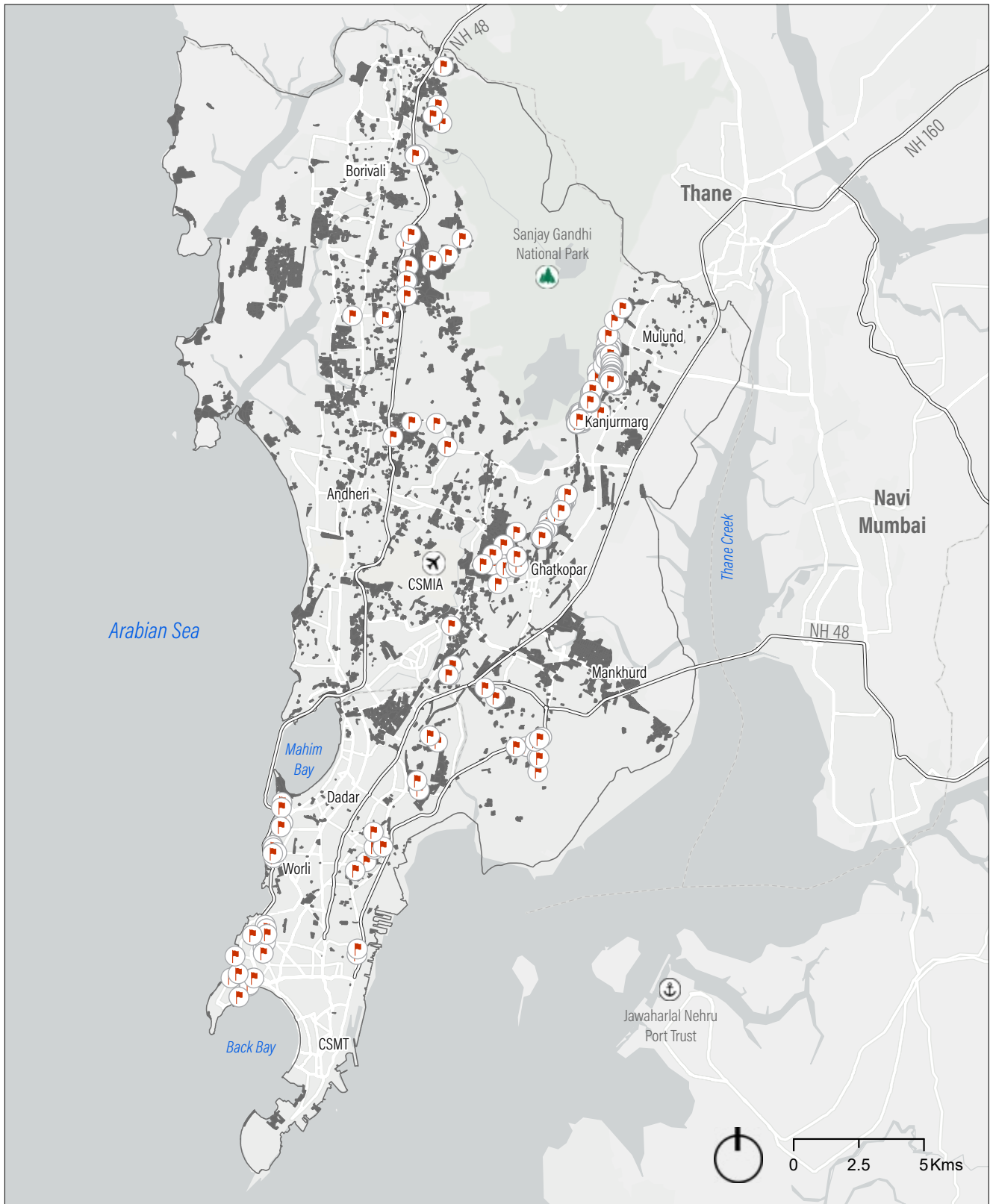
Figure 35 | Stormwater Drainage Network and Built-up Footprint



- Stormwater Drain
- Built-up
- Green Cover
- Waterbody
- BMC Boundary
- 🌳 National Park
- ✈️ Airport
- ⚓ Sea Port
- Railway Line

Source: WRI India; BMC

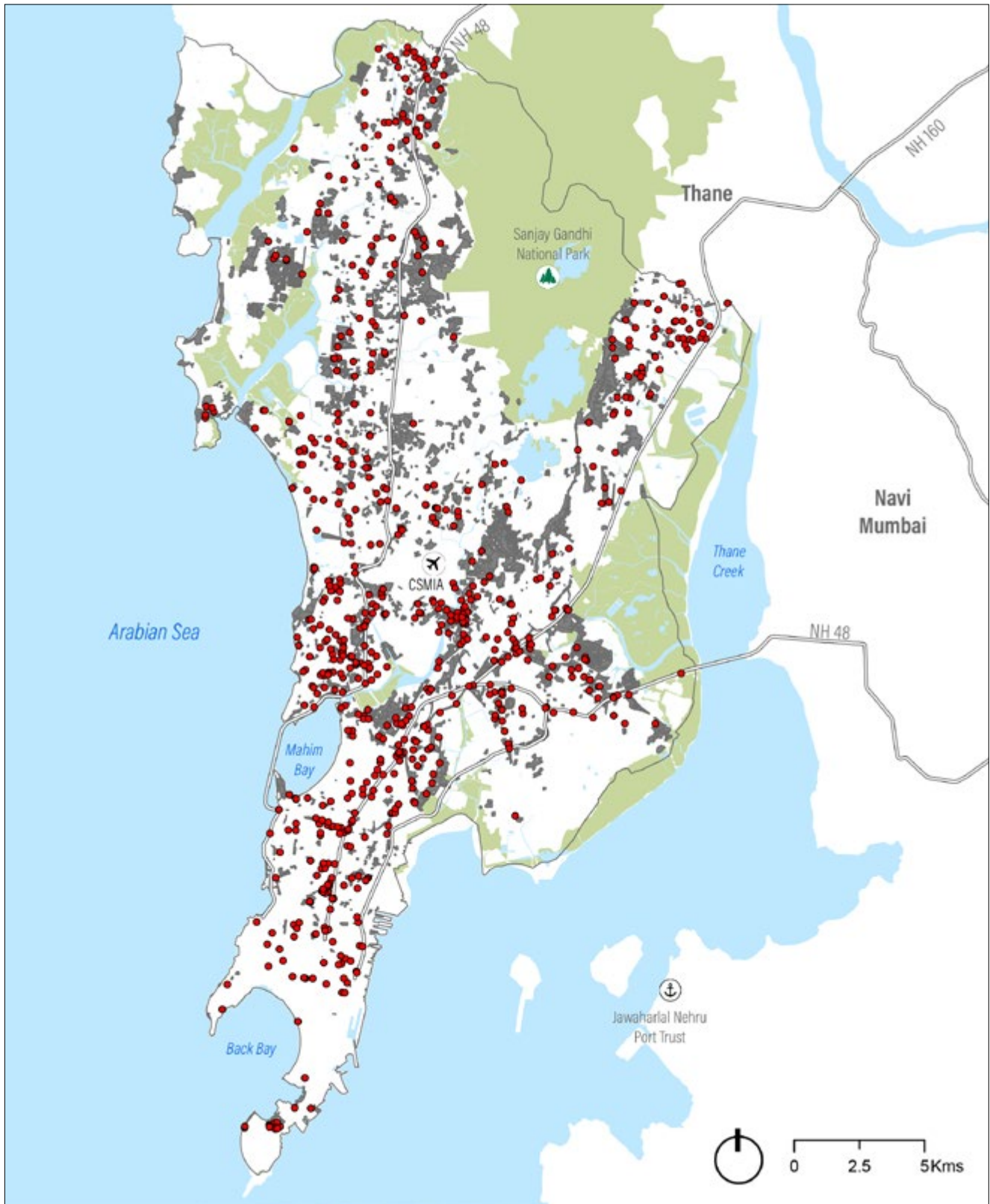
Figure 36 | Landslide Prone Locations and Informal Settlements



- | | | | |
|----------------------------|---------------|--------------|----------|
| Landslide Prone Location | BMC Boundary | Highway | Airport |
| Informal Settlements/Slums | National Park | Railway Line | Sea Port |

Source: WRI India; BMC

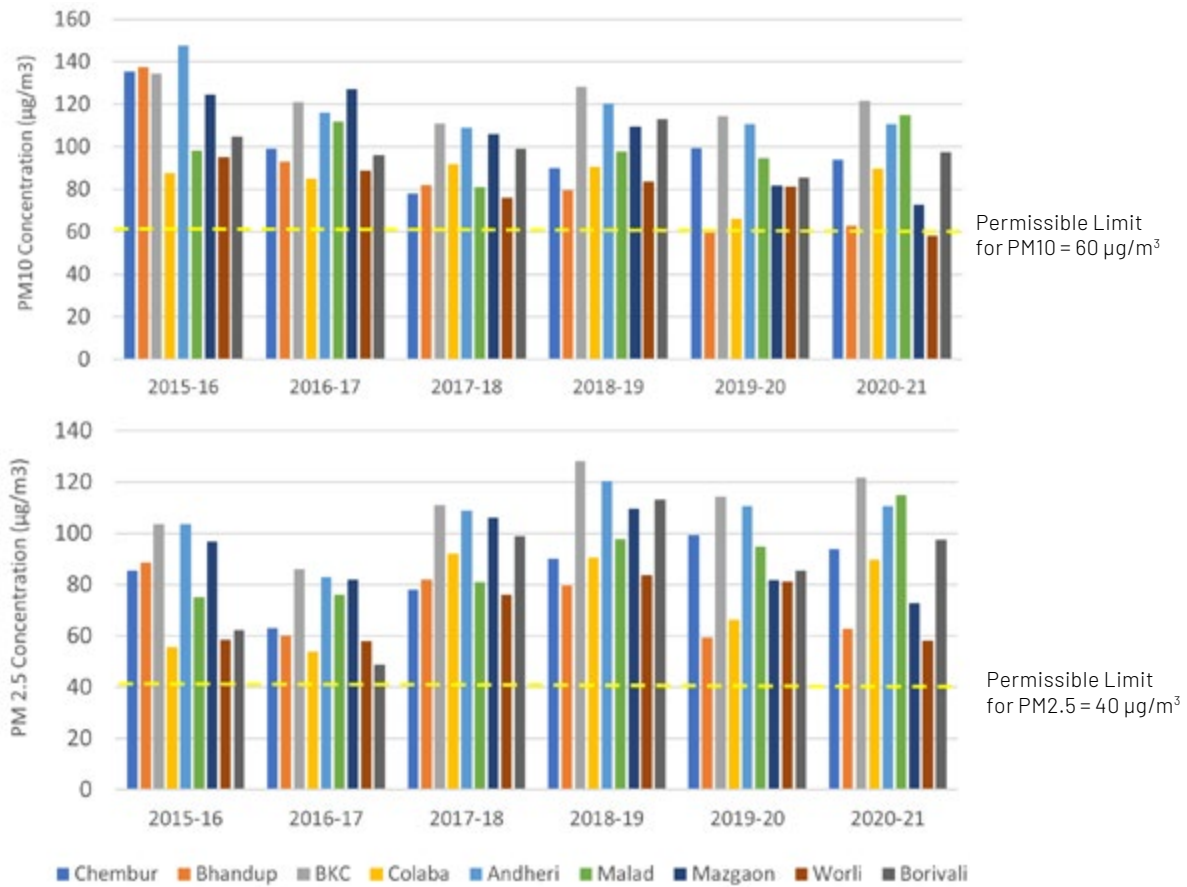
Figure 37 | Flooding Hotspots and Informal Settlements



- Flooding Hotspots
- Informal Settlements/Slums
- Forests & Mangroves
- Waterbody
- BMC Boundary
- 🌳 National Park
- ✈️ Airport
- ⚓ Sea Port

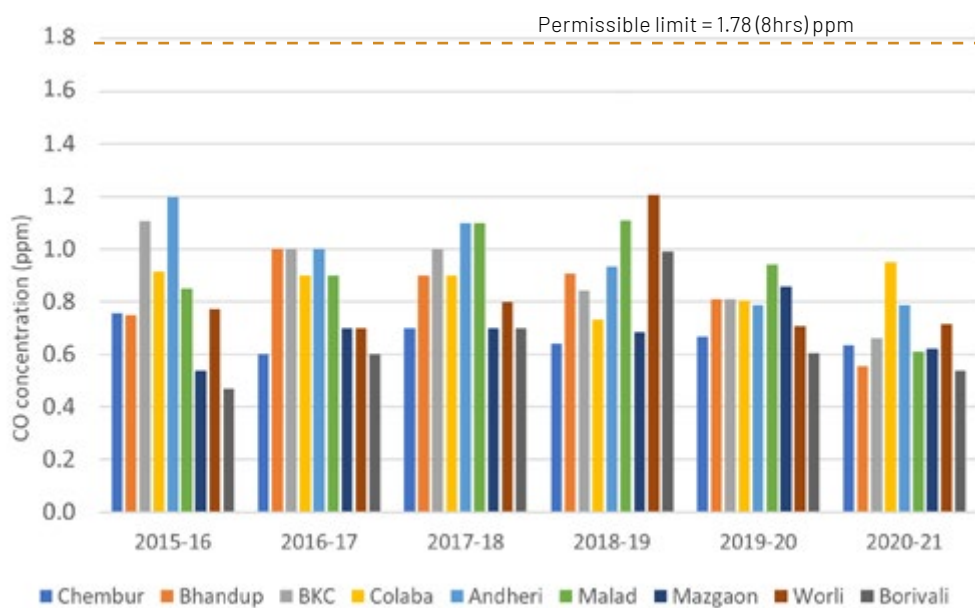
Source: WRI India; BMC

Figure 38 | Annual Average Concentration of PM10 and PM2.5 for SAFAR Monitoring Stations from July 2015 to March 2021.



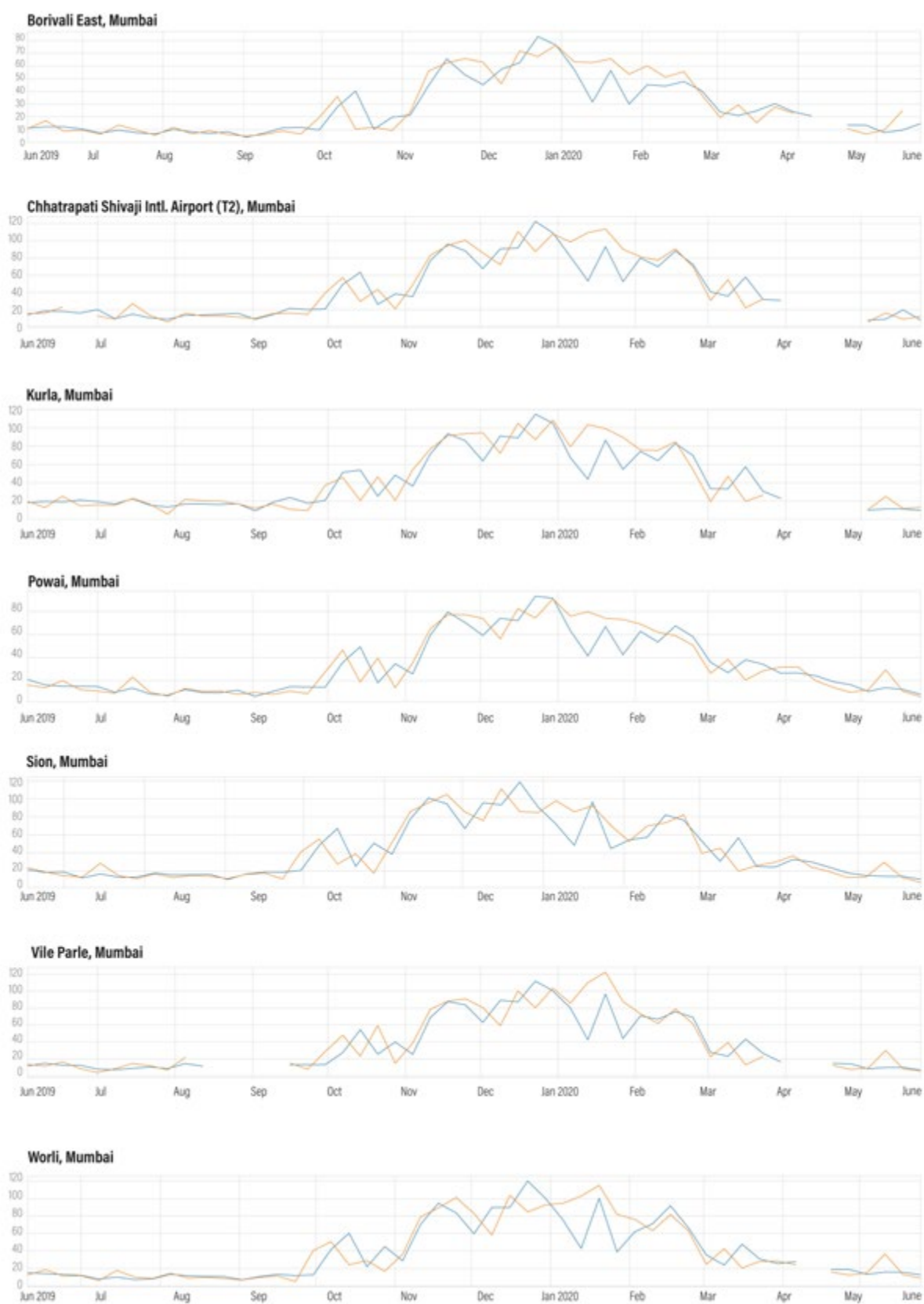
Source: 9 monitoring stations - SAFAR, Mumbai

Figure 39 | Station-wise annual average Carbon Monoxide (CO) Levels at Monitoring Stations in Mumbai from July 2015 to March 2021



Source: Source: 9 Monitoring stations - SAFAR, Mumbai; NAAQ Standards, CPCB

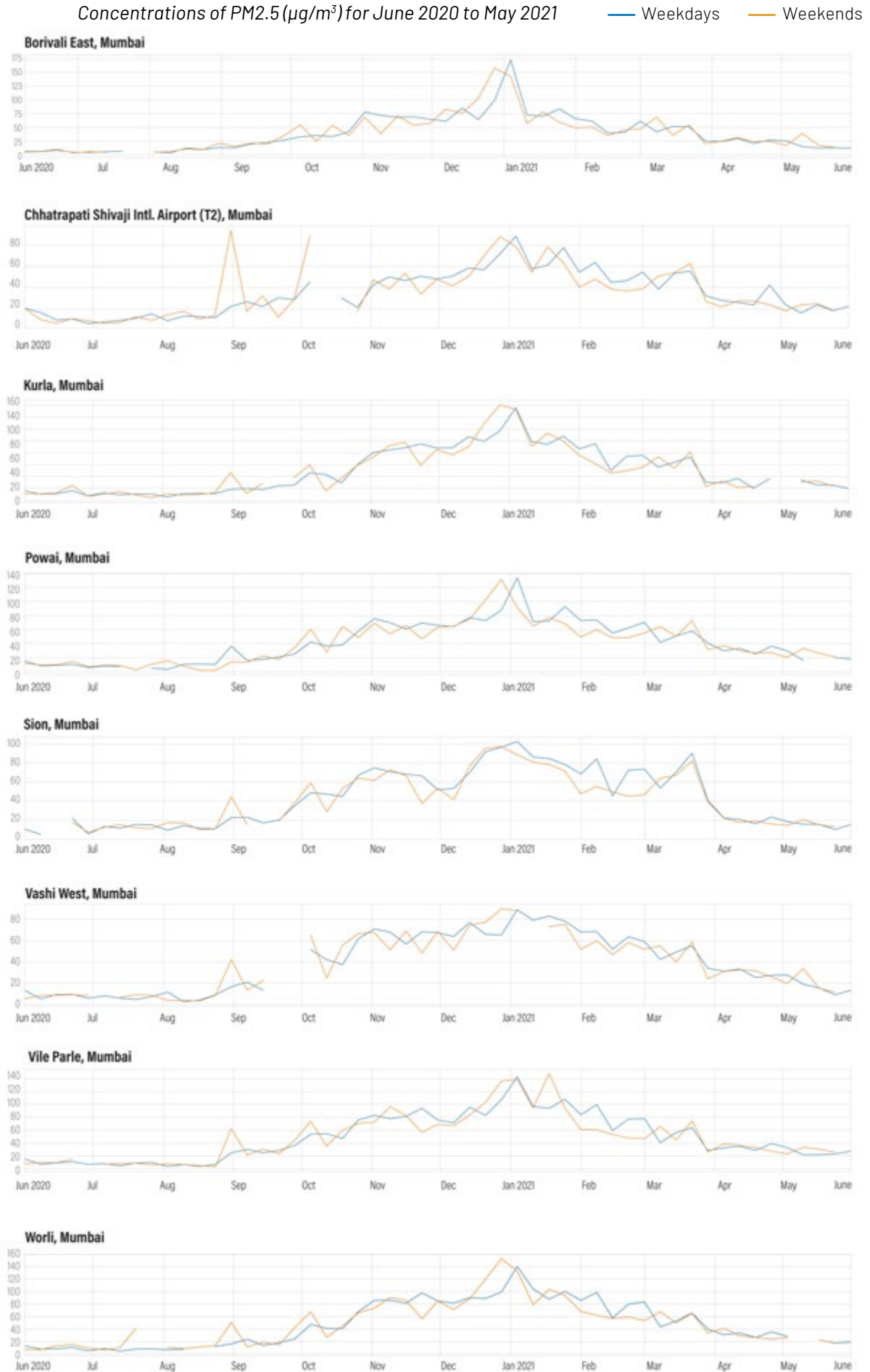
Figure 40 | Monthly Variation using Mean Weekday and Weekend Concentrations of PM2.5 ($\mu\text{g}/\text{m}^3$) for June 2019 to May 2020



Source for Figures 40, 41: 9 monitoring stations - CAAQMS, CPCB 2021

Note: For Bandra and Colaba PM2.5 Concentrations please refer to Figure 22

Figure 41 | Monthly Variation using Mean Weekday and Weekend Concentrations of PM2.5 ($\mu\text{g}/\text{m}^3$) for June 2020 to May 2021

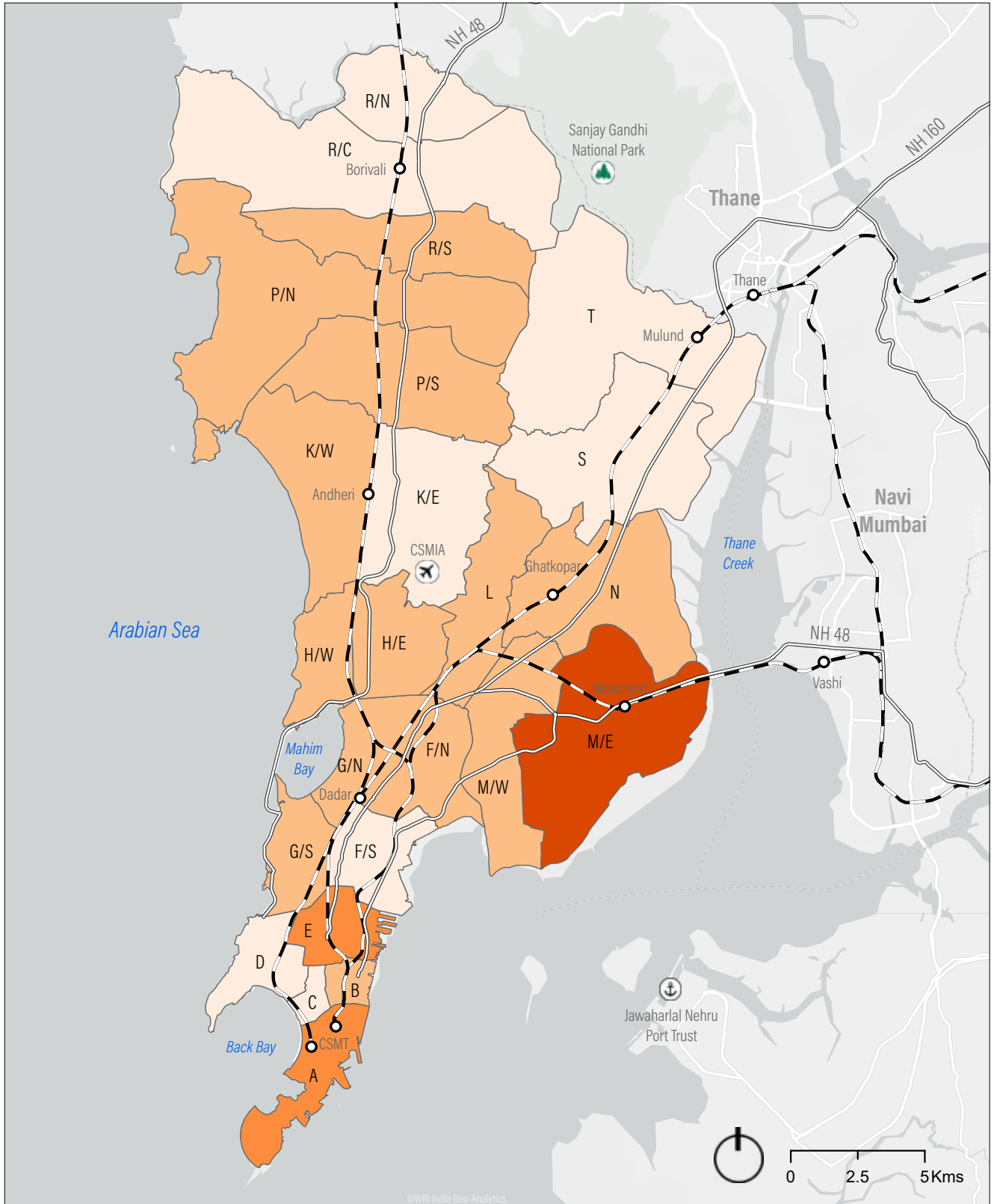


A.2 Demographic Context



Image Credit: Abhinand Gopal

Figure 42 | Ward-wise Effective Literacy Rate

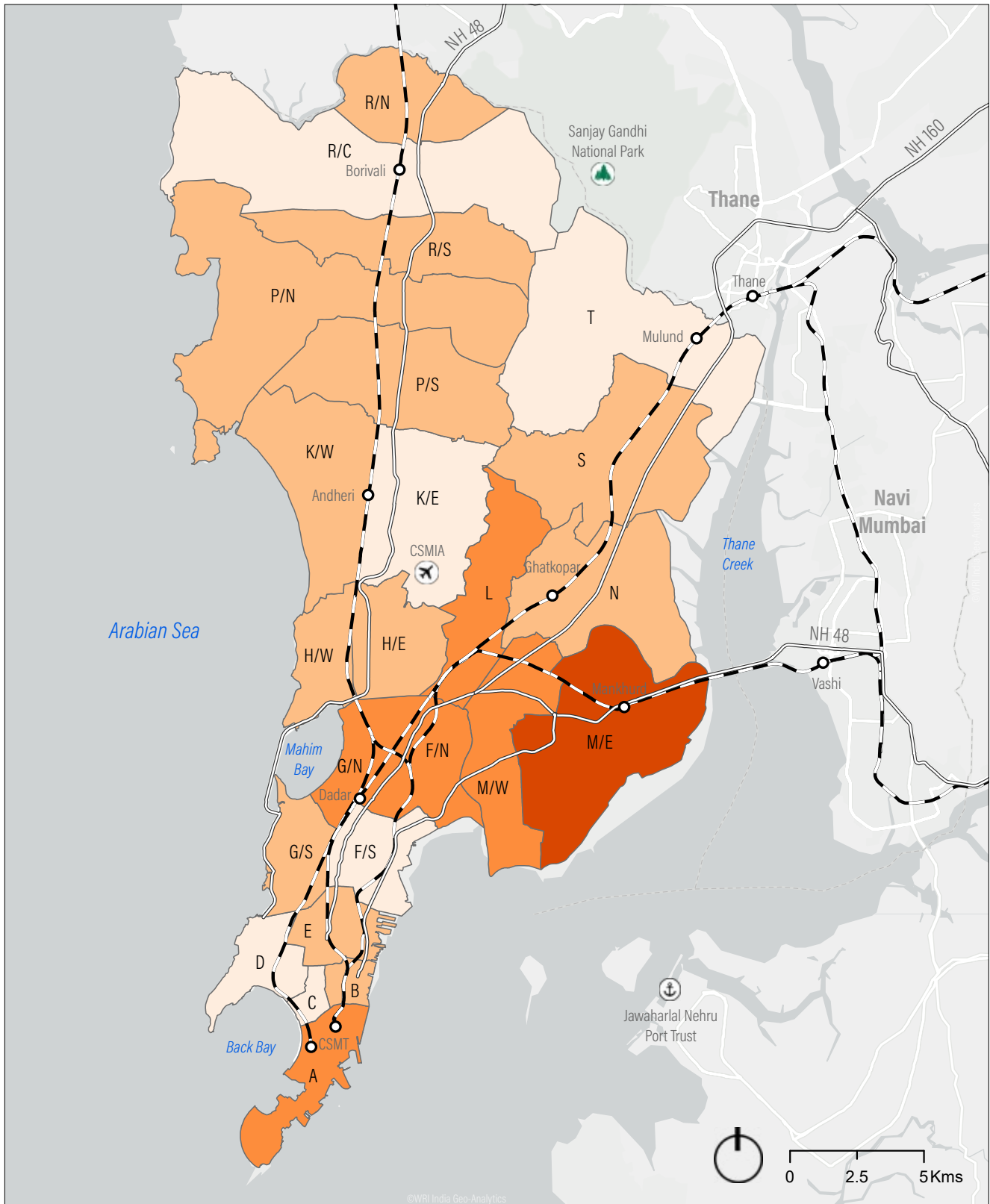


Effective Literacy Rate (%): ■ 83 - 85 ■ 85 - 88 ■ 88 - 91 ■ 91 - 94

— Highway —+— Railway Line ○ Station ✈ Airport ⚓ Sea Port 🌳 National Park

Source: WRI India using Census 2011

Figure 43 | Ward-wise Effective Female Literacy Rate

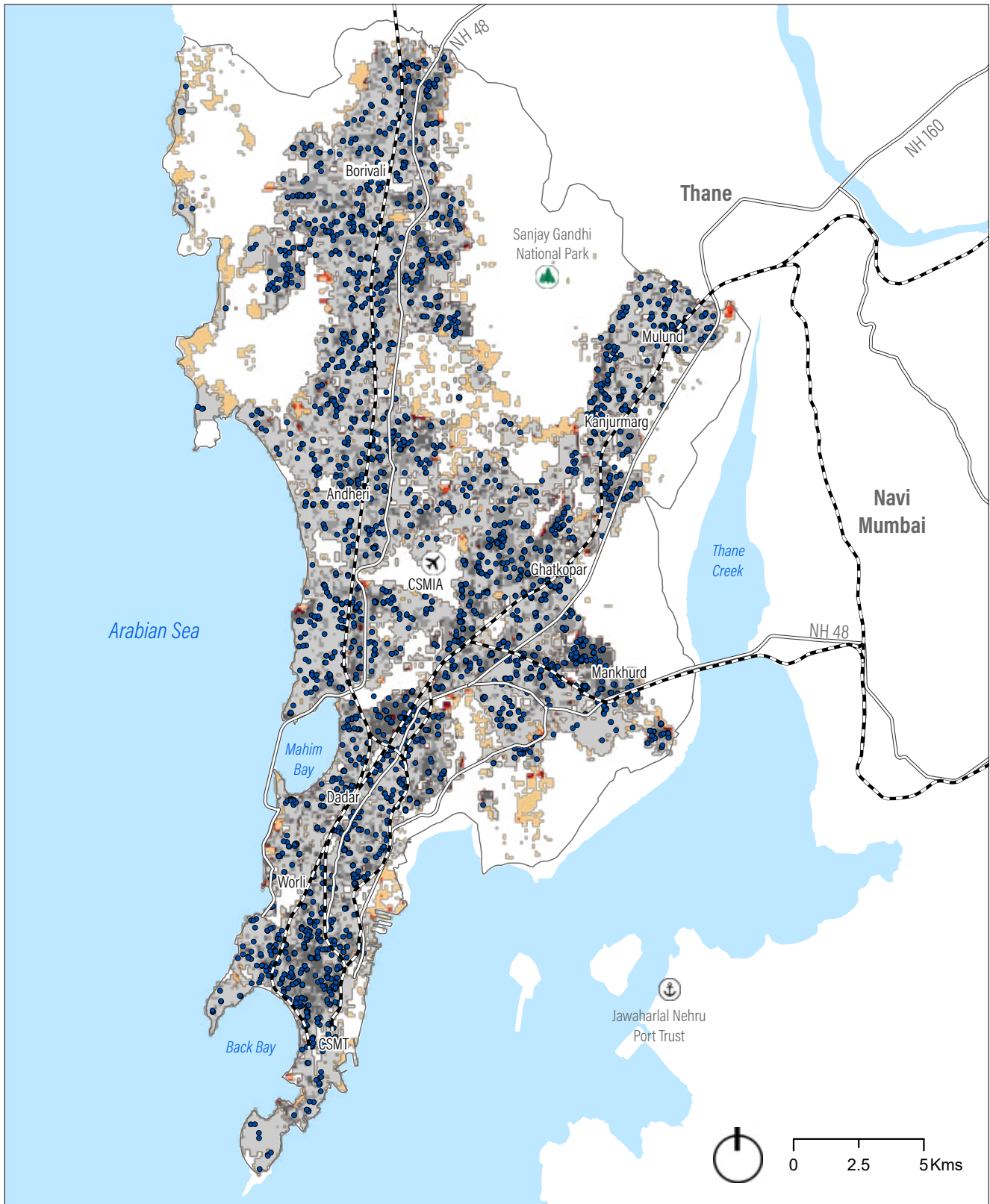


Effective Female Literacy Rate(%): ■ 78-81 ■ 81-85 ■ 85-88 ■ 88-92

— Highway - - - Railway Line ○ Station ✈ Airport ⚓ Sea Port 🌳 National Park

Source: WRI India using Census 2011

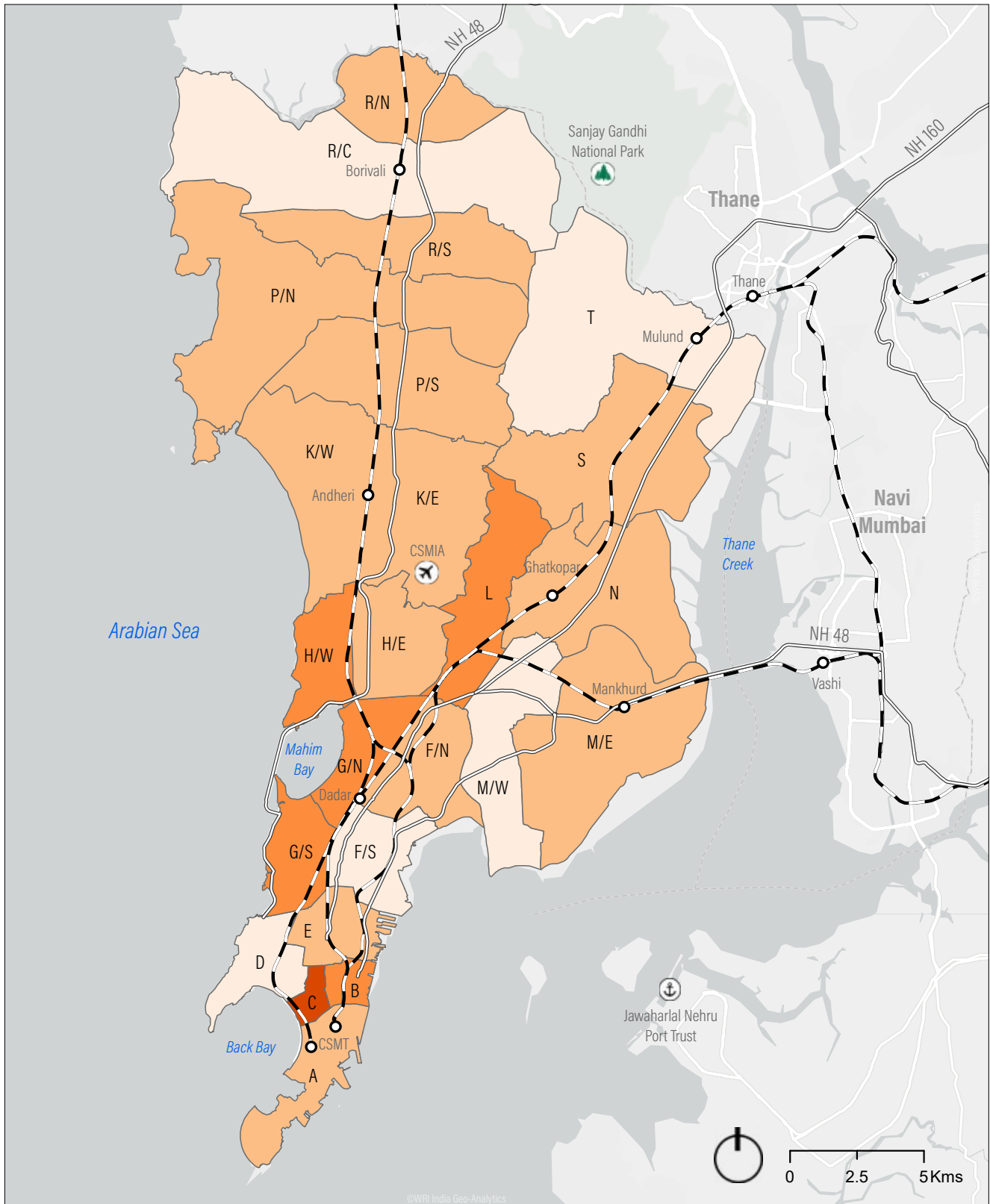
Figure 44 | Access to Educational Institutions



- | | | | | |
|--|----------------|---------------|------------------|-----------------|
| Population lacking Access to Schools: | ■ 5 - 500 | ■ 500 - 1,000 | ■ 1,000 - 13,800 | ● School |
| Population having Access to Schools: | ■ 5 - 500 | ■ 500 - 1,000 | ■ 1,000 - 13,800 | □ BMC Boundary |
| — Highway | — Railway Line | ○ Station | ✈ Airport | ⚓ Sea Port |
| | | | | 🌳 National Park |

Source: WRI India using data from BMC; Census 2011; OpenStreetMap Note: Service area defined by 1 km walking distance; Population in persons per hectare (Ha)

Figure 45 | Gender Imbalance - Sex Ratio

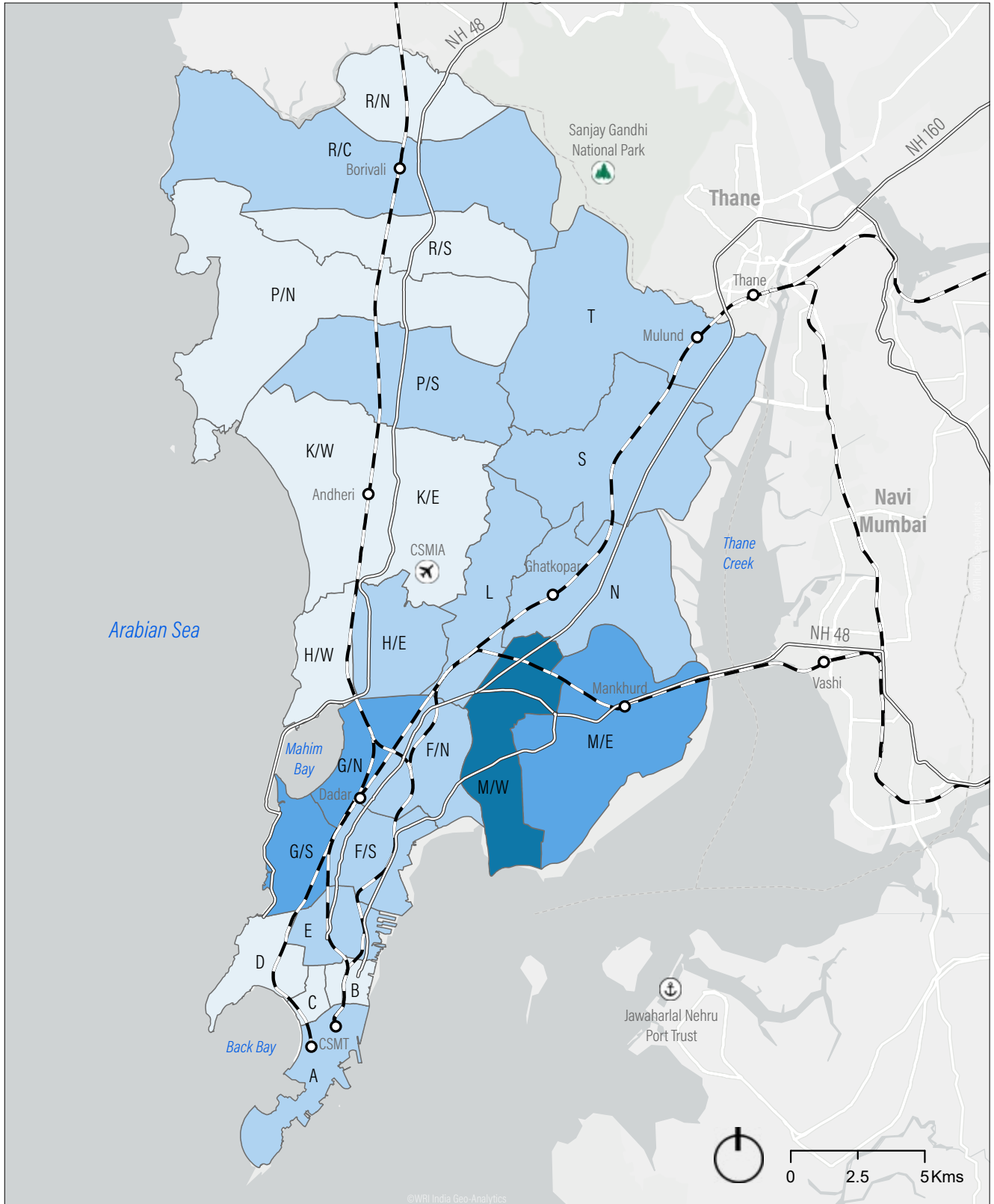


Sex Ratio: ■ 690 - 750 ■ 750 - 820 ■ 820-890 ■ 890-950

Highway Railway Line Airport Station
 Railway Line Sea Port

Source: WRI India using Census 2011

Figure 46 | Social Composition - Percentage of SC/ST Population



Percentage of SC/ST Population: □ 1 - 6 □ 6 - 10 □ 10 - 14 □ 14 - 19
 — Highway - - - Railway Line ○ Station ✈ Airport ⚓ Sea Port 🌳 National Park

Source: WRI India using Census 2011

A.3 Vulnerability Assessment



Image Credit: Sonika Agarwal; Modified by WRI India

Figure 47 | Access to Information based on Asset Ownership - Information Access via Broadcast Media

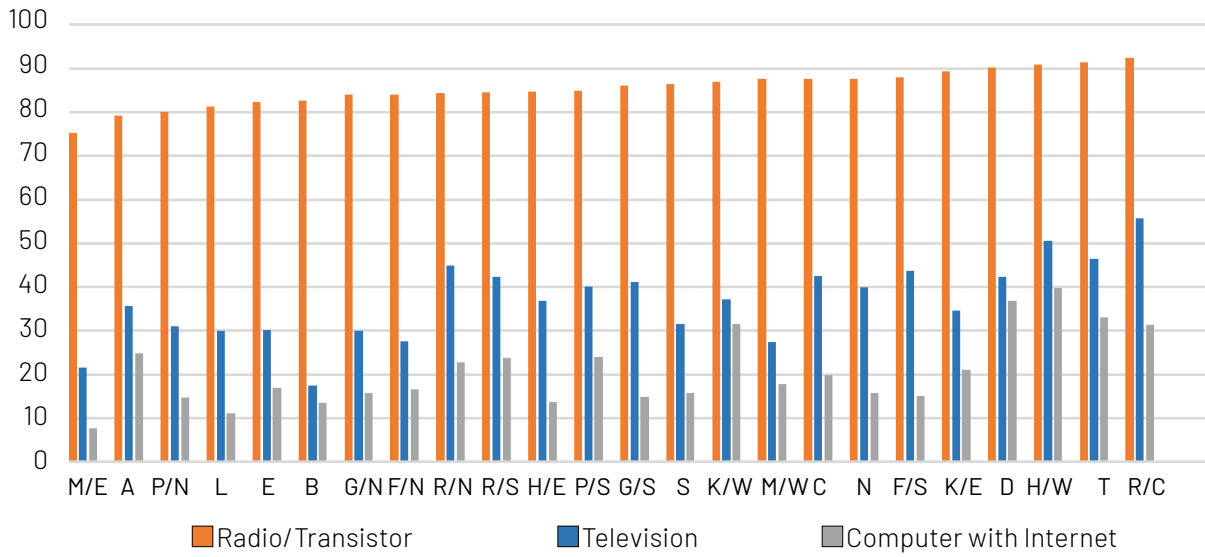
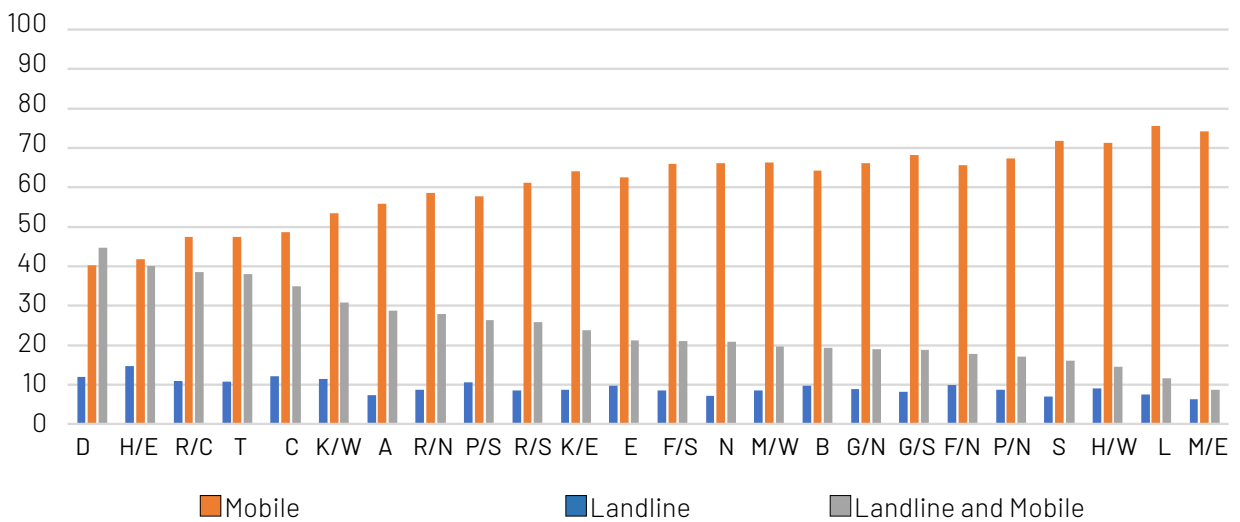
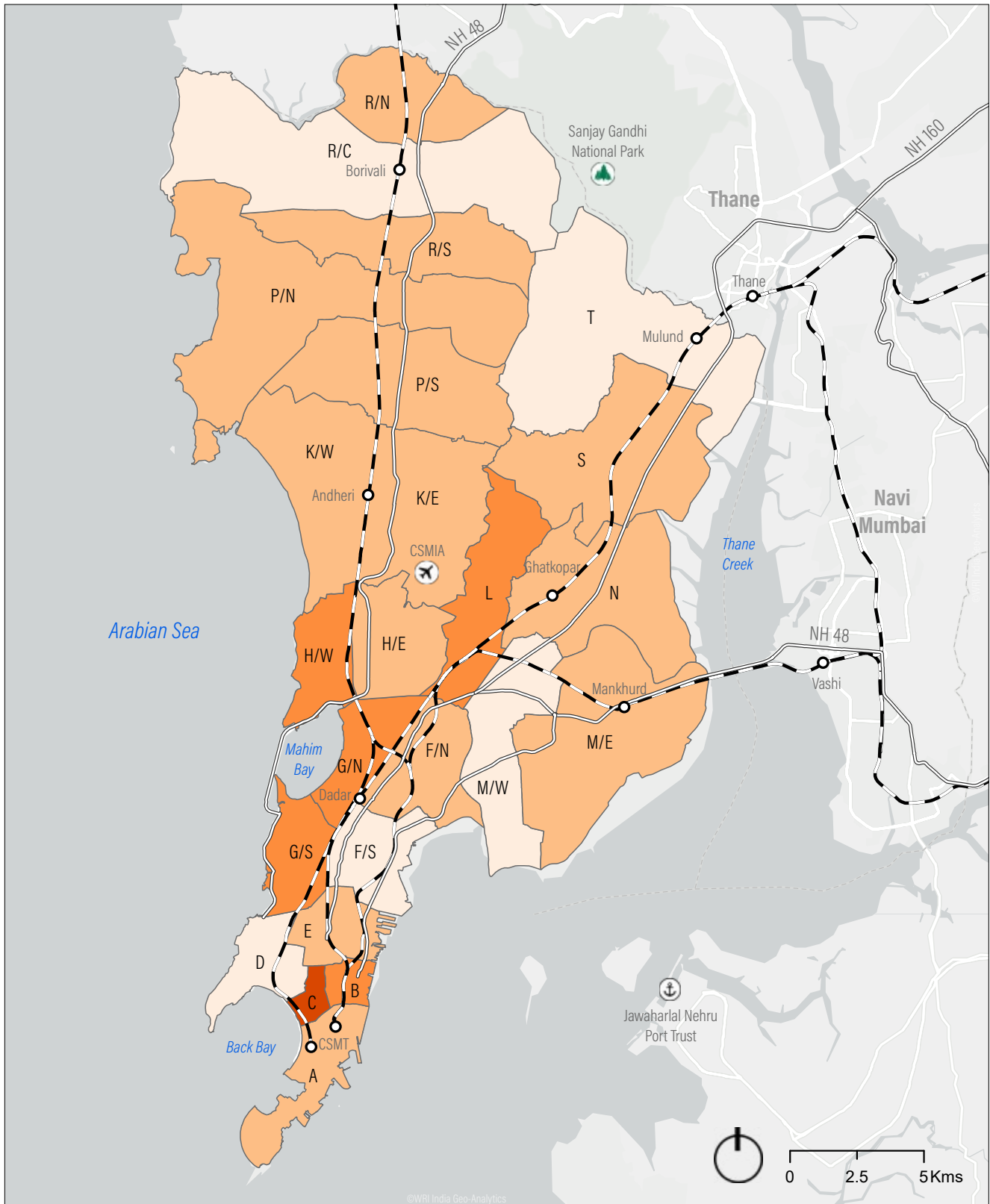


Figure 48 | Access to Information based on Asset Ownership - Information Access via Telephone



Source for Figures 47,48: WRI India using Census 2011

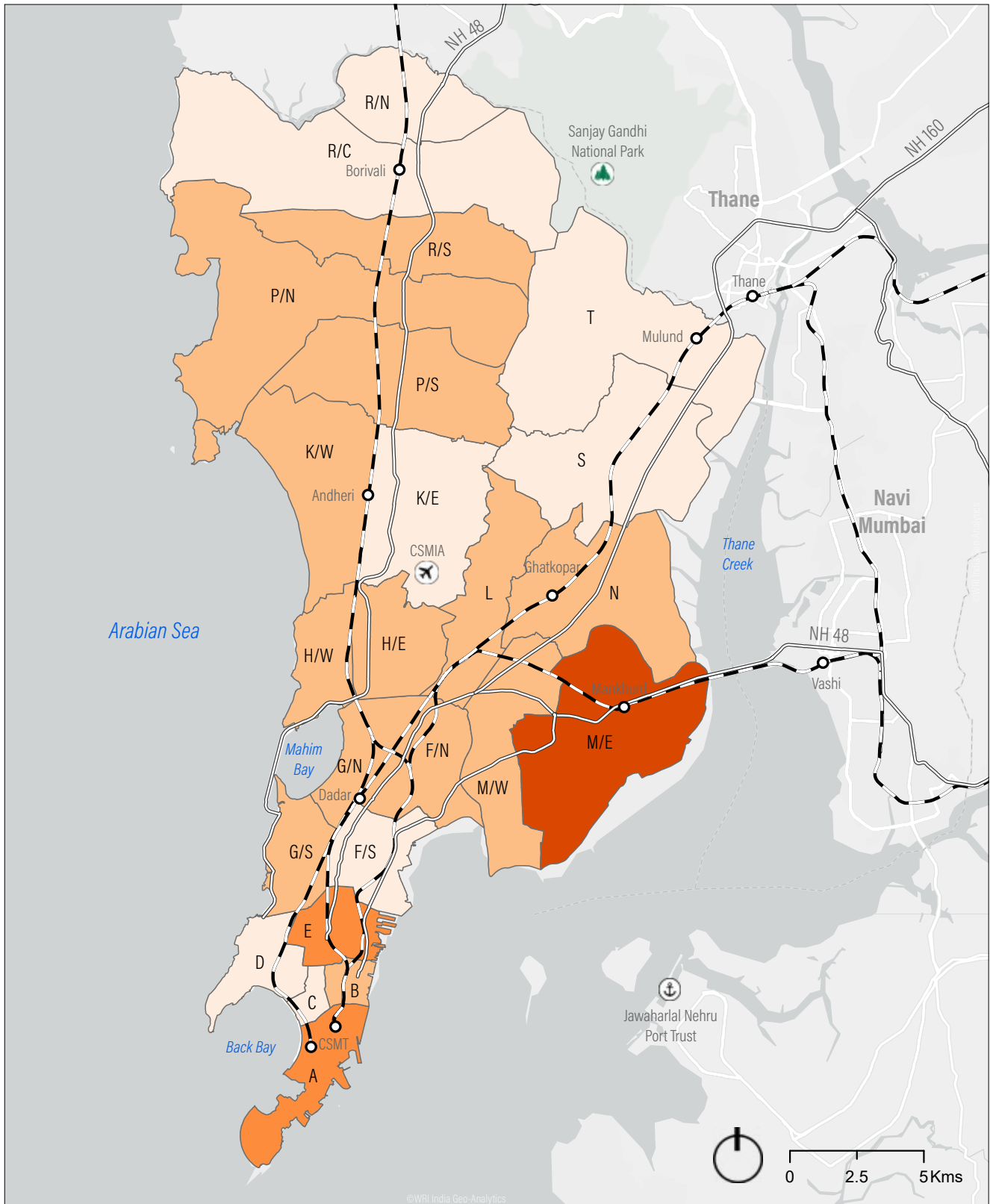
Figure 49 | Home Ownership



Percentage of Households Living in Own House: 54 - 61 61 - 68 68 - 75 75 - 83
 — Highway - - - Railway Line ○ Station ✈ Airport ⚓ Sea Port 🌳 National Park

Source: WRI India using Census 2011

Figure 50 | House Condition

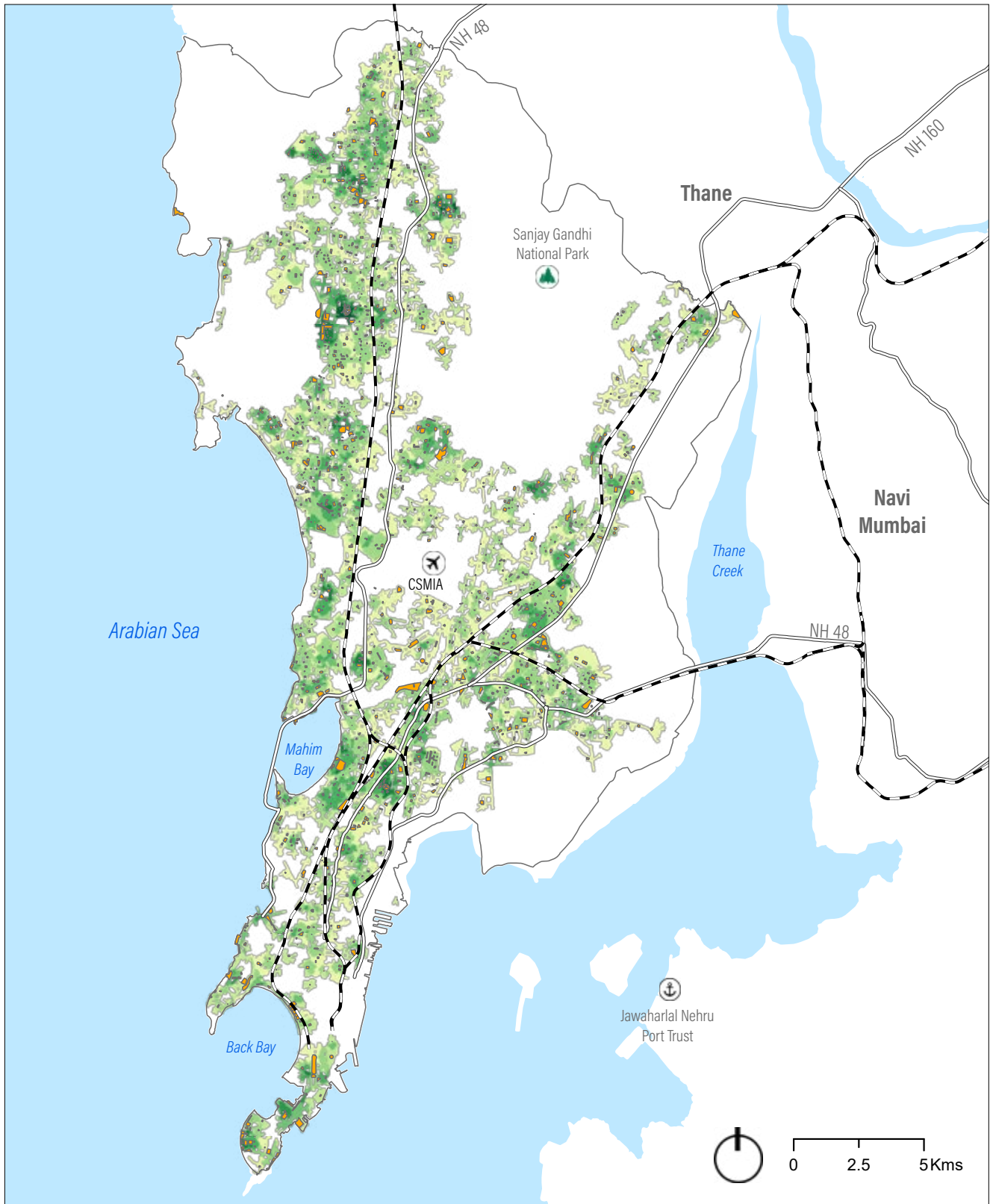


Percentage Households with Temporary Roofing Material: 10 - 22 22 - 36 36 - 50 55 - 65

— Highway - - - Railway Line ○ Station ✈ Airport ⚓ Sea Port 🌳 National Park

Source: WRI India using Census 2011

Figure 51 | Access to Daily Urban Recreation Spaces

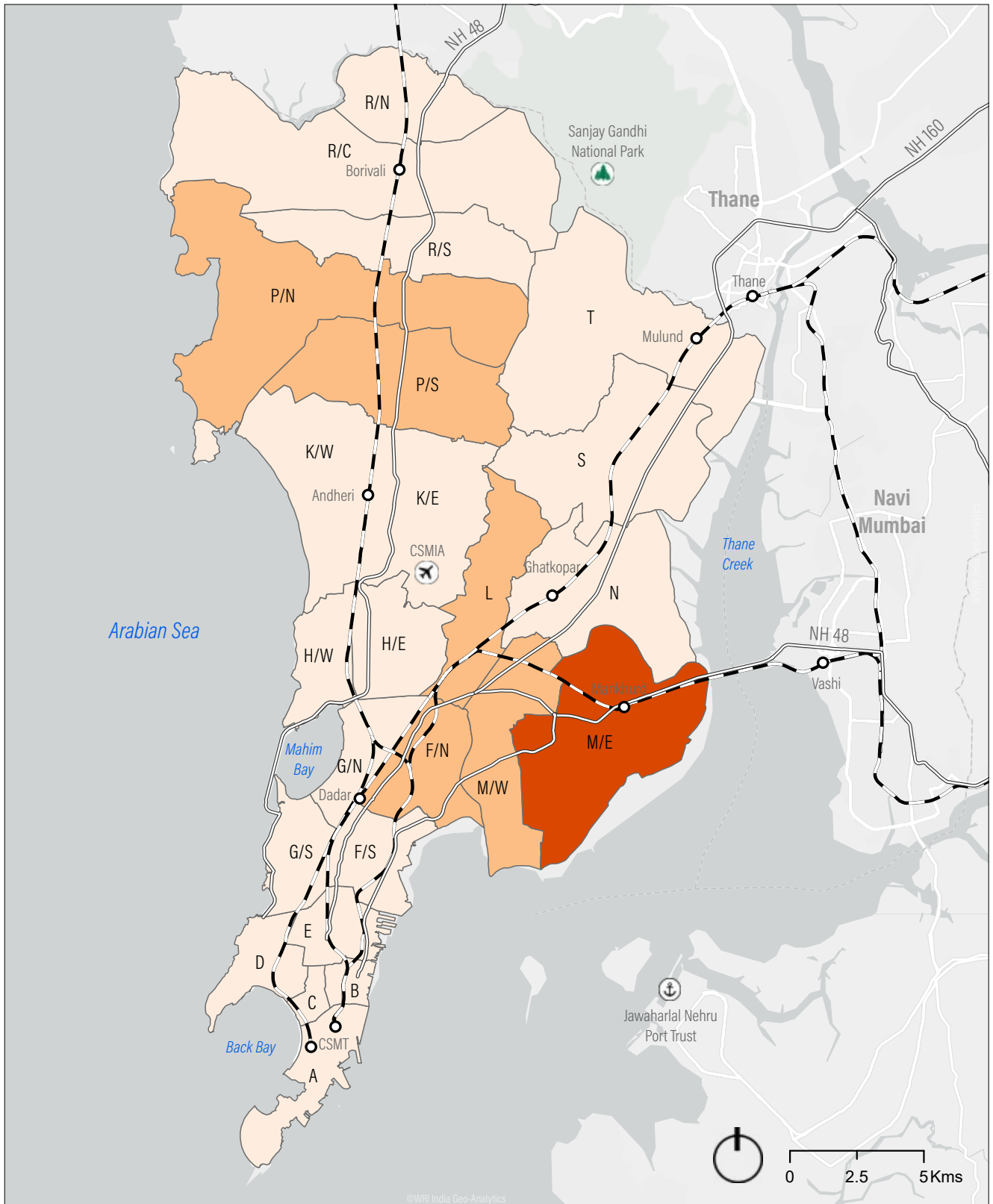


Access to Daily Urban Recreation Spaces: Low Access High Access Recreational Open Spaces
 — Highway —+— Railway Line ○ Station ✈️ Airport ⚓ Sea Port 🌳 National Park

Source: WRI India using data from BMC; OpenStreetMap

Note: Assumed service radii - Children's Park- 250 m, Neighborhood Park- 500 m, Institutional Playgrounds, Maidans & District Park- 1,000 m

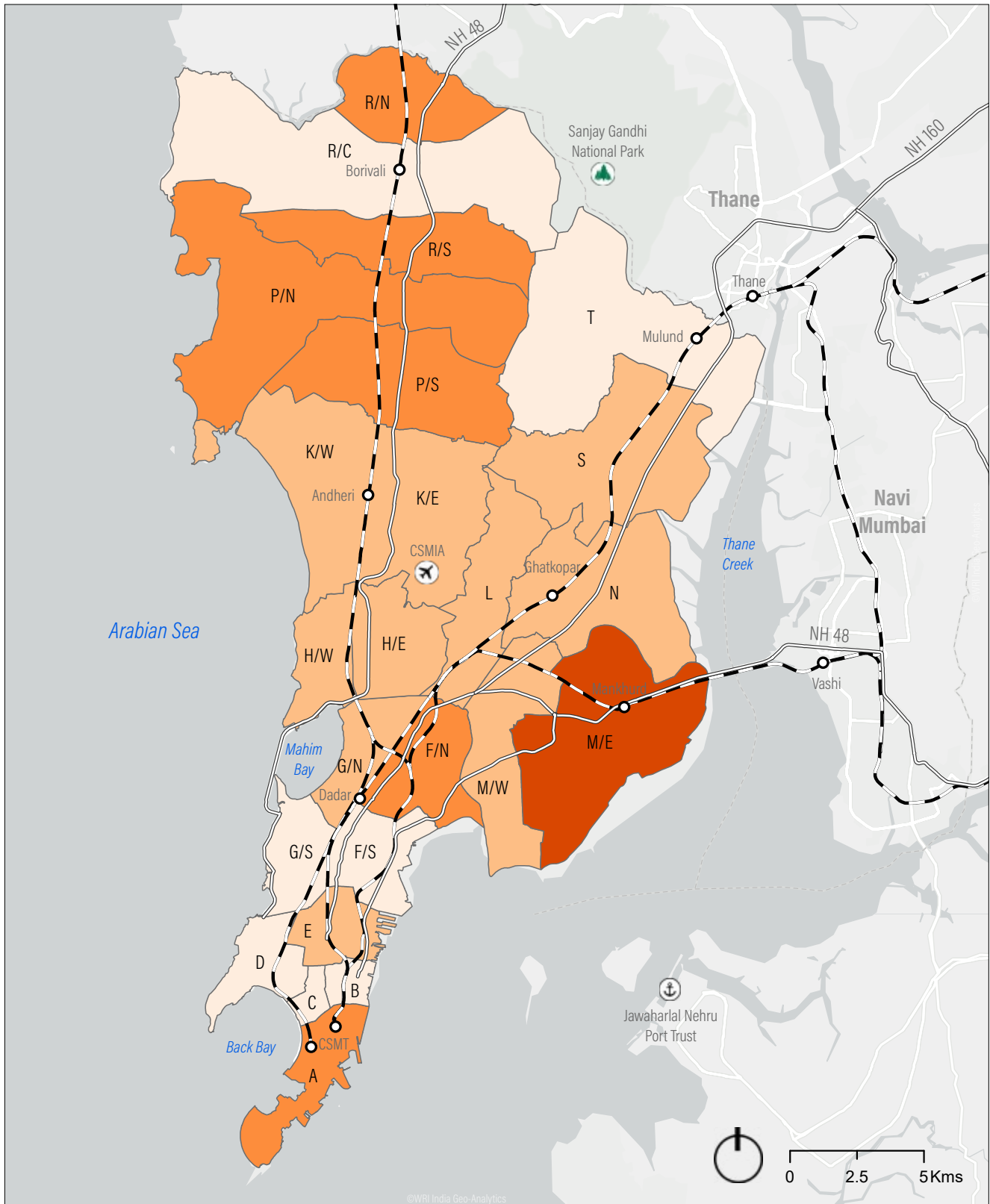
Figure 52 | Access to Drinking Water



Households having Access to Tap Water from Treated Source (%): ■ 82 - 86 ■ 86 - 90 ■ 90 - 94 ■ 94 - 98
 — Highway - - - Railway Line ○ Station ✈️ Airport ⚓ Sea Port 🌳 National Park

Source: WRI India using Census 2011

Figure 53 | Access to Drinking Water

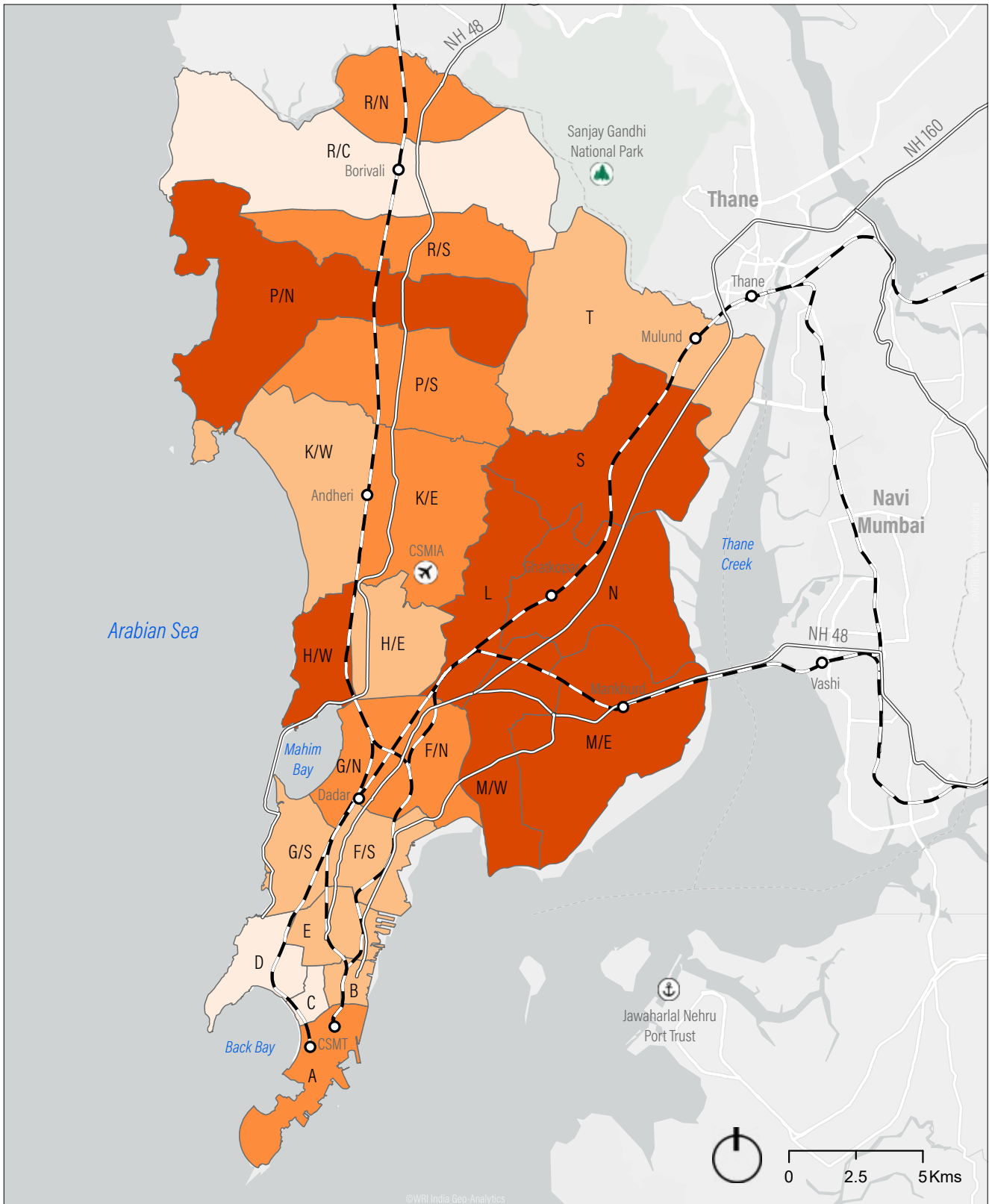


Households with Drinking Water Source within Premises (%): ■ 53 - 64 ■ 64 - 75 ■ 75 - 87 ■ 87 - 99

— Highway - - - Railway Line ○ Station ✈️ Airport ⚓ Sea Port 🌳 National Park

Source: WRI India using Census 2011

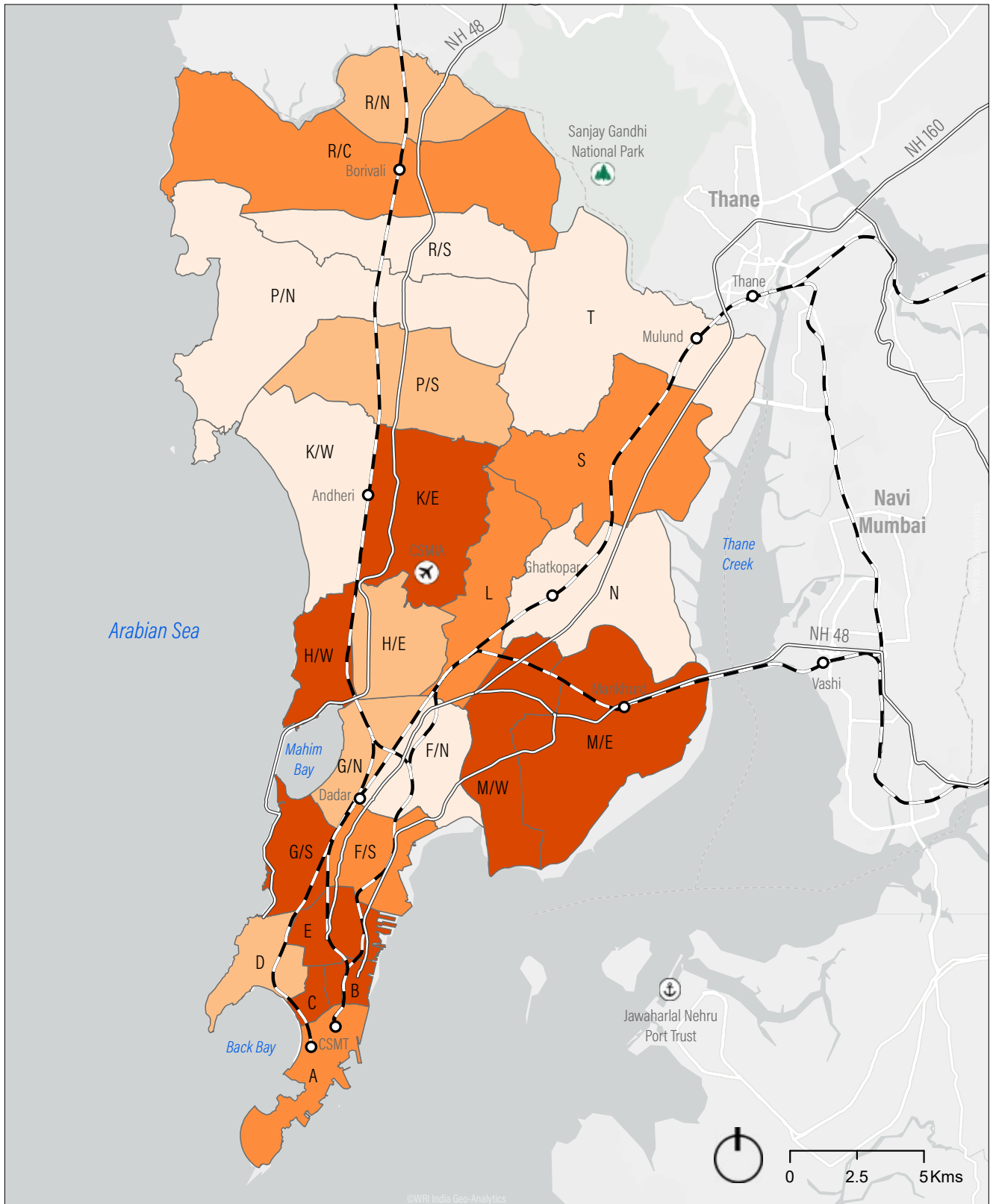
Figure 54 | Access to Sanitation



Households having Latrine within Premises (%): ■ 35 - 50 ■ 50 - 65 ■ 65 - 80 ■ 80 - 95
 — Highway - - - Railway Line ○ Station ✈ Airport ⚓ Sea Port 🌳 National Park

Source: WRI India using Census 2011

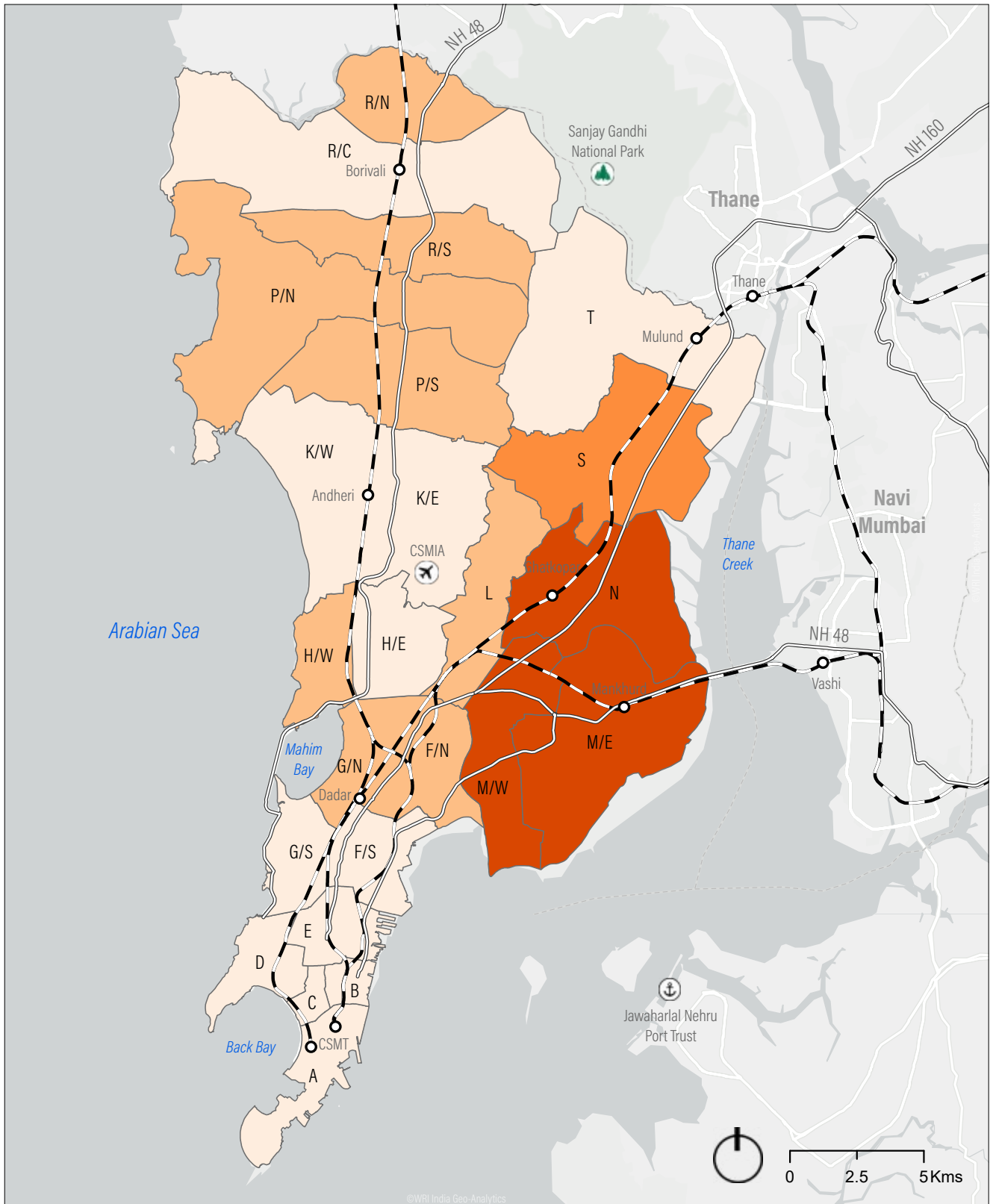
Figure 55 | Access to Sanitation



Households following Unhygienic Sewage Disposal (%): ■ 1.6 - 2.2 ■ 2.2 - 2.8 ■ 2.8 - 3.4 ■ 3.4 - 4.1
 — Highway - - - Railway Line ○ Station ✈ Airport ⚓ Sea Port 🌳 National Park

Source: WRI India using Census 2011

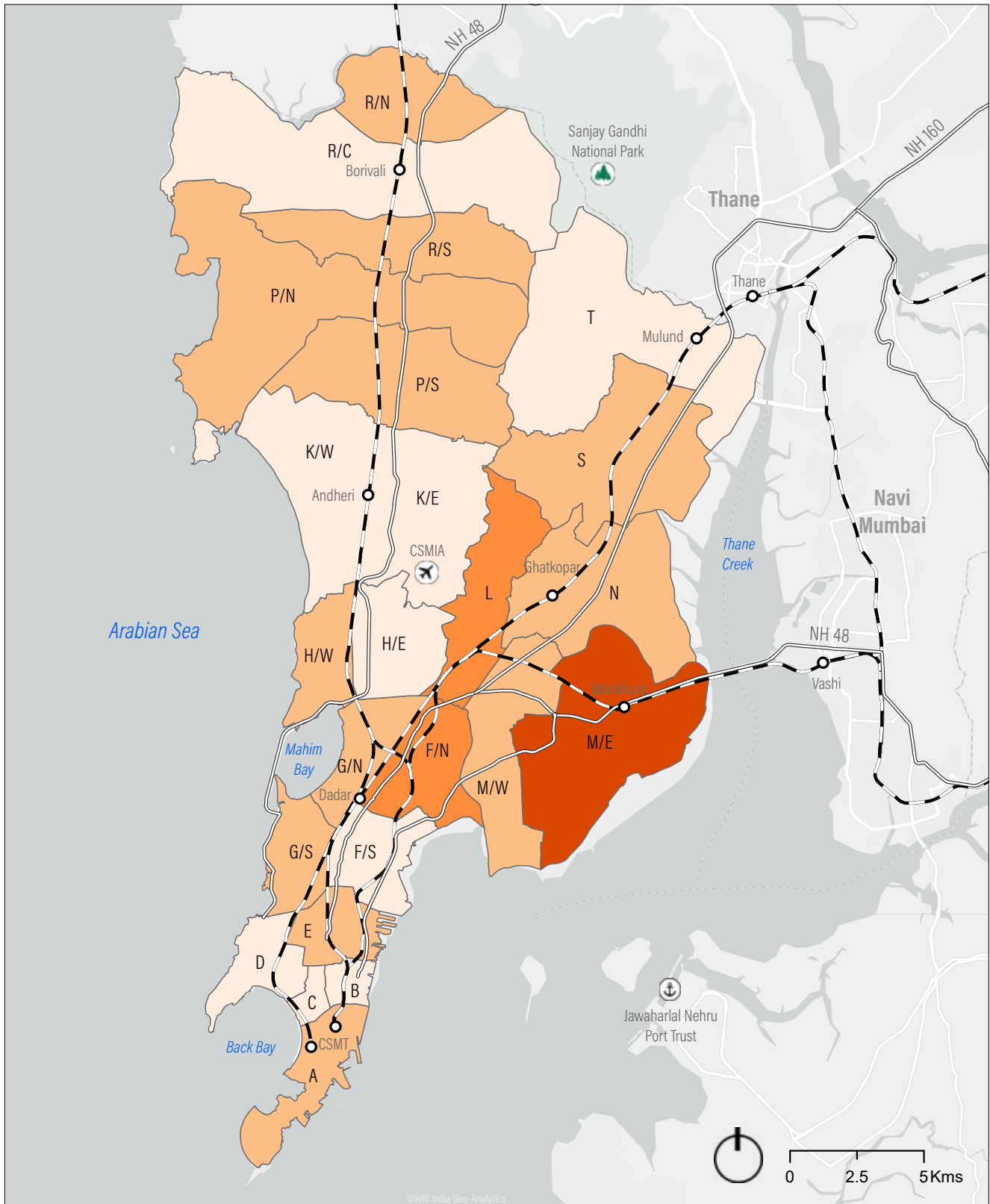
Figure 56 | Access to Sanitation



Households following Unhygienic Waste Water Disposal (%): 1 - 12 12 - 24 24 - 36 36 - 48
 — Highway - - - Railway Line ○ Station ✈ Airport ⚓ Sea Port 🌳 National Park

Source: WRI India using Census 2011

Figure 57 | Access to Clean Cooking Fuel

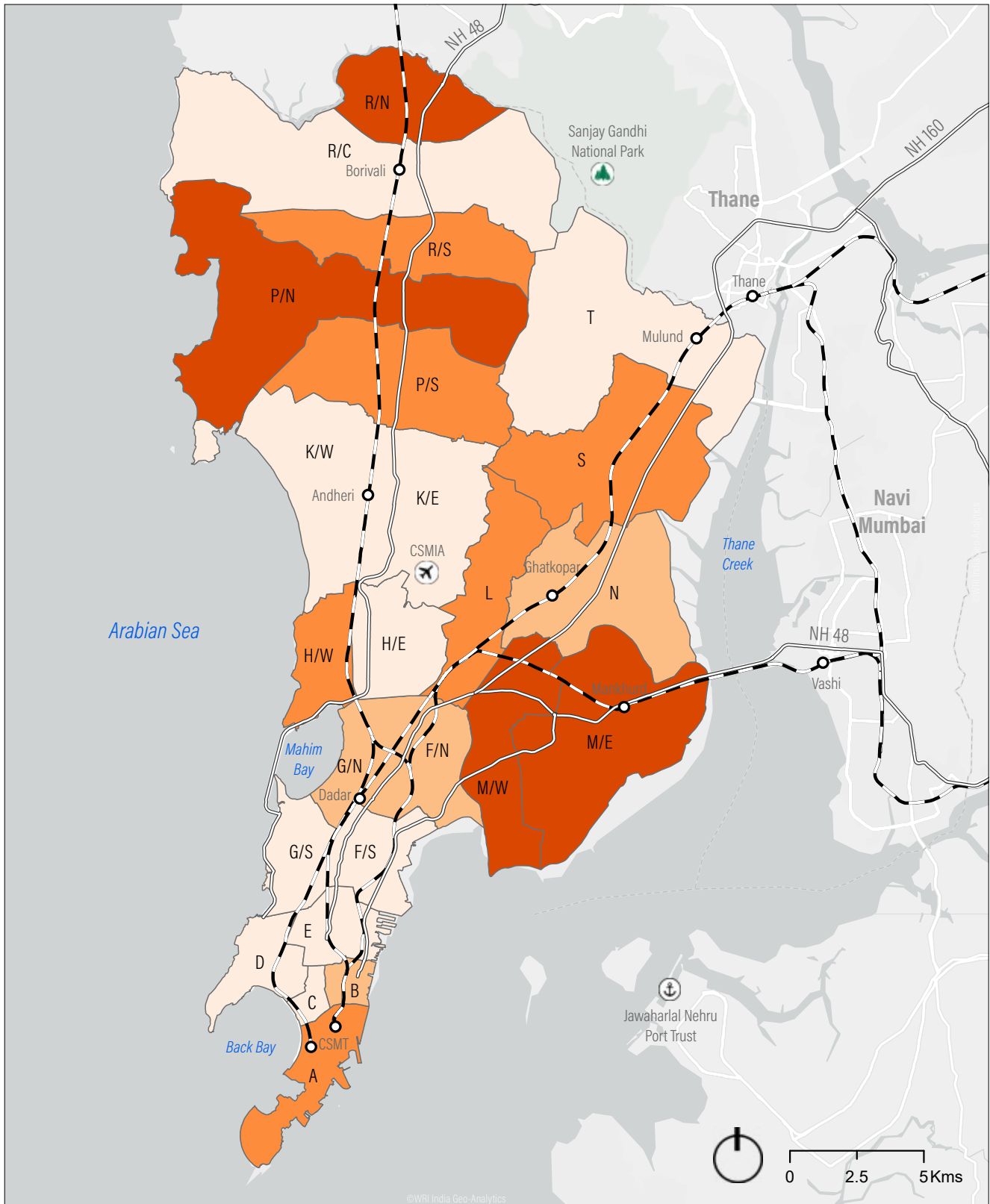


Households using Clean Cooking Fuel (%): ■ 54 - 63 ■ 63 - 72 ■ 72 - 81 ■ 81 - 92

— Highway - - - Railway Line ○ Station ✈ Airport ⚓ Sea Port 🌳 National Park

Source: WRI India using Census 2011

Figure 58 | Access to Electricity



Households with Electricity as Main Source of Lighting (%): ■ 95 - 96 ■ 96 - 97 ■ 97 - 98 ■ 98 - 100

— Highway - - - Railway Line ○ Station ✈ Airport ⚓ Sea Port 🌳 National Park

Source: WRI India using Census 2011

Figure 59 | Access to Mass Transit Stations on a Regular Day

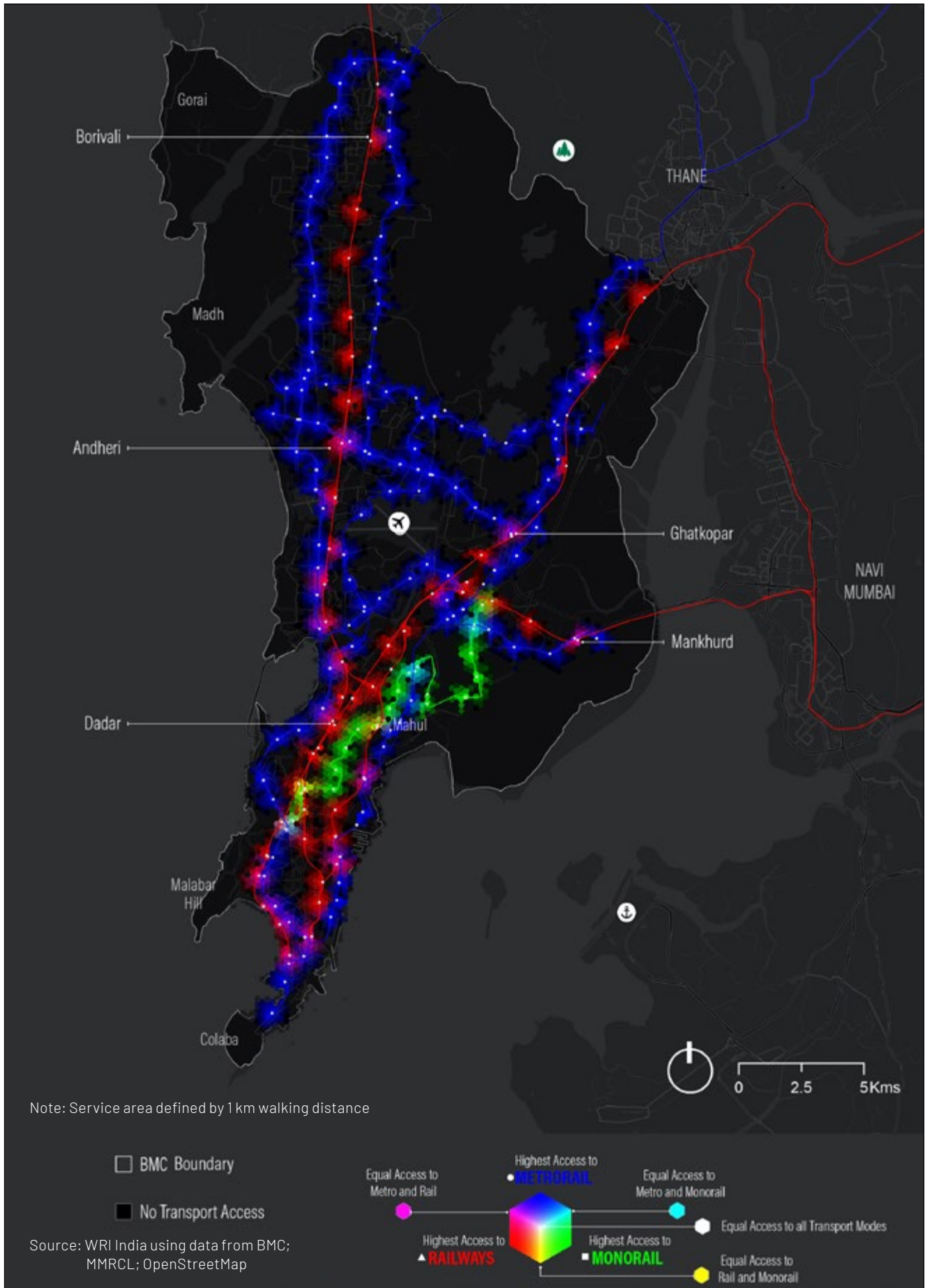
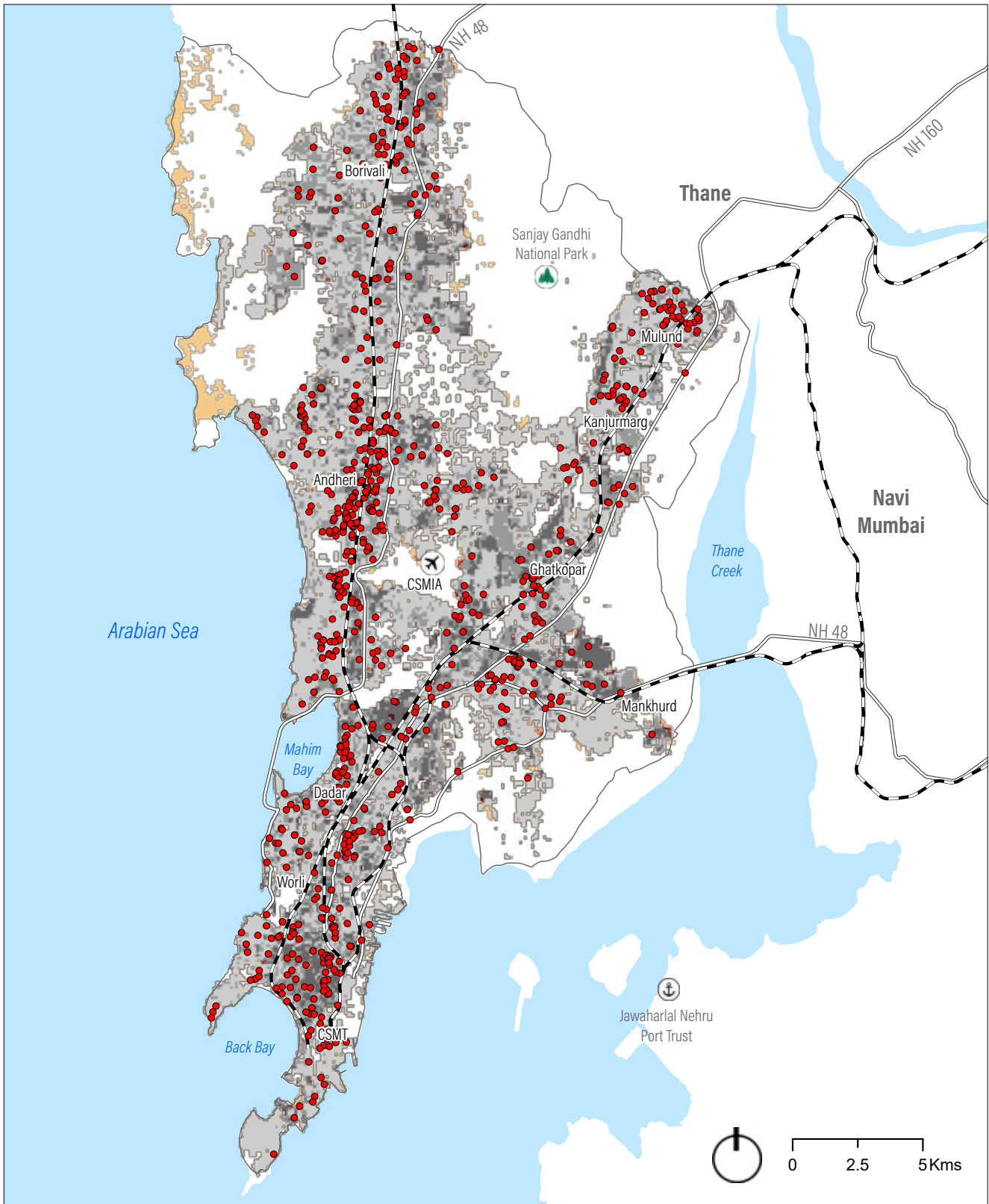


Figure 60 | Access to Healthcare



Population lacking Access to Hospitals: 5-500 500-1,000 1,000-13,800 Hospitals

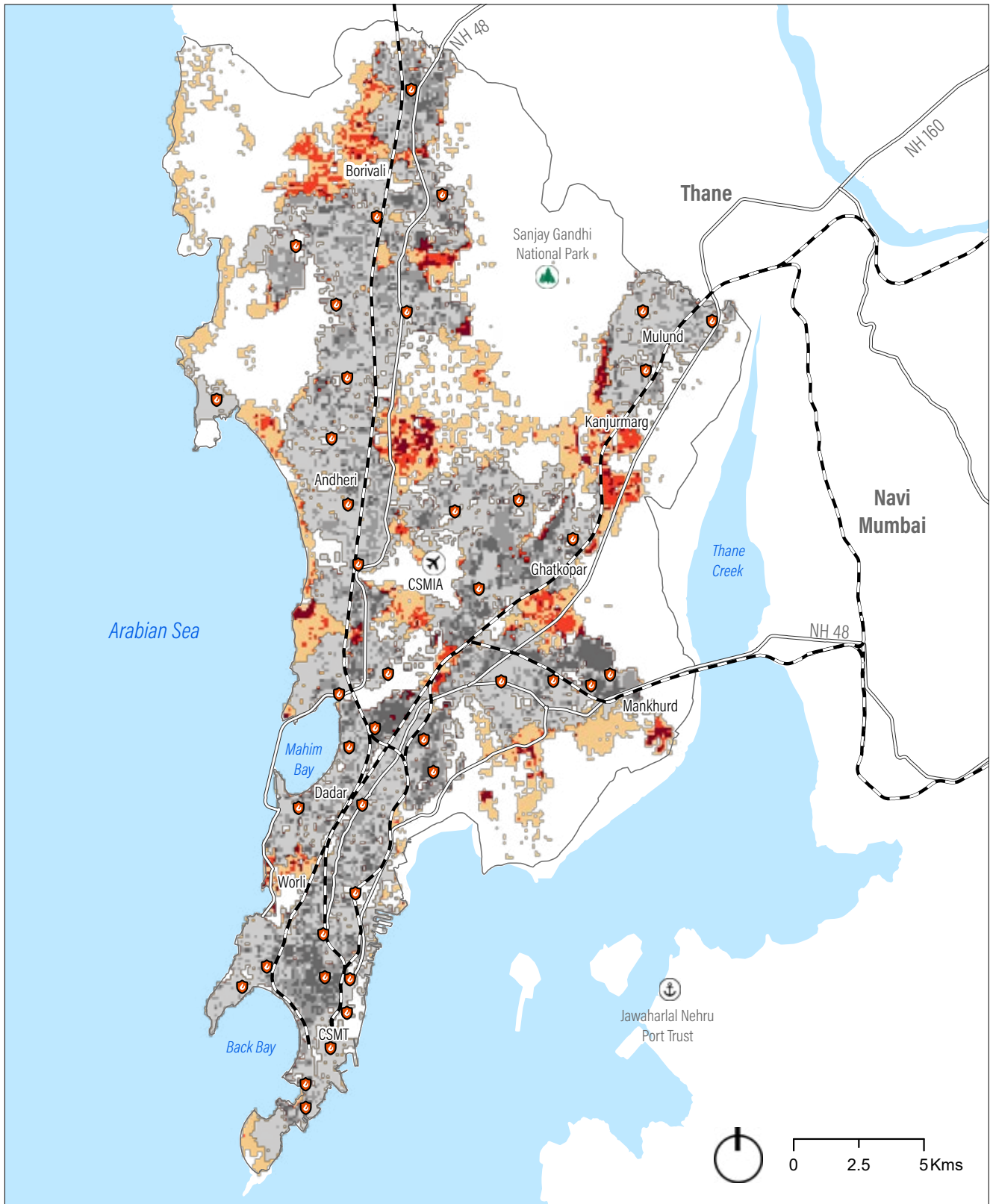
Population having Access to Hospitals: 5-500 500-1,000 1,000-13,800 BMC Boundary

— Highway - - - Railway Line ○ Station ✈️ Airport ⚓ Sea Port 🌳 National Park

Source: WRI India using data from BMC, Census 2011, OpenStreetMap

Note: Service area defined by 5 km driving distance; Population in persons per hectare (Ha)

Figure 61 | Access to Fire Services



Population not served by Fire Stations: 5-500 500-1,000 1,000-13,800 Fire Stations

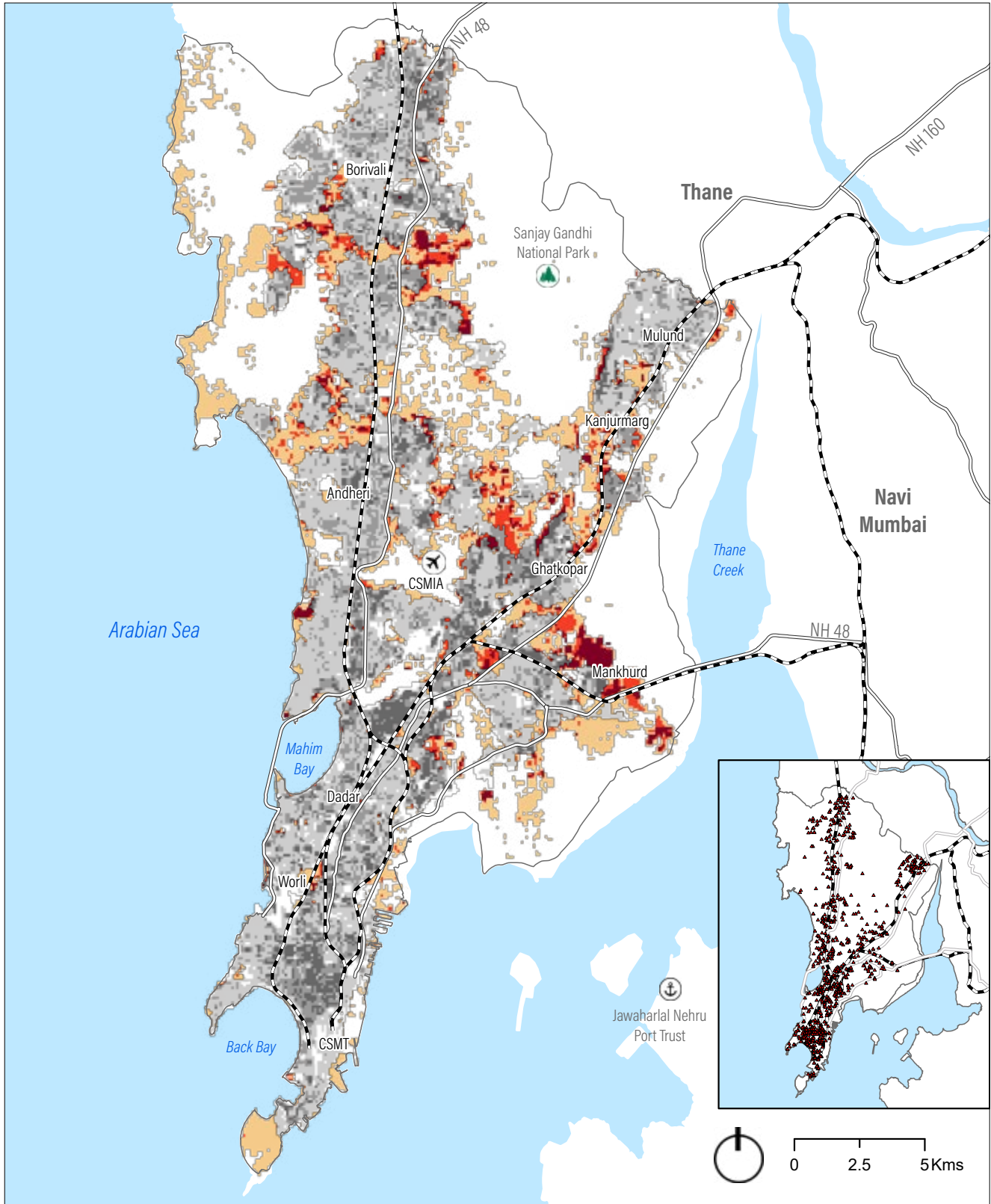
Population served by Fire Stations: 5-500 500-1,000 1,000-13,800 BMC Boundary

— Highway - - - Railway Line ○ Station ✈️ Airport ⚓ Sea Port 🌳 National Park

Source: WRI India using data from Google API; Census 2011

Note: Service area defined by 5 mins response time at 35 km/hr; Population in persons per hectare (Ha)

Figure 62 | Access to Flood Shelters



Population lacking Access to Flood Shelters: ■ 5-500 ■ 500-1000 ■ 1,000-13,800 ▲ Flood Shelters

Population having Access to Flood Shelters: ■ 5-500 ■ 500-1000 ■ 1,000-13,800 BMC Boundary

— Highway - - - Railway Line ○ Station ✈️ Airport ⚓ Sea Port 🌳 National Park

Source: WRI India using data from BMC; Census 2011

Note: Service area defined by 1 km walking distance; Population in persons per hectare (Ha)

Endnotes

I - Background – Air temperature anomalies indicate the degree of deviation of average annual air temperature with respect to the baseline temperature or long-period average. The 30-year period between 1981 and 2010 is used to estimate the baseline average air temperature (IMD, 2021). The direction of deviation from the baseline reflects whether a particular year was cooler or warmer compared to the baseline period. A year is deemed cool or warm if the average annual air temperature is lower or higher than the baseline average, respectively. The magnitude of deviation from the baseline indicates the departure from the normal or long-period average.

II - Background – Trend analysis involves assessing for the presence of the underlying annual rate of change at a statistically significant confidence level. The objective here is to determine the magnitude and direction of the annual air temperature trend across different timescales – inter-annual, intra-annual, inter-seasonal, and intra-day. Trend detection algorithms allow us to test for the presence of a statistically significant trend between time and the dependent variable i.e., air temperature. Mann-Kendall and Theil-Sen's Slope Estimator are non-parametric statistical tests used for the detection of direction and magnitude from timeseries data, respectively.

Results – Annual air temperatures have increased at a rate of 0.24°C per decade between 1973 and 2020 (Figure 3). The intra-annual, inter-seasonal, and intra-day trends show that the rate of change is highest for post-monsoon (November) and winter (February) months between late-evening (6-9 pm) and midnight hours. An increasing trend is observed for October, November, and December (OND) months, which likely indicates a warming post-monsoon season and corresponds well with the October heat phenomenon. An increase in night-time temperatures is associated with increased urbanization, especially built-up of tall structures and paved roads. Paved roads are made from asphalt and concrete that absorb more heat, whereas tall structures trap heat during the day that is released back into surrounding atmosphere during the night. This might point to the idea that night-time temperature increase has been responsible for post-monsoon warming.

III - Background – Change-point detection algorithms identify the location in the timeseries where the statistical properties change significantly, marking an abrupt shift in overall trend. Pettitt's test (Pettitt, 1979) examines the presence of a statistically significant location parameter (a period on the timeline) where a change or abrupt shift in trend likely occurs.

Results – According to Pettitt's test, the overall annual trend for air temperature changed significantly in the years 1995 and 2002.

IV - According to the IMD, in coastal areas a heat wave can occur when the maximum temperature departure from the normal is 4.5°C or more, provided the actual maximum temperature is 37°C or more.

V - Background – The heat index equation was derived by Rothfus in 1990 using multiple regression analysis of Steadman's equations (Rothfus, 1990) (Steadman, 1979). National Weather Service (NWS) under NOAA uses heat index for assessing the combined impact of temperature and humidity on the human body. The NWS guideline on heat-related health implications (National Weather Service, 2021) has categorized the heat index values into four health categories – caution (26-32°C), extreme caution (32-41°C), danger (41-54°C), and extreme danger (above 54°C). For analysis, maximum daily heat index values are used to classify daily

timeseries into NWS defined health categories. The variation in each category is used to derive an inter-annual trend using Mann-Kendall test.

Results – On average, in a year there are 174 and 187 days that fall under caution and extreme caution, respectively. The inter-annual variation of caution and extreme caution days shows that there is an inverse relationship between the two categories. Between 1973 and 2020, the annual trend shows a decrease of 2.2 caution days per year and an increase of 2.3 extreme caution days per year. Intra-annual variation of heat index timeseries shows that, on average, between 1973 and 2020, approximately 75% or more of October and November months were classified as extreme caution days.

VI - Background – According to the IMD, a heatwave event is based on the departure or deviation from the normal air temperature. IMD defines normal temperature for a particular day based on long-period average of maximum air temperature for that day. Based on IMD's definition, coastal areas such as Mumbai must meet two conditions for an event to be declared a heatwave:

1. Maximum daily temperature must exceed 37°C, and
2. The departure, or deviation of maximum daily air temperature from the long-period average (normal) must exceed 4.5°C on at least two consecutive days.

Once these conditions are met, a heatwave event can be further classified based on departure from the normal air temperature:

- Heatwave: departure from normal is greater than 4.5°C but less than 6.4°C, and
- Extreme Heatwave: departure from normal is greater than 6.4°C.

VII - Background – Ten stations are omitted from the analysis because their geographical location (coordinates) is unavailable. Out of the 50 stations left, only those stations are considered which have less than 30% data gaps (based on daily aggregated timeseries). There are 13 such stations, and therefore the analysis is based on the data from 37 stations.

VIII - Background – Sea Surface Temperature (SST) annual data product observed by MODIS Aqua was downloaded from NASA ocean color portal. The data product consists of two separate sets of images for daytime and nighttime at 4km spatial resolution. Study area boundary or the Arabian Sea extents have been adopted based on gazette issued by Marine Regions (Flanders Marine Institute) (*Marine Regions, 2022*) as illustrated below.

Set of sample points was created using a 500 km X 500 km grid within the study area keeping 200m buffer from the coast to minimize the effect of coastal area. The annual average values for the year 2003 – 2020 for each sample point across the study area was extracted and plotted as the range of observed SST.

Figure A.1 | Arabian Sea extent – study area reference boundary. Source: Marine Regions, 2022



IX - Background: Jawaharlal Nehru Port Trust (JNPT) tide gauge records sea surface height from three different sensors (radar, pressure, and float). The dataset consists of water level height observations recorded at a one-minute interval between 2011 and 2021.

The first step involves data cleaning and transforming the raw tide gauge dataset using harmonic least squares regression. Annual trends are estimated using hourly resampled tide height timeseries, whereas sea level variations due to storm surge events are examined at one-minute intervals.

Trend analysis of annual sea level variation from tide gauge data involves resampling the tide height timeseries to hourly interval and deriving the residual timeseries by removing the signal associated with periodic tidal motion. The magnitude and significance of trend is estimated using the modified Mann-Kendall test, which is a non-parametric statistical test used for monotonic trend detection.

Results - The direction of the trend exhibited by changes in sea levels based on tide height measurements from both radar and float (shaft encoder) sensors is slightly downward with a magnitude of 0.062 cm/year and 0.096 cm/year, respectively (Figure 14). Radar sensor is slightly downward with a magnitude of 0.03 cm/year.

X - Background: Because the astronomical tidal motion can be predicted, any abnormal rise in water level due to a storm surge event can be deduced by removing the observed water level from the predicted water level. Information related to cyclone events are made publicly available courtesy of the Cyclonic Weather Division, IMD. The preliminary reports and meteorological information related to all cyclone events that have been observed in the west coastal region of India were examined to identify potential surge events. After potential surge events are identified, the residual timeseries are computed at one-minute intervals.

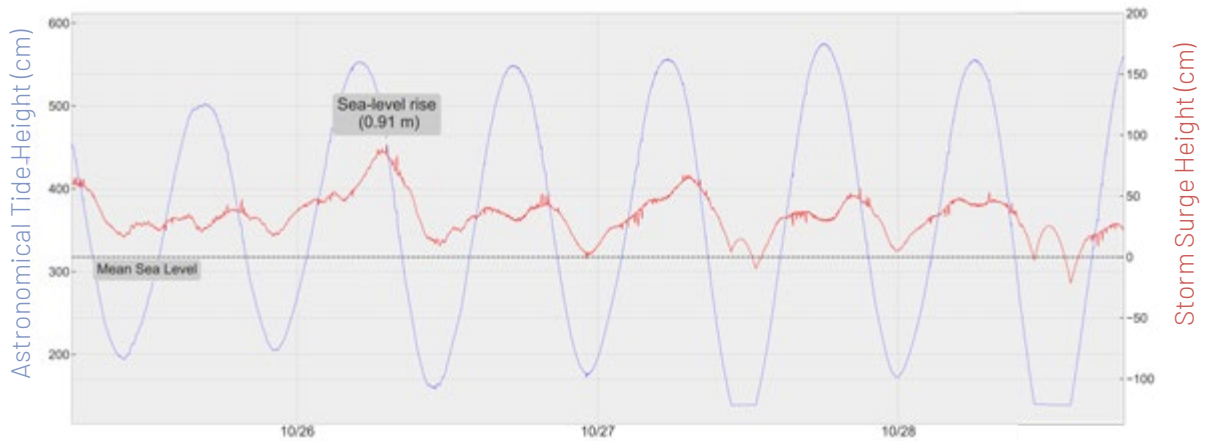
Results – Cyclones usually tend to occur around May-June period and October-November period. Eleven of the 18 cyclones have occurred in the last four years, refer to the “list of cyclone storms” below. Despite the absence of a significant sea level trend, climate change-induced increase in frequency of high intensity storms and extreme rainfall events can wreak havoc on coastal communities by causing damage to infrastructure and inundation of low-lying areas. Storms surge events that coincide with high tide formation are more likely to contribute to higher sea level increase. This is highlighted by Cyclone Kyarr (2019) and Cyclone Takutae (2021), both of which reached their highest potential during a high tide. Figure 15 and Figure A.2 below illustrate the sea level rise associated with both the events was 0.91 m and 0.93 m, respectively.

List of Cyclone Storms Over the Arabian Sea between 2011 – 2021

S.no	Cyclonic Storm	Duration
1	Keila	29 Oct – 4 Nov, 2011
2	Murjan	23 – 26 Oct, 2012
3	Nanauk	10 – 14 Jun, 2014
4	Nilofar (Very Severe)	25 – 31 Oct, 2014
5	Ashobaa	7 – 12 Jun, 2015
6	Chapala (Extremely Severe)	28 Oct – 5 Nov, 2015
7	Megh (Extremely Severe)	5 – 10 Nov, 2015
8	Sagar	16 – 21 May, 2018
9	Mekunu (Extremely Severe)	21 – 27 May, 2018
10	Luban (Very Severe)	6 – 15 Oct, 2018
11	Vayu (Very Severe)	10 – 17 Jun, 2019
12	Hikaa (Very Severe)	22 – 25 Sep, 2019
13	Kyarr (Super Cyclone)	24 Oct – 2 Nov, 2019
14	Maha (Extremely Severe)	30 Oct – 7 Nov, 2019
15	Pawan	2 – 7 Dec, 2019
16	Nisarga (Severe)	1 – 4 Jun, 2020
17	Gati (Very Severe)	21 – 24 Nov, 2020
18	Tauktae (Super Cyclone)	14 – 19 May, 2021

Source: Regional Specialized Meteorological Centre (RSMC), IMD

Figure A.2 | Storm Surge Associated with Super Cyclone Kyarr (2019)



Source: INCOIS Radar tide gauge data from JNPT Port

XI - Background: To assess the changes of mangroves, the spatial and temporal changes which occurred along the Mumbai suburb was analyzed using satellite imagery viz., 2008-2010 and 2018-2021 (Landsat Thematic Mapper). The median of imageries from 2008 - 2010 and 2018 - 2021 were compared for the analysis. Satellite data was classified using Random Forest Classification algorithm in Google Earth Engine to delineate different land cover features. Imageries were subjected to the supervised classification to delineate various classes viz., vegetation, water, barren and built up within the study area. The Area of Interest (AOI) consists of the mangrove boundaries as described by the Mumbai Development Plan 2034.

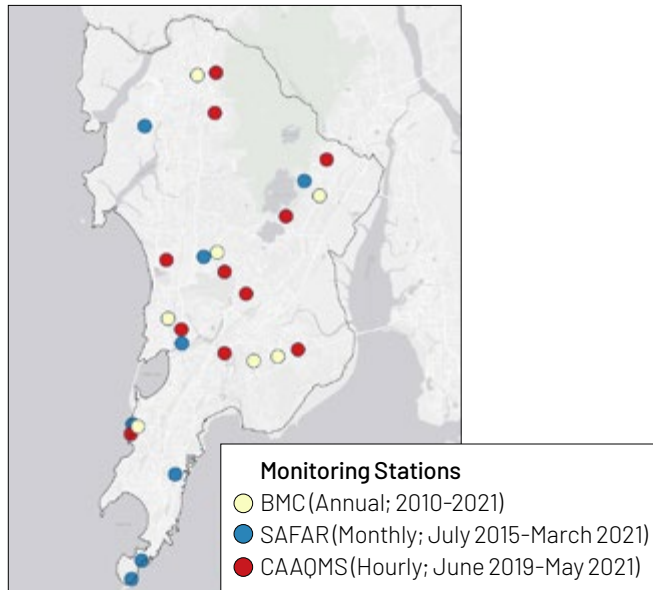
Baseline Period (2008 - 2010)	Change/ Transition Observed				Total Mangroves with Reduced Density by 2018-2021
	Mangroves	Water	Built-up	Sparse Mangroves/Mudflats	
Mangroves	2,785.83	62.38	6.22	256.45	325.05
Water	21.71	38.57	0.65	25.18	
Built up	8.1	0.14	9.7	41.68	
Sparse Mangroves or Mudflats	275.91	25.4	30.03	670.28	
Total Mangroves Gained/Increase in Density by 2018-2021	305.73	All units in hectares			

XII - Background: The coastline change calculation was done using LandSat 5 and LandSat 8 satellites, the data of which was provided by the United States Geological Survey (USGS). The raw images were chosen from the years of 1990 and 2020. Images which had less than 10% cloud cover over the land area were chosen. Based on the tidal levels, images were chosen from both the years which were in the same phase of the tide so that they are comparable over years. A Normalized Difference Water Index (NDWI) was calculated for both the images with the short-wave infrared and the green bands of satellite images were used for the same. Using a threshold of 0.2 value, the NDWI rasters were reclassified to differentiate land and water and the raster was finally vectorized to produce the coastline for the respective years.

XIII - Background: The availability of pollutants' data over the period of analysis varies for different stations. For analytical coherence within the analysis the following monitoring stations have been used considering that these had maximum consistency in the data:

- For NO₂, SO₂, and NH₃, BMC data for seven monitoring stations during April 2010 to March 2021 has been used to determine overall annual average concentration and station-wise annual averages.
- For CO, PM_{2.5} and PM₁₀, SAFAR data for nine monitoring stations from July 2015 to March 2021 has been used to derive overall annual average concentration and station-wise annual averages based on monthly averages received.
- For PM₁₀ and PM_{2.5}, CAAQMS data for nine monitoring stations from May 2019 to June 2021 at hourly resolution has been used to derive extensive hourly-weekly-monthly-annual comparisons for overall and station wise annual averages.

Figure A.3 | Spatial Distribution of Monitoring Stations



XIV - Background: In order to estimate the indoor household concentration of PM_{2.5}, the semi-empirical model was followed, a method provided by Balakrishnan, K, Ghosh, S, et.al., 2013 in their paper, 'State and national household concentrations of PM_{2.5} from solid cookfuel use: Results from measurements and modeling in India for estimation of the global burden of disease'. In this model data on cooking fuel type, kitchen area location and ventilation were used, derived from the Census of India, 2011, National Sample Survey, 2013-14 and Human Index Survey, 2012 (Balakrishnan, Ghosh, Ganguli, Bruce, & Barnes, 2013).

XV - Caveat: Accessibility analysis is limited to physical provision and proximity evaluation. Enrolment, teacher-student ratio, drop-out etc. are not included. Access to educational institutions is mapped using service area polygons that are created for the schools analyzing access within 1 km.

XVI - Assumption: Local news and updates are broadcast on radio, telecast, can be accessed via the internet or circulated via mobile phone SMS.

Caveat - Since this data is from 2011, population owning mobile phones is lower than 2021. No data is available for print media.

XVII - Caveat: While ownership as a single parameter cannot illustrate exposure or sensitivity as it depends on the condition and location of the house, this indicator only includes tenure. Cases of displacement and damage to houses caused due to a climate-induced hazard are not included.

XVIII - Approach: Proximity and per capita space are equally important to understand access to recreation spaces. Daily urban recreation spaces include children's park, neighborhood park, institutional playgrounds, maidans and district park. Each daily urban recreation space is categorized and assigned weightages. Service area polygons are created for each type of daily urban recreation open space using network analysis based on standard distances adopted through extensive literature study. A higher number on the scale indicates better access to various types of daily urban recreation spaces. The summation of access to each type was calculated which resulted in values in the range of 0-5, with 0 being no access to recreational open space within the walkable distance (low access) and 5 being access to all types of recreational spaces (high access). The summation of access to each type was calculated which resulted in values in the range of 0-5, with 0 being no access to recreational open space within walkable distance (low access) and 5 being access to all types of recreational spaces (high access).

Categories of Daily Urban Recreation Space, Area, Service Radius and Weightage

Categories of Daily Urban Recreation Space	Area in m ²	Service Radius (used as shed distance in meters)	Weightage and Justification
Children's Park	Less than 5,000	250	1
Neighborhood Park	5,000 - 10,000	500	1
Institutional Playgrounds		1,000	0.9 (limited usage based on institution hours)
Maidans		1,000	0.5 (multi-use space, may be used for other activities)
District Park	Above 10,000	1,000	1

Source: (Nochian, Tahir, Maulan, & Rakhshandehroo, 2015)

XIX - Assumption: Tap water from treated source is assumed to be a safe source for drinking water. Spatial data regarding frequency, quantity and coverage of supply network are unavailable and hence not considered.

XX - Assumption: Kitchen is assumed to be located inside the premises for this analysis. Percentage of households HHs using non-polluting cooking fuels to total households.

XXI - Caveat: Off-grid sources of electricity are not accounted for in this analysis.

XXII - Assumption: Analysis includes operational and proposed (including under construction and planned) stations for Monorail, Metro, and suburban rail networks.

Caveat - Affordability of specific transit modes, reliability and quality of service are not included in this analysis.

Approach - Access to mass transit networks such as suburban railway, Metro and Monorail in Mumbai is measured within hexagonal grids within a 1 km buffer zone around the stations. Distance to nearest suburban railway/Metro/Monorail station for a location which is represented by a hexagonal grid is calculated using OD matrix. These distances are inversely rescaled to 0 to 255 from 0 to 1,000 m. This implies, farther the location, lower the number on the 0 to 255 scale. Access to each mode is represented by one primary color from the standard RGB color model, Red for Suburban railways, Green for Monorail and Blue for Metro Rail.

XXIII - Caveat: The real-time traffic is not accounted for in the city level analysis while in live circumstances it does impact the time taken to reach the destination. Affordability, quality of service, medical staff to patient ratio are not included in the city-level access analysis. For the population-to-bed ratio, this analysis uses bed data from 2021 while the population data is from Census 2011 and hence the current population-to-bed ratio might be lower given increase in population. Based on the data from the BMC Health Department, access to urban health amenities is mapped using service area polygons for hospitals analyzing access within 5 km.

Number of Hospital Beds by Wards

Administrative Ward Name	Hospital Beds
A	1,991
B	316
C	135
D	2,336
E	5,127
F/N	4,534
F/S	5,202
G/N	1,627
G/S	1,182
H/E	1,074
H/W	1,976
K/E	3,643
K/W	4,556
L	1,523
M/E	1,128
M/W	1,622
N	2,878
P/N	2,349
P/S	1,027
R/C	1,956
R/N	1,054
R/S	2,546
S	2,098
T	1,806
Total	53,686

Source: BMC Health Department

Number of Hospitals by Administration and Number of Beds

Hospital Type Based on Hospital Administration	Number of Hospitals	Total Beds
GOVT - Government	17	5,835
BMC-GEN - BMC General Hospital	5	6,923
BMC-MH - BMC Maternity Home	28	958
BMC-PH - BMC Primary Health Centre	15	3,122
BMC-SPL - BMC Specialty Hospitals	5	1,909
BMC-UHC - BMC Urban Health Centre	1	50
PVT - Private Hospital	1,521	34,889
Total	1,592	53,686

XXIV - Approach: Analysis at the city level includes vehicular access from the location of fire stations based on a constant speed assumed at 30 km/hour (LEA Associates, 2016) within 5 -7 minutes response time standard. Variation in traffic conditions, road conditions and capacity of individual fire stations are not accounted for.

XXV - Approach: Access to flood shelters is mapped using service area polygons for flood shelters analyzing access within 1 km.

XXVI - Persons potentially at risk due to floods (Source: WRI India Analysis using data from BMC; Census 2011)

Ward Name	Population Potentially Exposed to the Risk of Flooding (Within 250m Buffer)	Percentage Population Potentially Exposed to the Risk of Flooding (Within 250m Buffer)
A	33,152	17.9
B	53,911	43.4
C	36,010	21.7
D	1,05,583	30.4
E	1,47,930	37.5
F/N	3,55,766	66.8
F/S	1,44,576	40.3
G/N	3,04,429	50.3
G/S	1,53,522	41.7
H/E	3,29,774	61.6
H/W	2,00,342	61.2
K/E	1,87,389	22.5
K/W	2,66,733	35.9
L	3,12,960	34.5
M/E	2,75,491	34.1
M/W	1,82,542	45.1
N	1,08,962	17.4
P/N	1,43,697	15.4
P/S	1,43,846	31.0
R/C	1,45,800	25.6
R/N	1,75,520	41.1
R/S	2,09,665	30.0
S	1,90,113	26.4
T	1,78,542	49.5
Total	43,86,255	35.3

Climate & Air Pollution Risks and
Vulnerability Assessment for Mumbai, India
March 2022

Cover Image: Saikiran Kesari